Meereswissenschaftliche Berichte
MARINE SCIENCE REPORTS

No. 40

Data report of R/V "Poseidon" cruise 250
ANDEX'1999

von

M. Schmidt, V. Mohrholz, T. Schmidt, H.-Ch. John,
S. Weinreben, H. Diesterheft, A. Iita, V. Filipe, B.-B. Sangolay,
A. Kreiner, V. Hashoongo, D. da Silva Neto

Institut für Ostseeforschung
Warnemünde
2000

Contents

Appendix

Zusammenfassung

Die Poseidon Reise POS250 war eine gemeinsame Expedition von Wissenschaftlern und Studenten aus Angola, Deutschland und Namibia. Die Messungen erfassen den östlichen äquatorialen Atlantik, den Angola-Dom sowie die Angola-Benguela Front. CTD-Messungen wurden in Kombination mit Strömungsmessungen sowie chemischen, Phytoplankton- und Zooplanktonuntersuchungen durchgeführt. Die Stationsdaten werden durch Unterwegsmessungen mit dem Thermosalinographen, dem schiffsgebundenem ADCP und der Schiffswetterstation ergänzt. Die Daten vermitteln einen Überblick über das äquatoriale Stromsystem und seine südwärtige Fortsetzung vor der angolanischen und namibischen Küste.

Die beobachten Stromfelder spiegeln die bekannte Struktur der Äquatorialströme wider, wobei der nach Osten gerichtete äquatoriale Unterstrom das stärkste Signal lieferte. Die Äquatorialströme werden durch ostwärtige Gegenströme bei 2°N (NECC) and 4°S (SECC) berandet. Von 4°S to 8°S war in den oberen 100 m östliche Strömung vorherrschend. Vor der Küste Angolas wurde die Strömung nach Süden abgelenkt und ging in einen Wirbel mit dem Angola-Dom im Zentrum über. Im Tiefenhorizont von 125 m bis 175 m gibt es Anzeichen für ein Stromband, das sich von Namibia, 20°S, bis Angola, 8°S, erstreckt.

Der Angola-Dom, mit Zentrum bei 9°S 8°E, war mit einer zyklonalen Zirkulationszelle an der Oberfläche verknüpft, deren nördliche Berandung in den südwärts abbiegenden Südäquatorialen Gegenstrom übergeht. Dieses Gebiet ist durch gewaltige Flußwasserfahnen beeinflußt, die auf effektiven Austausch zwischen Küste und offenem Ozean hinweisen.

Die Angola-Benguela Front bei etwa 16°S trennt ein Band kalten Auftriebswassers (etwa 15°C) vor der Namibischen Küste südlich der Front von warmem tropischen Wasser (etwa 29°C) nördlich der Front. Während der Reise wurde durch ein Starkwindereignis neuer Kaltwasserauftrieb angeregt, der die Lage der Front nach Norden verschob.

Die Planktonuntersuchungen demonstrieren den Einfluß der hydrographischen Bedingungen und Strömungen auf Diversität, Häufigkeit und Vertikalverteilung von Phyto- und Ichthyoplankton. Durch die aus den Küstengewässern eingetragenen Plankter wächst die Ichthyoplanktonhäufigkeit in Richtung der angolanischen Küste. Im Zentrum des Angola-Doms wurden normalerweise tief lebende Larven in extrem flachen Horizonten angetroffen, während in und oberhalb der Thermokline eine normale Verteilung gefunden wurde.

Nach Süden hin wurde ein Anstieg von Diversität und Größe von mesopelagischen Fischarten beobachtet. An der Angola-Benguela Front traten Küstenfische in Proben aus dem offenen Ozean auf, was auf eine Westdrift entlang der Front hindeuted. Südlich der Front zeigt die küstenferne Fauna die Charakteristik des Südatlantischen Zentralwirbels.

Im gesamten Untersuchungsgebiet wies die Sauerstoffkonzentration ein Minimum bei etwa 300 m Tiefe auf. In Äquatornähe ist die sauerstoffarme Wassermasse auf eine dünne Schicht beschränkt, die sich zur angolanischen Küste hin aufweitet. Sie setzt sich durch die ABF nach Süden hin fort. Während der Reise wurden keine anoxischen Bedingungen beobachtet.

Summary

The Poseidon cruise POS250 was a joint survey of scientists and students from Angola, Namibia and Germany. The measurments covered the eastern equatorial Atlantic, the Angola Dome area and the Angola-Benguela Front. On a grid of hydrographic stations CTD measurements have been carried out combined with direct current measurements and chemical, phytoplankton and zooplankton investigations. The station data are supplemeted with underway measurements with Thermosalinograph, Vessel Mounted ADCP and ship's weather station. The data set provides a large scale view on the East Atlantic equatorial current system and its continuation to the south off the Angolan and Namibian coast.

The observed current patterns resemble the known structure of the equatorial current system. The eastward equatorial undercurrent was the dominating signal. The equatorial currents were bounded by eastward counter currents at 2°N (NECC) and 4°S (SECC). From 4°S to 8°S the prevailing flow direction in the upper 100 m was eastward. Near the Angolan coast, the current was deflected to the south and merges into a circular structure with the Angola Dome in its center. There is indication for a northward stream band of varying strength in the 125 m to 175 m layer extending from Namibia, 20°S, to Angola at 8°S.

The Angola Dome was found near 9°S and 8°E associated with a cyclonic circulation cell in the near surface currents. It's northern limb merges with the southward bending South Equatorial Counter Current but it is also influenced by giant river plumes indicating efficient exchange with the coastal ocean.

The Angola-Benguela Frontal Zone at 16°S separates a band of cold, i.e. 15°C upwelled water off the Namibian coast south of the front from warm, i.e. 29°C, water north of the front. During the cruise a strong wind event forced new upwelling which moved the frontal zone to the north.

The plankton investigations show the influence of hydrographic conditions and currents on phytoplankton and ichthyoplankton diversity, abundance and vertical distribution. The ichthyoplankton abundance increases towards Angolan waters by entrained planktonic organisms originating from distant coastal areas. In the center of the Angola Dome extremely shallow vertical distributions of normally deep living larvae and shallow diversity gradients were found, but normal patterns in and above the thermocline.

An increase in diversity and size of mesopelagic fish species was noticed towards the south. At the Angola-Benguela-Front coastal fishes appeared in samples from the open ocean, which suggests westward flow along the front. South of the front the offshore fauna revealed characteristics of the South Atlantic Central Gyre.

In the whole area of investigation oxygen content reveals a minimum at about 300 m depth. Near the equator the minimum concentration is confined to a thin layer which broadens towards the Angolan coast. The oxygen depleted water mass continues southward through the ABF. However, no anoxic conditions have been met during the cruise.

1 Background

The area of investigation covers the two major eastern boundary currents of the Southern Atlantic. In a rough conceptual picture the northern branch is the Angola Current consisting of a pole-ward directed surface current with a vertical extent of about 50 m and a pole-ward undercurrent. The Angola Current is considered as continuation of the South Equatorial Counter Current (SECC) which bends southward at the Angolan coast. Another source is the Gaboon-Congo Undercurrent, a pole-ward undercurrent at the shelf break at 1°S to 6°S, reported by WACOGNE and PITON (1992), which is conjectured to be fed from the southward turning South Equatorial Under Current (SEUC) and the Equatorial-Under-Current (EUC) as well.

The Angola Current surface part disappears at about 15°S and is separated from the Benguela upwelling area by a pronounced frontal system, MEEUWIS and LUTJEHARMS (1990). However, the undercurrent is believed to extend southward and advects tropical plankton into the Benguela ecosystem. In light of the presently available data, the seaward Ekman transport component removes mass from the Angola Current and plays a major role in its mass balance, LASS, MOHRHOLZ, SCHMIDT (1999). It remains to be investigated, whether along the front a westward recirculation into the South Equatorial Current (SEC) occurs, and whether filaments penetrate through the front pole-ward; symmetrically to the situation as along the Cape-Verde-Frontal-Zone, FIEKAS et al. (1992), JOHN and ZELCK (1997).

Geostrophic analysis reveals the Angola Current as coastal branch of a cyclonic gyre in the Angola Basin centered at about 13°S and 4°E, MOROSHKIN et al. (1970), GORDON and BOSLEY (1991). It extends to about 300 m depth with subsurface velocities of about 50 cm s^{-1} in a narrow coastal band. The dynamic topography indicates a closed clockwise circulation between the Angolan coast and 5°W and 5°S and 15°S respectively. On the northern side the gyre is closed by the eastward flowing South Equatorial Undercurrent (SEUC), REID (1964),MOLINARI et al. (1981), MOLINARI (1982) and the South Equatorial Counter Current. According to WACOGNE and PITON (1992) both currents are driven by different dynamics. The SEUC appears to be tied to the equatorial thermostad, whereas the SECC is determined by the Sverdrup balance with local negative wind stress curl.

The Angola Dome is a rise of the thermocline near 10°S and 8°E to 10°E which has been analyzed by MAZEIKA (1967) on basis of oceanographic data. It is undetectable in the sea surface temperature but can be clearly seen in the field data from 20 m to 150 m depth. It corresponds also to lower salinity (0.3 to 0.5) and lower oxygen (2 to 3 ml l^{-1}). However, although appearing in the thermocline only seasonally from January to May, there is a permanent subthermoclinic doming of isotherms, VOITUREZ (1981), VOITUREZ and HERBLAND (1982).

The position of the Angola Dome determined from quasisynoptic field measurements varies considerably. So VOITUREZ and HERBLAND (1982) determined the Dome at about 10°S and 10°E but FILIPE (1998) reported a Dome structure at 12°S and 12°E.

The dynamics of the Angola Dome is still under discussion and leaves open many questions. The seasonal thermocline uplift suggests that it is linked with the seasonal cycle of the SECC. In turn SECC's variablility is believed to be triggered by the seasonal cycle of the local wind stress curl, WACOGNE and PITON (1992). The minimum wind stress curl is two degrees south of the position of the Angola Dome and suggests upwelling in the open ocean due to horizontal Ekman transport divergence. However, in the light of numerical model simulation results the situation appears much more complex. Seasonally, warm saline water mass from the equatorial current system penetrate with a downwelling signal as baroclinic Kelvin waves southward and produce the eastern limb of the Dome. An interplay of horizontal and vertical convergence of the flux near the thermocline with the surface heat flux generates a seasonal cycle of the heat balance of the Angola Dome area, YAMAGATA and IIZUKA (1995).

The Angola Basin gyre excludes the water masses from the general South Atlantic gyre and forms a shadow zone with a residence time of 4 to 10 years, GORDON and BOSLEY (1991). In his analysis of the age of South Atlantik Central water, Tomczak has detected the oldest water mass in the area of the cyclonic gyre, TOMCZAK (1998). Consequently there is a significant minimum in the oxygen concentration ($< 1\,\mathrm{ml\,l^{-1}}$) compared with the underlying Antarctic intermediate water and thermocline water. This oxygen deficient water seems to propagate pole-ward into the Benguela current system and may contribute to the oxygen budget of the Benguela upwelling area.

For an introduction to the background of the biological investigations especially for the expected correlations of hydrography and currents with ichthyoplankton distribution see Section 9.4.1

2 The extent of measurements

The area of investigation covers the area of the Angola Dome and the Angola-Benguela Front off southern Angola and northern Namibia from 9°5′S to 21°S. Seven off shore sections and one longshore section at 8°E have been worked. Especially in the Angola Dome area gaps between the sections have been filled by additional stations. The typical distance between the stations is 10 n.m. near the coast up to 30 n.m. in the open ocean. The distance between the sections varies from 60 n.m. to 90 n.m. (see figures 2.1 and 2.2). CTD casts have been carried out to the bottom in shallow water or to 1300 m in the open ocean.

The way from Las Palmas has been used to sample a long section across the equatorial current system from 1°27.6′N, 5°45.17′W to 8°39′S, 12°49′E.

At each CTD station water samples for nutrient and oxygen estimation have been taken. Up to 11 bottles have been closed at depth which have been chosen to meet the most important water masses in the profile.

Phytoplankton samples could be taken only on a reduced station grid with more stations near the coast and a coarser station distance in the open ocean. Samples have been taken from three depth above, within and below the fluorescence maximum.

Neuston samples and Ichthyoplankton have been sampled on selected transects. The equatorial transect was worked completely. Cross-slope profiles were one transect along 17°S, and a second transect slanting east-northeast and crossing 20°S offshore at 9°E. Furthermore a shorter line at 20°S, coinciding with the Namibian Sea Fisheries Institute's time series line, was repeated to elucidate any slope-undercurrent transport. These four more zonal transects were expected to show the ichthyoplankton structures north of the ABF, in the frontal zone itself, and (if it would have been a climatologically normal year) about 100 n.m. south of the ABF. The outmost station of each off shore section was at 8°E and form a long meridional section from 6.5°S to 20°S. The Ichthyoplankton was sampled in depth layers 200 to 150 m, 150 to 100 , 100 to 50 m, 50 to 25 m and 25 to 0 m, unless bottom depths shallower than 200 m interfered.

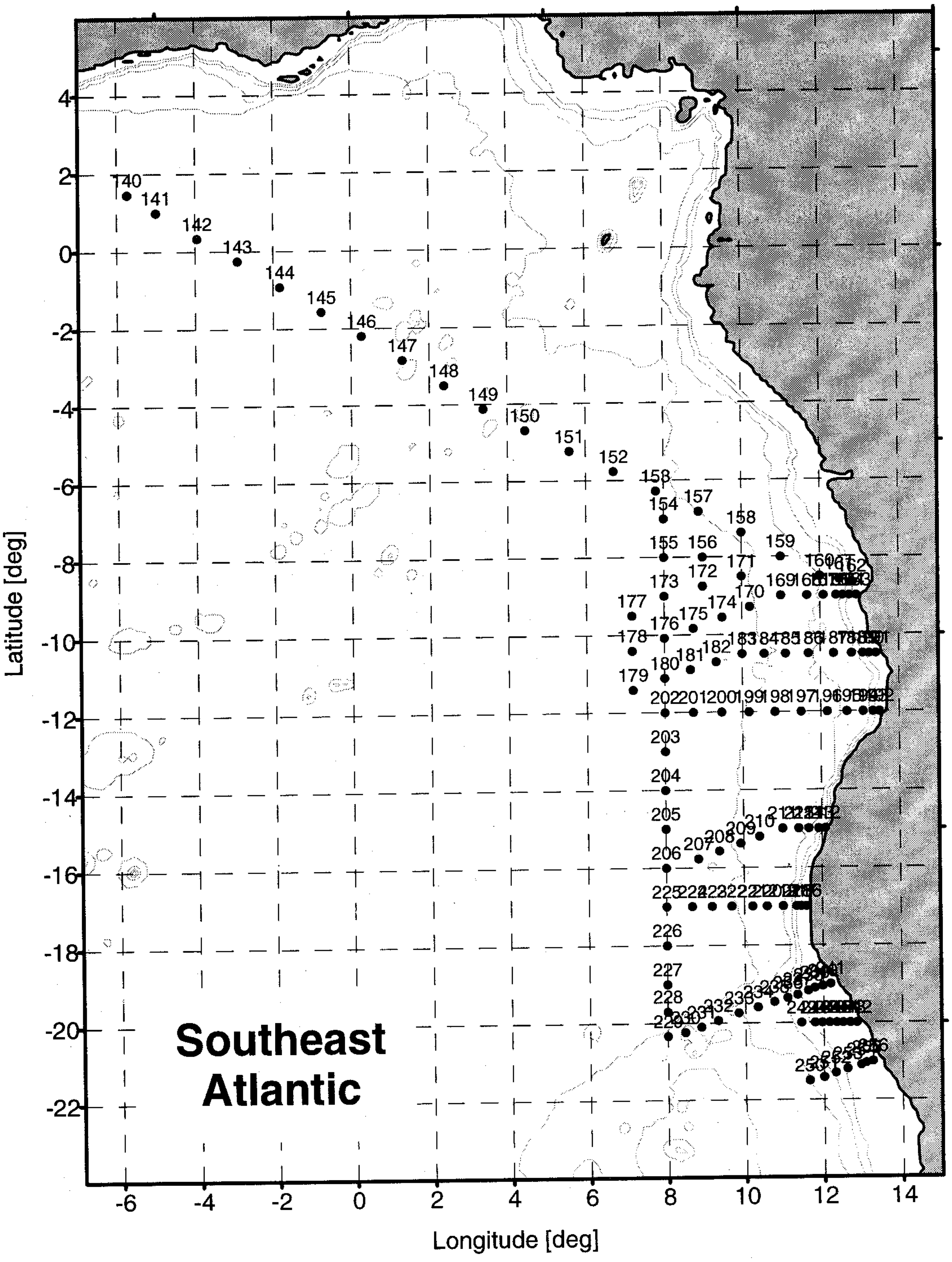

Figure 2.1: Map of hydrographical stations of the cruise POS250 (02. - 28. April 1999)

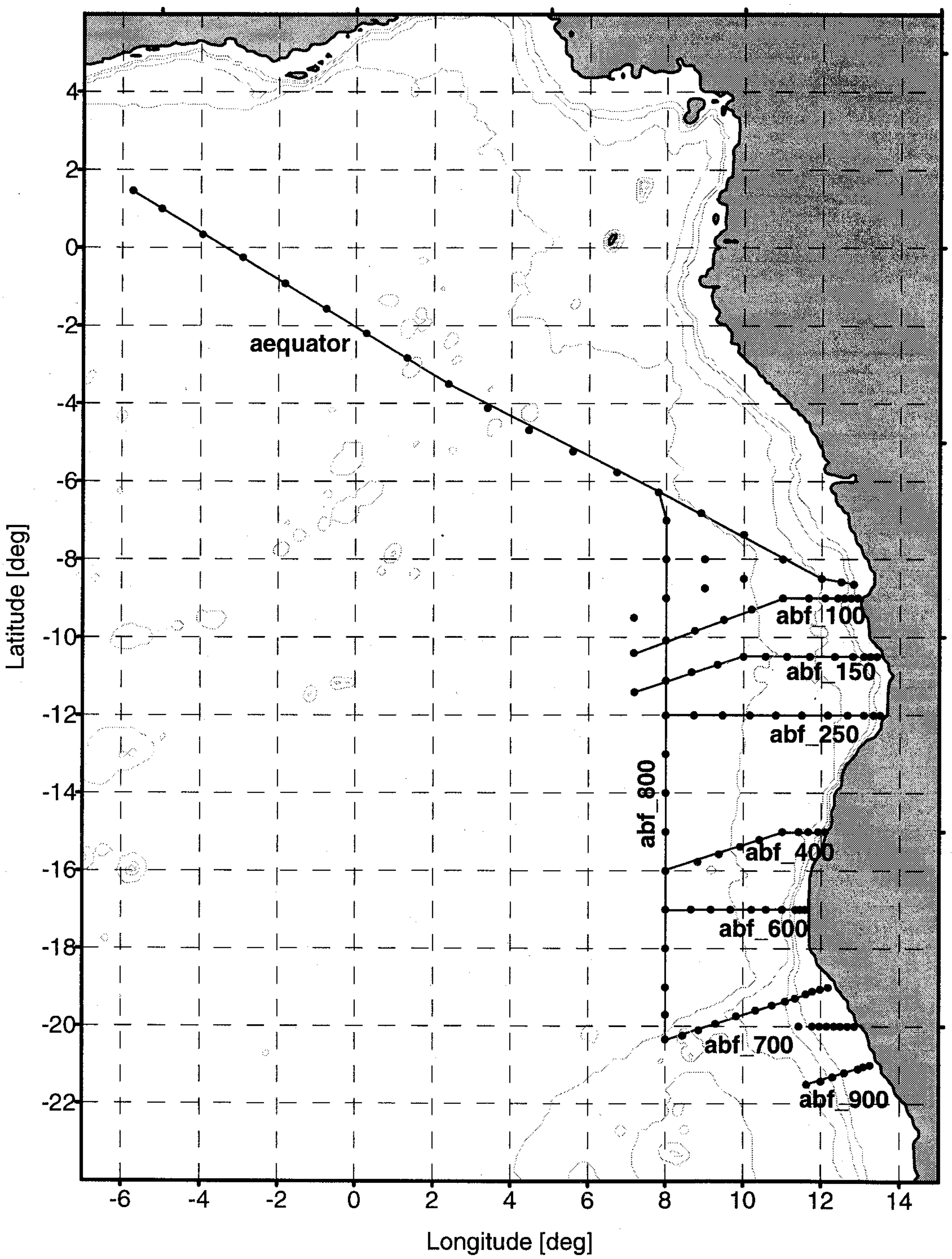

Figure 2.2: Map of hydrographical sections of the cruise POS250 (02. - 28. April 1999)

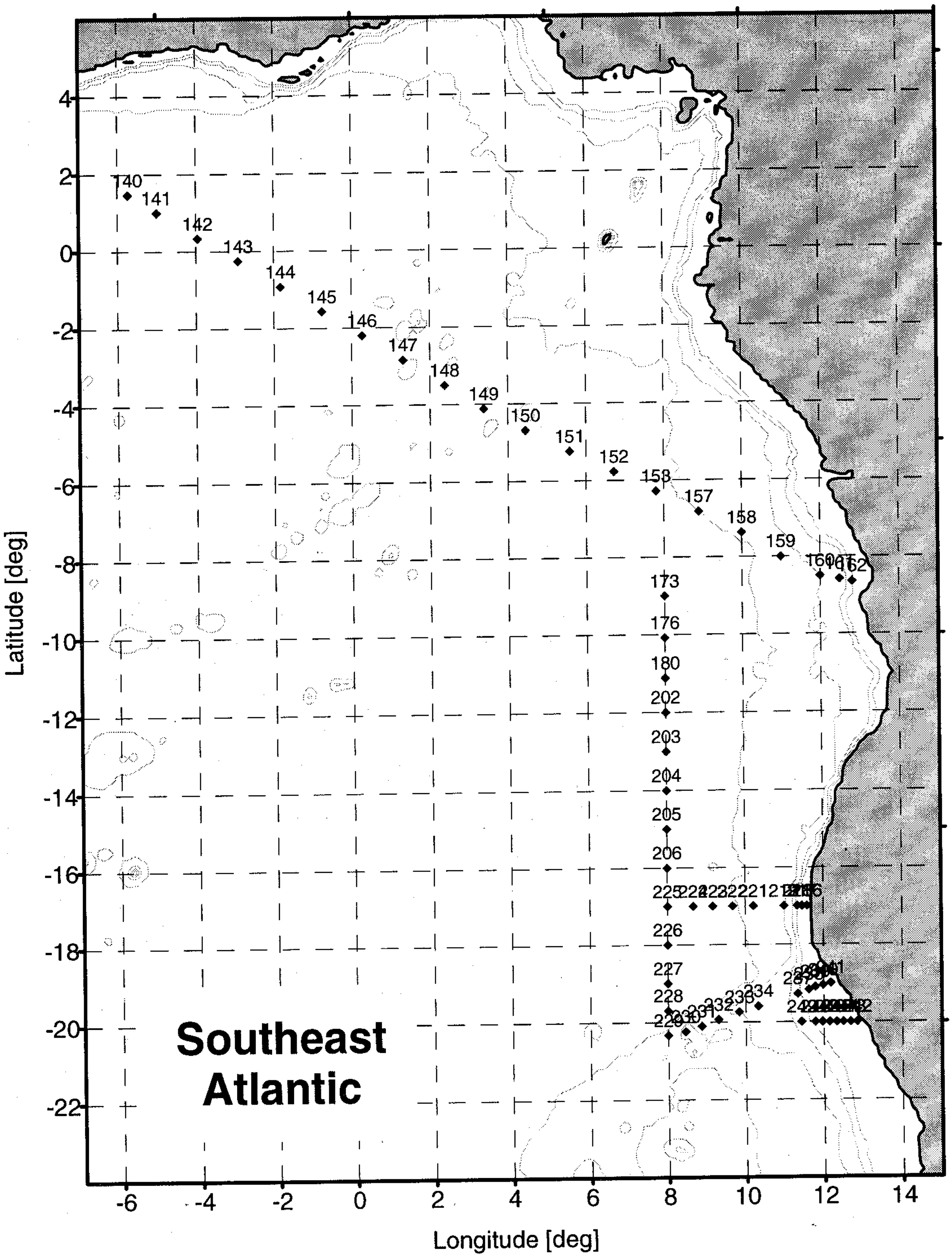

Figure 2.3: Map of ichthyoplankton stations of the cruise POS250 (02. - 28. April 1999)

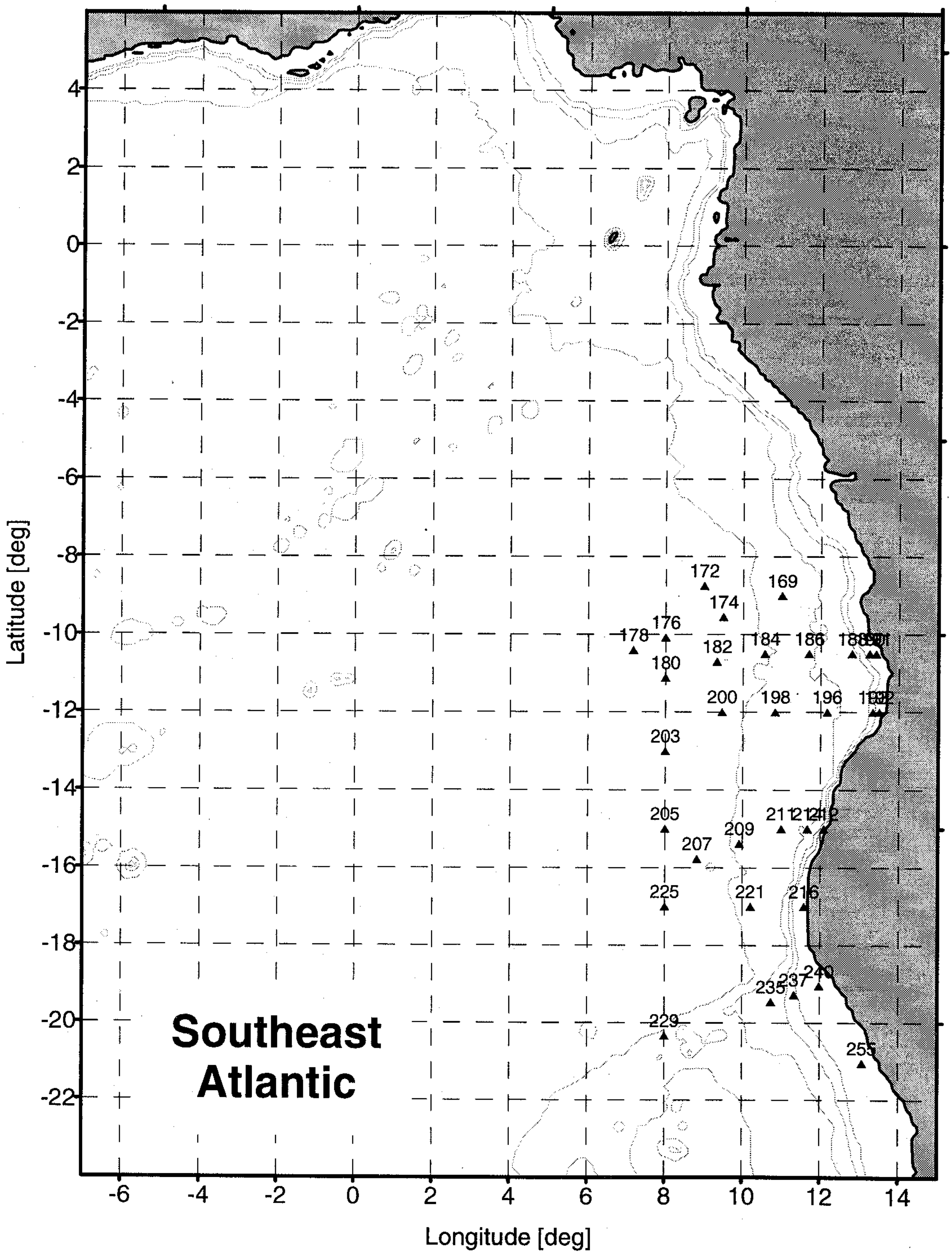

Figure 2.4: Map of phytoplankton stations of the cruise POS250 (02. - 28. April 1999)

3 Survey chronology

Investigation	date
Boarding in Las Palmas	17th March
Unloading container installing and testing equipment	18th March
Calibration of the LADCP	
ESTOC station for cruise POS249	19th March
boarding of Vianda Filipe and Bomba Bazik Sangolay	20th March
start of the cruise	
encounter of the northern trades	22th March
calibration of the VMADCP	24th March
equator crossing celebration	27th March
Equatorial section CTD, VMADCP, LADCP, Multinet and neuston sampling	28th March - 5th April
ITCZ latitudes but weak signal, clouds only	28th March
equator crossing	29th March
EUC in VMADCP	30th March
encounter of the southern trades	1th April
fresh water plume (Zaire river?)	3th April
three stations south of the section worked	
Eastern	4th April
calm weather in a fresh water plume	
sampler rosette malfunction fixed	
safety exercise	5th April
port of Luanda	6th April
reception in the German embassy	
boarding of Domingos da Silva Neto	
Aina Iita, Anja Kreiner, Victor Hashoongo	

Investigation	date
survey of Angola Dome	6th - 14th April
CTD, VMADCP, LADCP, water samples,	
neuston, Multinet, phytoplankton	
working section abf_100	6th - 10th April
Angola Dome becomes visible in CTD data,	9th April
station grid adopted	
heavy rain over the Angolan coast	
working section abf_150	10th - 12th April
exceptional lightning over Angolan shore	12th April
giant river plume with drifting plants	
working section abf_250	13th - 14th April
salinity fronts up to > 2PSU	13th April
stations on the 8°E section	14th - 16th April
survey of the Angola Benguela front	16th - 21th April
CTD, VMADCP, LADCP, water samples,	
neuston, Multinet, phytoplankton	
working section abf_400	16th - 18th April
celebration of half survey time	17th April
stations on the along shore section	18th April
must be skipped due to whitecaps	
working section abf_600	19th - 21th April
stations on the 8°E section	21th - 22th April
working sections south of the	21th - 26th April
Angola Benguela front	
CTD, VMADCP, LADCP, water samples,	
neuston, Multinet, phytoplankton	
working cross shore section abf_700	22th - 24th April
working ichthyoplankton section, no CTD	25th -2 6th April
working CTD section abf_900, CTD only	26th April
port of Walvis Bay	27th April
loading container, social event	28th April
press conference, disembarking	29th April

4 Personnel

Participants	Function	Institute	Department
Dr. Martin Schmidt	chief scientist	IOW[1]	Phys. Oceanogr.
Dr. H.-Christian John	scientist	FIS[4]	Marine Biology
Dr. Thomas Schmidt	watch leader	IOW[1]	Phys. Oceanogr.
Dr. Volker Mohrholz	watch leader	IOW[1]	Phys. Oceanogr.
Stefan Weinreben	technical staff	IOW[1]	Phys. Oceanogr.
Henry Disterheft	technical staff	IOW[1]	Marine Chemistry
Aina Iita	trainee	NatMIRC[3]	Phys. Oceanogr.
Vianda Filipe	trainee	IIP[2]	Phys. Oceanogr.
Sangolay Bomba-Bazik	trainee	IIP[2]	Marine Chemistry
Anja Kreiner	trainee	NatMIRC[3]	Marine Biology
Victor Hashoongo	trainee	NatMIRC[3]	Marine Biology
Dr. Domingos da Silva Neto	trainee	IIP[2]	Marine Biology

Crew of R/V 'Poseidon' (18), Master R. Priebe

Service and support of the crew is greatly acknowledged here.

[1] IOW	Baltic Sea Research Institute Warnemünde Seestraße 15, D18119 Rostock-Warnemünde, Germany
[2] IIP	Fisheries Research Institute PO Box 2601, Luanda, Angola
[3] NatMIRC	National Marine Information and Research Center PO Box 912, Swakopmund, Namibia
[4] FIS	Taxonomische Arbeitsgruppe Forschungsinstitut Senckenberg, Hamburg

5 Equipment

5.1 CTD

The CTD-system "SBE 911plus" (SEABIRD-ELECTRONICS, USA) was used to measure the parameters:

- pressure, temperature, conductivity, bottom distance
- fluorescence (683 nm, "chlorophyll-a“), backscattering (520 nm, "turbi dity“) by a Dr. Haardt BackScat II-Fluorometer.
- oxygen with IOW - oxygen sensor

Additionally the CTD-probe was equipped, with a Rosette water sampler with 11 free flow bottles of 5 l volume. A CTD-system configuration sheet is included in appendix A.1.

5.2 Vessel mounted Acoustic Doppler Current Profiler (VMADCP)

A 75 kHz narrow band Vessel Mounted Acoustic Doppler Current Profiler (VMADCP), manufactured by RDInstruments, was installed in the sea chest of the ships hull. The data output of the ADCP was merged on-line with the corresponding navigation data (see subsection 5.5.1, 5.5.2 and 5.5.3) and stored on the hard disc of a PC using the storage system DAS.

A list of configuration parameters used for the Vessel Mounted Acoustic Doppler Current Profiler (VMADCP) is included in appendix A.3.

5.3 Lowered Acoustic Doppler Current Profiler (LADCP)

During the cruise an LADCP was used to obtain full depth velocity profiles of currents at each CTD-station. An ADCP WH-300 was mounted at the CTD-probe. The ADCP was equipped with an external battery case for elimination of magnetic disturbations by battery packs. The ADCP was used in upward looking mode to get current data as close as possible to the surface.

The maximum range of the LADCP current measurements amounts 110 m with using 4 m depth cell size and 120 m for 8 m depth cell size. The standard deviation are $3\,\mathrm{cm\,s^{-1}}$ respectively $2\,\mathrm{cm\,s^{-1}}$. The Workhorse ADCP produce two profiles, one for velocity and one for echo intensity. Additionally the temperature inside the ADCP case is recorded.

5.4 Thermosalinograph

The thermosalinograph is installed in the ship bow. A measurement chamber serves as filter and bubble trap and contains an OTS probe equipped with temperature and a conductivity sensor. The PT 200 temperature sensor has a resolution of 0.0006°C, the 7 electrode conductivity sensor resolves $0.001\,\mathrm{mS\,cm^{-1}}$. For salinity determination a second temperature sensor is attached to the conductivity cell. The calibration of the thermosalinograph is described in section 7.5.

5.5 Navigation

5.5.1 GPS-System

The ship is equiped with ASHTEC GG24 receiver which involves American (GPS) and Russian (GLONAS) navigational satellites. So up to 24 satellites could be available, the Russian ones without artificial noise. The time provided by the GPS system was included in the data distribution system.

5.5.2 Attitude Determination Unit

An ASHTECH Attitude Determination Unit ADU2 antenna array was installed on ships RADAR mast. It provides additional information on ships heading without the typical gyrocompass deviations.

5.5.3 Gyrocompass

The Gyrocompass signal was included in the VMADCP record and in the permanent datalog as well. The gyrocompass deviation is shortly described in section 7.4

5.5.4 Echo Sounder

The research vessel was equipped with an deep sea echo sounder "ELAC LAZ 4700" (Honeywell ELAC Nautik GmBH Kiel) used for depth measurements within the permanent data logging system.

5.6 Meteorological data and weather station

The following quantities have been measured by the ship wheather station

- apparent wind speed and direction
- air pressure
- wet and dry temperature

- global solar radiation

For wind speed and direction a pair of anemometers were installed symmetrically at both sides of the RADAR antenna mast in 19 m height. Two psychrometers were at both sides of the bridge in 11 m height measuring wet and dry temperature. Air pressure was measured by a barometer up on the foremast. The radiometer was installed in ships bowsection. However, the starbord psychrometer and the port anemometer were giving wrong data.

5.7 Permanent data loggin

The data logging system PC-LOG, Vers. 5.4, Rathlev (1996), was used to combine meteorological, navigational and thermosalinograph data to a unique dataset. The data are averaged over one minute and are stored in daily log files on the hard disk of a PC.

The data are distributed as a data telegram to the REISE software (Wlost, 1999) and are provided to build the header of the CTD data files.

5.8 Equipment for intercomparison measurements

5.8.1 Salinometer

A salinometer "AUTOSAL Model-8400A" (GUILDLINE INSTRUMENTS LTD., Canada, Serial No. 58 648) was used as reference for conductivity measured by the CTD.

5.8.2 Reversing thermometer

Reversing thermometers (THERMOMETERWERK GERABERG, GDR), i.e. sets of four pieces - manufactured for temperature ranges of -2 to 30°C, protected, numbers 1, 2, 3 and 5, served as check for the CTD-temperature sensor.

5.8.3 Oxygen determination

Titration was performed with a DMS Titrino 702, METHROM AG CH-9101 Herisau (Switzerland), whereby the endpoint of the titration is determined potentiometrically. (See Grasshoff et al. (1983), WOCE Hydrographic Operations and Methods (1990)).

5.9 Zooplankton sampling

5.9.1 Multiple-opening-closing-net (Multinet)

For studies on the vertical distribution of zooplanktonic organisms, samples were taken with a Hydro-Bios multiple-opening-closing-net (MCN or Multinet). Obtaining several subsamples instead of an integrated tow has besides information on vertical distribution the advantage of minimized zooplankton abrasion. The underwater unit of the sampler consists of a stainless steel frame with canvas part to which five net bags are attached by means of zip fasteners. The net changings are actuated by push botton control from the deck command unit via a single- or multiconductor cable. The net bags are opened and closed by means of an arrangement of levers. The motor for actuating the net bags is powered by internal batteries. The mesh size of the nets was 300 μm. A CTD (ME) mounted at the MCN recorded pressure, temperature and salinity. The filtered water volume was determined by calibrated flowmeters attached inside of each net.

5.9.2 Neuston sampler

To sample the zooplankton community in the surface layer, between the water's surface and a few centimeters below, a David Neuston sampler was used. It consists of two nets with 30 cm wide mouths suspended from a katamaran swimmer body. It has asymmetric bridles which cause the nets to kite away from the ship's bow wave and consequently to fish in undisturbed water. The upper net sampled the surface layer (from 0 to 8 cm) and the lower net the layer from 10 to 25 cm. Nets with a mesh size of 300 μm were used. To determine the water filtered a calibrated flowmeter was attached at the lower net.

5.10 Nutrient measurements

The samples were gathered by Hydro-Bios free flow samplers attached to the CTD as described in section 5.1.

The inorganic nutrient ammonia, nitrite, nitrate , phosphate and silicate were measured using manual standard colorimetric methods which are described in detail by GRASSHOFF et al. (1983) and ROHDE and NEHRING (1979). The absorption was measured with a photometer Shimadzu UV1201V using 5 cm or 1 cm cuvette length depending on the intensity of the reaction colour.

6 Measurement strategy

The surveyed area is covered by a net of hydrographic sections, sailed as CTD sections. At the CTD sections a number of CTD stations has been defined. Each station has a station name and a consecutive station number. Near the coast the station to station distance is about 10 n.m. and is increased to 30 n.m. or 60 n.m. in the open ocean. The stations are starting or in some cases final positions of Neuston sampler and Multinet deployments.

This system of stations and sections is a compromise between the necessity of high resolution perpendicularly to the coast (to account for the coastal trapped baroclinic processes) and the available ship time.

6.1 CTD stations

During the CTD stations the ship was drifting with the bow kept in the wind. The CTD was lowerd to a maximum depth of about 1300 m or to 10 m above the bottom at shallower stations. The CTD was lowered with approximately $0.5\,\mathrm{m\,s^{-1}}$ above the thermocline (200 m) and $1\,\mathrm{m\,s^{-1}}$ below taking 24 scans per second.

6.2 LADCP measurements

The LADCP attached to the CTD probe was used at every CTD station. Before deployment, the deck unit PC-clock of the ADCP was synchronized with the CTD deck unit PC clock. This allows for later correction of the sound velocity profile with CTD temperature and salinity data. GPS position and time, when the CTD passed the 30 dBar horizon during both down and upcast, were kept as fixpoints for the calculation of the ADCP path. The LADCP configuration is given in table A.4. The selected parameters results in a mean ensemble time of 1.8 s.

6.3 VMADCP measurements

The vessel mounted ADCP was used during the whole cruise in the water tracked mode. Only the way between section abf_150 and transect abf_250 off the Angolan coast bottom tracking was possible. A list of configuration parameters used for the Vessel Mounted Acoustic Doppler Current Profiler (VMADCP) is included in appendix A.3.

6.4 Navigational and meteorological data sampling

Navigational and meteorological data as well as the data of the Thermosalinograph were online displayed (one value per second), but continously recorded with one value per minute only (daily datafiles during the survey). Wind data are online corrected for ships heading and speed.

During daytime every six hours cloudiness was observed. Later, the cloudiness was observed at every station. For cloudines the cloud index (0 to 8) as well as the cloud type was recorded. The observations followed the "Wolkentafel für Wetterbeobachter auf See" (1967).

6.5 Phytoplankton sampling

For the determination of Chlorophyll concentration at selected stations three depths are chosen for phytoplankton sampling guided by the fluorescence signal of the fluorometer of the CTD probe, one near the fluorescence maximum and one well above and below the maximum. From each depth level two 0.5 to 1l water samples are taken with CTD rosette sampler. They are filtered as soon as possible in subdued light, on Whatman G/F filters p glass microfibre filters (25 mm diameter) with a pressure not exceeding 200 Pa. The moist filter is folded with a tweezer into an Eppendorf tube. The tubes are stored frozen in the dark at −20°C to be further investigated onshore by HPLC and fluorometric methods.

For phytoplankton identification of delicate organisms as flagellates 250 ml samples from the same depth are mixed with 1 ml of acetic Lugol solution immediately after sampling. The samples are stored dark under room temperature. For studies of coccolithophorids, diatoms and thecate dinoflagellates 200 ml samples are mixed with 4 ml of neutralized Formaldehyde solution. These samples are stored dark at room temperature too.

6.6 Neuston sampling

At each station the Neuston sampler was towed alongside the ship for between ten and sixty minutes. The towing time was adjusted according to the clogging of the nets by jellyfish or phytoplankton. The ship speed was about 2.5 knots. At night, spotlights of the vessel shining on the water surface in front of the net have been switched off as far as possible to get undisturbed and representative night samples. When the nets were retrieved they were hosed down from outside. The cod-end buckets were retrieved and the samples preserved with 4% formol as soon as possible. Environmental data such as wave conditions, wind speed and direction, surface temperature and salinity were recorded.

6.7 Multiple-opening-closing net (Multinet)

The Multinet was lowered with a speed of $0.5\,\mathrm{m\,s^{-1}}$ at a ship speed of approximately 2.5 knots to a maximum depth of 200 m (where the bottom depth was less than 200 m, the sampling depth was adjusted accordingly) and the first net was opened. Depending on ship speed and currents the net was pulled up with between $0.2\,\mathrm{m\,s^{-1}}$ and $0.6\,\mathrm{m\,s^{-1}}$. Nets 2 to 5 were opened at 150 m, 100 m, 50 m and 25 m respectively. The exact time each individual net was open was recorded. Retrieving the nets they were hosed down from the outside. The cod-end buckets were retrieved and the samples preserved with 4% formol.

6.8 Nutrients and oxygen

During the cruise 1125 nutrient samples and 1147 oxygen samples were collected. Samples were taken from the surface down to 1200 m depth. Normally, the resolution was 10 m between surface and 100 m depth, below that 200 m steps were selected. But in many cases the sampled depth was adjusted to the stratification found from the CTD measurements, The samples were gathered by Hydro-Bios free flow samplers attached to the CTD as described in section 5.1.

6.8.1 Oxygen determination

Bottle oxygen samples were taken in calibrated glass bottles for the determination of dissolved oxygen immediately after the rosette sampler has been recovered before all other subsamplings. Strong attention was paid to this step and the subsequent fixation because this step is one of the main sources of error in the oxygen determination. The analysis of the fixed oxygen samples was carried out in the lab within 2 hours after the CTD cast. Titration was performed with a DMS Titrino 702, METHROM AG CH-9101 Herisau (Switzerland), whereby the endpoint of the titration is determined potentiometrically.

6.8.2 Nutrients

The subsampling for nutrients was perforemd immediately after oxygen sampling using 500 ml plastic bottles which were rinsed with seawater before and are used for these investigations exclusively. Bevor filling the bottles they were washed with the respective sample vigorously. Each water sample taken by the bottles of the rosette sampler was identified in a unique manner by combing the cruise number and the number of bottles closed so far since the beginning of the cruise.

The inorganic nutrients ammonia, nitrite, nitrate, phosphate and silicate were determined with colorimetric standard methods (see Section 5.10). In the Angolan waters the ammonia content was nearly constant and was therefore determined only occasionally. The analysis were performed immediately after sampling and were finalized latest after two hours, with exception of ammonia due to the longer reaction times of 6 hours.

6.9 Other measurements in relation to the cruise

Satellite images of sea surface temperature (SST) with 50 km resolution loaded from the NOAA server (http://las.saa.noaa.gov/las-bin/climate_server) have been used as guideline for the final station grid. High resolution SST images has been provided by Chris Smith, John Mantel and Chris Duncombe Rae, Marine and Coastal Management, South Africa.

7 Data quality assurance

Data Quality Assurance (QA) consists of operation manuals and procedures of the measuring units and devices, handling procedures in ship and measuring operation, intercomparison measurements and data validation procedures.

7.1 CTD data

At CTD stations the research vessel was operating with the bow in the wind keeping the CTD probe in undisturbed water. However, the ship induced stirring should be of minor importance compared to the general homogenisation by wind induced stirring and breaking waves. A CTD cast started below the sea surface with the pressure sensor usually at about 2 m depth. At heavy sea conditions this was not possible and CTD casts started at 5 to 7 m depth to protect bottles to be closed by waves at the surface and to prevent a contamination of the CTD pumping system with air bubbles.

After deployment the CTD was lowered to 10 m depth. It stayed there for about 3 minutes to equilibrate sensors heated by solar radiation and to remove air bubbles from the pumping system.

7.1.1 Intercomparison measurements

The CTD salinity, temperature and pressure sensor have been calibrated by the manufacturer or by the calibration lab of the IOW. However, during the survey stability of sensors has been monitored approximately once a day by help of intercomparison measurements at an overall number of 16 stations. A vertically homogenious layer was selected and the CTD probe was kept in this depth for about 10 minutes. After that a 2 minute cast was started and two bottles were closed. 6 water samples for salinity were taken and the reversing thermometers have been released.

After that a short downcast series through the homeogeneous layer was carried out and a bottle for oxygen samples was closed. This procedure was not necessary any more after station 200 where a new oxygen sensor was attached which is included in the CTD pumping system. This configuration has a stable sensor sensitivity independent off the CTD probe movement.

At the equatorial transect and off Luanda the statification was to high for intercalibration measurements.

Salinity

Conductivity (then salinity) of the samples was determined by means of a salinometer "AUTOSAL Model 8400A" (accuracy of ± 0.001). It was located in a lab with nearly constant temperature. The salinometer was calibrated by means of standard seawater (Ocean Scientific International) Batch P134 produced 4.6.1998. A statistically significant deviation

(0.0024 $\mathrm{mS\,cm^{-1}}$ with stdandard deviation of $\pm 0.0039\mathrm{mS\,cm^{-1}}$) between conductivity of the water samples and the CTD measurements (sensor 1150, last calibration 2.1.1999) was found. With respect to conductivity 2 of the intercomparison measurements have been disregarded (as outlayers).

Temperature

Bias and stability of the temperature sensor (accuracy of ± 0.001 K) has been checked only by help of a bundle of four reversing thermometers, (Thermometerwerk Geraberg, GDR), manufactured for temperature ranges of -2 to 30°C, protected, numers 1, 2, 3 and 5, with graduation of ± 0.1 K. The statistically significant temperature deviation (mean deviation -0.0065 K with stddev. of ± 0.0077 K) between reversing thermometers and CTD data (sensor 1592, last calibration 1.2.1999) was not corrected, because it is primarily caused by the lesser readout accuracy of the reversing thermometers.

Oxygen

The sensitivity (slope) of the oxygen sensor, (O023, last calibration 5.2.1999) has been determined by help of water samples, gathered while lowering the probe. Oxygen content of the samples was determined by help of a titration set (Winkler method, accuracy of $\pm 0.02\,\mathrm{ml\,l^{-1}}$). The Weiss salinity correction for the oxygen saturation partial pressure is part of the data conversion run with SeaSoft. Influence of temperature on the oxygen saturation pressure was corrected by a sensor internal thermistor network.

The sensor of this type was used until station 200. Since station 173 the signal was overlaid with spikes. As an attempt to solve the problem the sensor membran was renewed before stations 175 and 195. After station 200 it failed due to a leakage in it's temperature compensation unit.

At station 176 a new developed sensor was mounted. The sensor provides an output signal that is proportional to the current of the oxygen-electrode and a signal of the temperature. This temperature sensor has the same relaxation time as the oxygen-electrode. The sensor is integrated in the pumping system of the CTD and the calibration casts can be carried out at a fixed depth. However, the temperature compensation procedure is not finalized and the data will be postprocessed.

To improve the calibration statistics and to estimate the sensor drift at the equatorial transect with only a few calibration measurements available, all oxygen samples have been included in the calibration procedure. Only measurements at depth with strong gradients have been discarded.

No indication was found for a significant dependence of the sensor sensitivity neither on pressure nor on conductivity or oxygen content (titration values). A slight temperature dependence was found especially in tropical water with a surface temperature of 29 to 31°C. Highest deviation occured at the surface and the O_2-minimum in 300 to 400 m depth, where the CTD oxygen values are generally lower than titration values. This indicates either an overtitration or a sensor nonliniarity at low concentrations.

On the equatorial transect below the surface sometimes oversaturation was met again with lower CTD values at the surface. The influence of strong gradients has been excluded.

Finally, at stations with strong gradients the low response time > 5 s became visible indicating the need for both bottle sampling and continuous electronic mesurements.

Pressure

An online precorrection of CTD pressure measurements (with Digiquartz-pressure sensor (SN 51392), calibrated 1993) on air pressure was done by a default value of 1006 hPa. Pressure sensor values of air pressure (on deck registration) have been compared to air pressure values of the ships weather station.

At some stations the pressure sensor calibration has been carried out prior the CTD cast, at other stations after the CTD cast. Both groups of stations show a significantly different offset which can be traced back to the pressure sensor hysteresis. This behaviour indicates a possible pressure offset error of about ± 50 hPa. However, since only downcasts have been used, this error should be a constant and does not influence the calculated geostrophic currents.

Fluorescence and backscattering

An intercomparison measurement for the fluorometer data has not been done. The Dr. Haardt BackScat II-Fluorometer (Dr. Haardt, Germany, Model 1303 MP/Chla/Phy/2R/MO, SN 7091) is calibrated by the manufactor (valid from 27.04.1998). Backcsatter (turbidity) is given in reflectance units (percent). 100% reflectance is defined by a white reflectance standard (Lambertian) and 1%, 0.1% and 0.01% scales are realized by calibrated optical attenuators. Attempts will be made to attain a postcorrection by correlating the fluorescence channel and the chlorophyll from HPLC-absorption spectra of filtered water samples.

7.2 ADCP data

For the data quality assurance of ADCP-data see section 8.3.

7.3 Multinet and neuston sampler

To good quality of the samples certain procedures had be attended to. The samples have been preserved in 4% formol as soon as possible. To ensure minimum loss of sample quality the samples taken at the lower depth are preserved first as they undergo the most intense temperature and light intensity changes when brought to the surface.

As far as time allowed a first sample analysis was done under the microscope. If possible, fish larvae were identified to species level and counted, while for other zooplankton only the order or the subclass was recorded.

7.4 Navigational and meteorological data

Navigation

The GPS based navigation permitted sailing at ADCP transects and to predefined CTD station locations with sufficient accuracy of about between 30 m and 100 m. Generally, distances between waypoints have been calculated based on spherical co-ordinates.

In many cases, GPS was not available and wrong data were in the log files. This is of minor importance for the CTD header files but may be significant for the LADCP position determination.

The gyro-compass error F is given by

$$\sin F = -\frac{v \cos\theta}{902.46 \cos\varphi}, \tag{7.1}$$

where v is the ships velocity in earth co-ordinates, θ the ships gyro heading and φ the geographic latitude. In the area of investigation F is smaller than $\pm 0.5°$.

During CTD operation the ship was drifting. During CTD casts of about 1h drifts from 1 to 2 n.m. are possible.

Echo sounding

Calibration of the echo sounder unit has not been done. At the CTD stations the echo sounder signal disappeard in many cases from the permanent data log and had to be reintroduced in the CTD header files by hand.

Meteorological instruments

The meteorological instruments at R/V "Poseidon" belong to the Institute für Meereskunde, Kiel. A calibration is not documented. Generally, a lot of instrument failures occured.

- The starboard psychrometer gave wrong data.
- The portside psychrometer lost water and had to be repaired.
- The portside anemometer was fixed by corrosion in the beginning of the cruise. It was repaired by the ships crew but failed again later showing zero wind direction.
- The starboard anemometer showed reasonable results in the beginning of the cruise but showed a wrong wind direction, possibly by a cable failure, later.

Thus the most accurate wind observation came from the ship mate's eyes and experience. The radiometer was not calibrated.

Permanent data logging

The permanent data logging was disturbed if the GPS data were not available. In that case wrong position and time data went into the logs. Switching off the data logging system to clean the thermosalinograph conductivity cell yields a wrong date in the data logging system causing a data loss of about two days after 16th April. Later, the date error occured again because of a wrong GPS time at midnight.

The data logging of the REISE software was of little help since the sensor channels cannot be selected by the user. This results in the registration of data from the damaged psychrometer and anemometer. Additionally, the radiometer data could not be included in the data telegram.

7.5 Thermosalinograph

The thermosalinograph unit was precalibrated from former cruises. As a result of inter-comparison with a CTD T90 on survey POS247 a difference $T_{TS} - T_{T90} = 0.025°\mathrm{C}$ and $S_{TS} - S_{T90} = 0.1$ has been reported. Details on this procedure are unknown. To calibrate the salinity-measurements of the Thermosalinograph, waterbottles were filled simultaneously. 6 Bottles each time were determined by means of the salinometer Autosal.

Additionally, on each station the salinity and the temperature have been compared to the values of the CTD. For this check stations with a well mixed surface layer have been selected and thermosalinograph data and the CTD data have been tested for a drift with time. Figures 7.1 and 7.2 show the difference between the thermosalinograph data and SeaBird CTD data. For temperature the statistical analysis gives

$$
\begin{aligned}
T_{TS} - T_{CTD} &= -0.0229018°\mathrm{C} + 0.000435136\,\mathrm{K}\,d^{-1}t \\
\text{time range} &: \text{day 87 to day 116} \\
N &= 84 \\
r^2 &= 0.096 \\
\sigma &= 0.01,
\end{aligned}
$$

where T_{TS} and T_{CTD} denote thermosalinograph temperature and SeaBird CTD temperature. t is the time since 1th January 00:00, N is the number of points, r^2 describes the statistical significance of the linear trend. So, the slight trend is of no statistical significance and a constant correction of $\Delta T_{TS} = -0.021\,\mathrm{K}$ is used. σ is the residual error of regression.

Salinity requires a more detailed correction, since a large drift due to sensor pollution was met. After sensor cleaning the salinity calibration changed suddenly and a piecewise data correction is necessary, see Figure 7.2. In the beginning of the cruise S_{TS}, and CTD salinity shows a slight decreasing trend. This trend stopped at 10th April 6:00 UTC followed by a

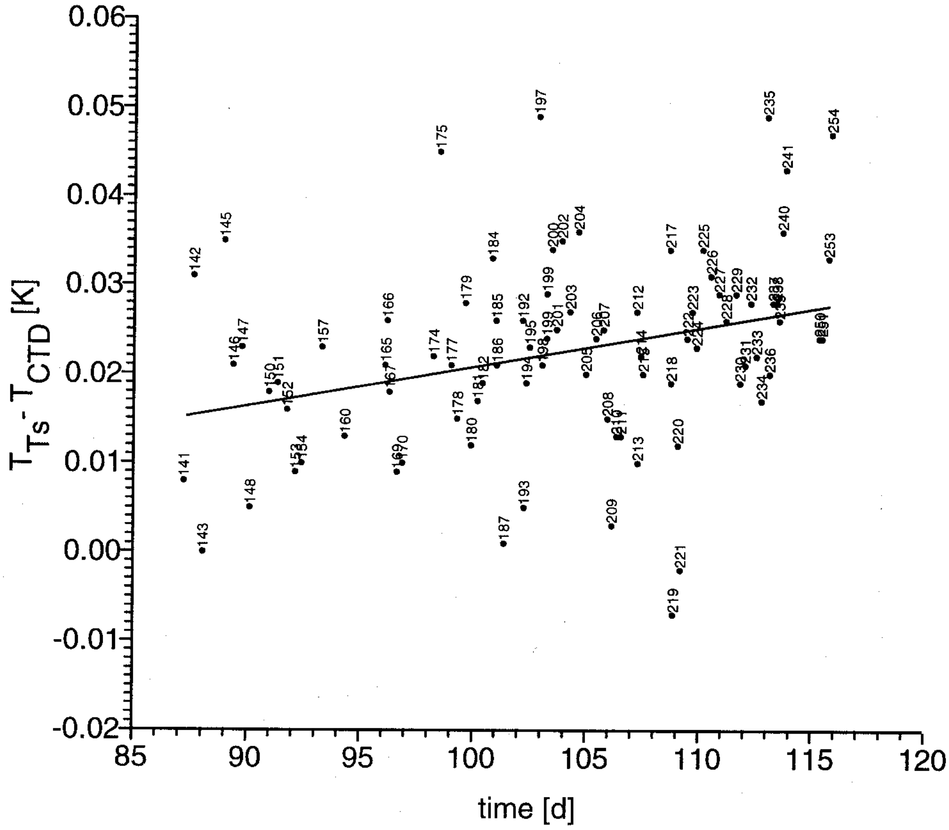

Figure 7.1: Calibration of the therosalinograph - temperature

steep decrease. There is no obvious reason for this behaviour but the ship was in a river plume during this time. 13th April the sensor drift changed again. At 15th April the conductivity cell was cleaned resulting in a different sensor charcteristics. The piecewise corrections can be summarized as

$$S_{TS} - S_{CTD} \quad = \quad a - bt \tag{7.2}$$

where S_{TS} and S_{CTD} denote thermosalinograph salinity and SeaBird CTD salinity. t is the time (in days) since 29th March 0:00 UTC. The coefficients a and b are:

time range	[day]	a	b $[d^{-1}]$	N	r^2
87.0	- 99.0549	0.206	- 0.0016447	31	0.57
99.0549	- 102.7326	3.355	- 0.03329	13	0.96
102.7326	- 104.6	- 1.609	0.015056	9	0.67
104.9	- 110.5258	- 0.422	0.004433	21	0.67
110.5258	- 116	0.333	- 0.002394	20	0.46

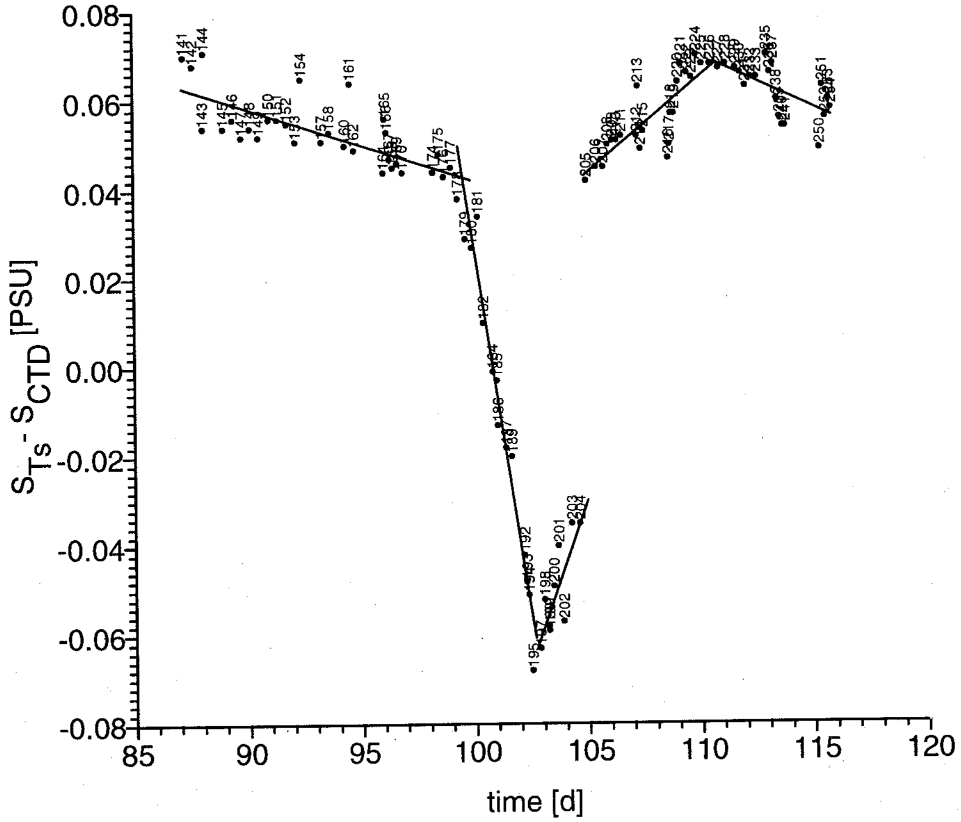

Figure 7.2: Calibration of the therosalinograph - salinity

After applying these corrections outliers have been eleminated with a median filter (MATLAB procedure *outmedi(_,9,1.5)*).

7.6 Oxygen and nutrient titration

7.6.1 Oxygen

The thiosulphate solution used for the titration is not a primary standard. Therefore, a calibration is done in regular intervals with potassium iodate.

The accuracy of the determination is at least $\pm 0.02\,\mathrm{ml\,l^{-1}}$.

7.6.2 Nutrients

The calibration of the methods used was performed in regular intervals during the cruise and compared with expierenced calibration factors (Shewart charts). The methods are used over long periods within HELCOM Monitoring Programme. Beside the above mentioned internal quality control, the methods are crosschecked twice a year since 1993 within QUASIMEME (general: good overall performance).

The accuracy of the methods is:

Ammonium	:	$\pm 0.05\,\mu\mathrm{mol\,l^{-1}}$	(in the range under discussion)
Nitrite	:	$\pm 0.02\,\mu\mathrm{mol\,l^{-1}}$	
Nitrate	:	$\pm 0.05\,\mu\mathrm{mol\,l^{-1}}$	(low concentration range)
		$\pm 0.1\,\mu\mathrm{mol\,l^{-1}}$	(high concentration range)
Phosphate	:	$\pm 0.02\,\mu\mathrm{mol\,l^{-1}}$	
Silicate	:	$\pm 0.1\,\mu\mathrm{mol\,l^{-1}}$	

7.7 Instrument malfunctions, errors

At equatorial stations 140 - 158 the bottle firing mechanism malfunctioned, resulting in double closing (not double firing) at bottle numbers 1, 4 and 8 in most cases. The subsequent firing meets than a closed bottle (2, 5, or 9). But, to make the problem more complex, the third bottle may be closed just with the second fire impulse. Thus, the water samples have been checked for doubled values of oxygen, nitrite, nitrate, phosphate and silicate in the subsequent bottles, i.e. 2, 5 and 9. This doubling ensures that the correct depth is assingned to bottles 1, 4, and 8. The second of the double fired samples should be discarded since it may be distorted by vertical gradients. The problem of too early closed bottles 3, 6/7 or 10/11 has been corrected by comparison of the oxygen bottle values with correct profiles. Starting with cast 158, compared with casts 159 and 160, the transect was worked backwards and corrections of the depth levels for bottles 3, 6/7 and 10/11 have been proposed.

In order to correct wrong heading information in the data files some .dat files have been edited with the ASCII editor Notepad. This program has the property to replace bytes with Hex code 0 by bytes with Hex code 20. Since Hex code 20 is also a valid byte in the binary .dat files, this error cannot be corrected. However, after removing resulting pressure spikes the data look reasonable. Tests with other files show that errors concern mostly the last digits since larger errors are detected and removed by the SeaBird software. This concerns the station 140 to 149.

Several instrument malfunctions yielded a substantial loss of data in the meteorological dataset. If the GPS time was not available the date of the PC-log computer could be changed. As a result the data were written to wrong files. Thus, the meteorological data from 16th and 17th of April have been lost and several gaps in the records occured. At least after 19th of April all wind sensors gave wrong values.

8 Data Postprocessing

8.1 CTD data correction as result of the data validation

The following table list the corrections which was used in the CTD data processing.

parameter	correction
conductivity	not necessary
temperature	not necessary
pressure	a precorrection value of 954 hPa
	was used in the CTD data processing
oxygen	a sensor slope correction factor 0.74
	was applied for stations 140 - 175
fluorescence	not validated
backcattering	not validated

8.2 Navigational and meteorological data, thermosalinograph

For the validation raw data logged by the XLOG system of the ship were converted into matlab files. The data were interpolated to minute intervalls and reasonable physical thresholds were used to clip outliers and remove bad data. The validated data were averaged over intervalls of 1, 10 and 60 minutes and stored in Matlab files.

8.2.1 Navigation

Ship positions collected by the VM-ADCP system were added to the XLOG meta data. All data were scanned for outliers and bad values. The detected bad data were deleted from the data base.

8.2.2 Echo sounding

A median filter has been applied to remove outliers and bad data.

8.2.3 Thermosalinograph

After applying the corrections derived in section 7.5 outliers have been eleminated with a median filter (MATLAB procedure *outmedi(_,9,1.5)*). Additionally, the surface density σ_T was computed and added to the dataset.

8.2.4 Wind speed and direction

The original log data contain only the ships heading. Therefore the ships speed was calculated from the ship positions. The real wind vector was estimated from the relative wind data and ship speed, course and heading,

$$\begin{pmatrix} u_{ship} \\ v_{ship} \end{pmatrix} = \begin{pmatrix} U_{ship}\sin(D_s) \\ U_{ship}\cos(D_s) \end{pmatrix} \tag{8.1}$$

$$\begin{pmatrix} u_{ws} \\ v_{ws} \end{pmatrix} = \begin{pmatrix} U_{swind}\sin(H_s + D_{sw} - \pi) \\ U_{swind}\cos(H_s + D_{sw} - \pi) \end{pmatrix} \tag{8.2}$$

$$\begin{pmatrix} u_{w} \\ v_{w} \end{pmatrix} = \begin{pmatrix} u_{ship} \\ v_{ship} \end{pmatrix} + \begin{pmatrix} u_{ws} \\ v_{ws} \end{pmatrix} \tag{8.3}$$

$$U_{wind} = \sqrt{u_w{}^2 + v_w{}^2} \tag{8.4}$$

$$D_{wind} = \frac{3\pi}{2} - arctan2(v_w, u_w) \tag{8.5}$$

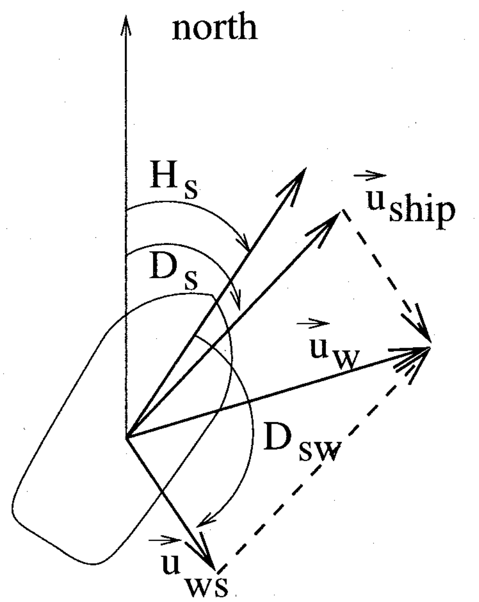

Figure 8.1: The calculation of the true wind from the wind relative to the ship, ship heading and ship course.

U_{ship} - ship speed

D_s	- ship course (GPS)
H_s	- ship heading (gyro compass)
U_{swind}	- relative wind speed
D_{sw}	- relative wind direction
U_{wind}	- true wind speed
D_{wind}	- true wind direction
u_{ship}, v_{ship}	- vector components of ship speed
u_{ws}, v_{ws}	- vector components of relative wind
u_w, v_w	- vector components of true wind

Outliers have been removed with a median filter. Due to problems with the wind sensors the wind vector is available until 23th April only.

8.2.5 Air pressure and global radiation

The MATLAB procedure *outmedi(_,7,3)* was applied to remove outliers.

8.2.6 Air temperature and humidity

The air temperature and relative air humidity was calculated from dry and wet temperatures of psycrometer. To remove outliers the MATLAB procedure *outmedi(_,9,3)* was applied.

8.2.7 Output file format

The following table lists all parameters and the residual errors of the validated meta data. The data are stored in Matlab format.

parameter	unit	residual error
time	[d]	0.000695
latitude	[deg]	0.001
longitude	[deg]	0.001
depth - echo sounder	[m]	-
ship-course	[deg]	5.0
ship-heading	[deg]	0.3
ship-speed	[$\mathrm{m\,s^{-1}}$]	0.3
wind vector east (10 m)	[$\mathrm{m\,s^{-1}}$]	1.0
wind vector north (10 m)	[$\mathrm{m\,s^{-1}}$]	1.0
air temperature (10 m)	[°C]	1.0
air moist relative (10 m)	[%]	7.0
global radiation	[deg]	-
air pressure	[dBar]	1.0
water temperature (3 m depth)	[°C]	0.011
salinity (3 m depth)		0.006
density (σ_T - 3 m depth)	[$\mathrm{kg\,m^3}$]	-

8.3 VMADCP

The validation and postprocessing of vessel mounted ADCP data was carried out with the CODAS software package written by FIRING et. al (1995).

Prior uploading into the CODAS database the data were checked for time errors. Some single point errors were found and corrected. A shift in the PC-time at the last track from Walfisbay to Las Palmas could not be corrected exactly. However, this error does not influence the data quality itself. The time shift amounts to nearly 18 days for all data. At GMT 28.05.1999 12:21:00 the PC-time was 10.05.1999 11:16:29. Therefore all data with sampling time later then 28.04.99 needs a time correction of +18.0448 decimal days.

During creation of the CODAS database 5 ensembles with a short ensemble time were excluded. As the next step the cruise track was calculated and the outlayers were eliminated. A correction of transducer temperature and salinity was not applied.

The statistical data analysis with the CODAS software gives the following values of error tresholds for the identification of bad data.

parameter	threshold
reference layer bins	5-15
w variance	600.0
w 2nd derivation	32.0
uv 2nd derivation	53.0
error velocity	50.0
amplitude	30.0

These parameters were used to flag the outlayers and bad data values in the profiles. The error of relative velocities amounts roughly 1 $\mathrm{cm\,s^{-1}}$.

The ship velocity was removed from the data using both the water tracking method and the bottom tracking method. Considering amplitude and phase of the calibration coefficients both methods give consistent results (see table).

parameter	Bottom tracking	Water tracking
amplitude	1.0058	1.0041
ampl. standard dev.	0.0045	0.0091
phase	-4.4002	-4.4033
ph. standard dev.	0.2816	0.4458

The calibration coefficients for amplitude (1.005) and phase (-4.4) added to the database. The residual heading error of 0.3 deg results in an error of 2.6 $\mathrm{cm\,s^{-1}}$ at the absolute current velocities. The absolute reference layer velocity was calculated and the navigation data were scanned for outlayers. After elimination of bad values the navigation data were smoothed.

The residual error of validated current data was estimated as 3 to 4 $cm\,s^{-1}$. Contour and vector plots of all data completed the validation.

8.4 Phytoplankton

The phytoplankton samples have be processed in the Fisheries Research Institute in Luanda. The chlorophyll concentration has been determined with HPLC. Unfortunately, no absolute calibration of the method was possible. Hence, the results are in relative units.

Additionally the abundance of typical phytoplankton groops as well as the typical cell size has been estimated. The results are summarized in Table B.4 and Table B.3

8.5 LADCP

Calibration

Prior the cruise the LADCP was calibrated at the IOW at 24.02. 1999. An residual error after the calibration of 0.3 deg was obtained. Just before the cruise started, this calibration was controlled at the port of Las Palmas. The same residual error of 0.3 deg was detected. Then the battery pack was removed from the ADCP case. Now the ADCP was recalibrated for using in upward looking mode with external battery case. This calibration procedure results in the following residual errors:

Heading error estimated after the field calibration update:	
overall error:	
Peak Double + Single Cycle Error (should be $< 5°$):	0.43°
detailed error summary:	
Single Cycle Error:	0.17°
Double Cycle Error:	0.32°
Largest Double plus Single Cycle Error:	0.49°
RMS of 3rd Order and Higher + Random Error:	0.12°
Orientation:	up
Average Pitch:	−1.52°
Pitch Standard Dev:	0.63°
Average Roll:	−0.05°
Roll Standard Dev:	0.63°
Compass field calibration procedure	
Total error before calibration:	3.6°
Total error after calibration:	0.4°

Local magnetic deviation

Local magnetic deviation was corrected by using the *heading bias* parameter of the LADCP configuration file. Data of local magnetic deviation are captured from German resp. British charts (release BSH-1991 resp. 1992). The yearly change of the magnetic deviation was taken into consideration. The applied magnetic deviation as well as the used heading bias parameter is given in table B.2.

Post processing

Postprocessing of LADCP data were carried out with MATLAB LADCP software by Martin Visbeck. First the velocity profiles were differentiated with respect to depth to eliminate the CTD-package's motion. Then a depth record was obtained by integrating the vertical velocity in time. Now the shear profiles were averaged together within depth bins. The average shear profile was then integrated vertically to obtain a baroclinic velocity profile. The barotropic correction was calculated with start and end position from GPS, wich were recorded if the CTD-probe pass the 30 dbar depth level.

Unfortunately resulting current profiles differ significantly from profiles measured with the vessel mounted ADCP. Especially the signature of the equatorial current system cannot be found in the LADCP data. This indicates data errors which can be traced back to an unsufficient vertical range of the backscattered signal. Consequently, the barotropic flow calculated from the LADCP data is not correct and the LADCP profiles cannot be used.

8.6 Data storage and distribution

The following table list the current stage of data processing and storage as well as the persons who are responsible for the particular measurements.

Data set	status	Format	responsible
CTD	validated	Seabird cnv-files (ASCII)	Volker Mohrholz
LADCP	no results	-	
VMADCP	validated	matlab binary files	Volker Mohrholz
Meteorology	validated	matlab binary files	Volker Mohrholz
Navigation	validated	matlab binary files	Volker Mohrholz
Oxygen	validated	ASCII-File	Günter Nausch
Nutrients	validated	ASCII-File	Günter Nausch
Phytoplancton	processed	ASCII-File	D. da Silva Neto
Neuston	processed	EXCEL-tables, figures	H.-C. John
Ichthyoplankton	processed	EXCEL-tables, figures	H.-C. John
Ichthyoplankton	unknown		Anja Kreiner

The raw data are available on CD-ROM for the cruise participants. A new edition with validated data is in progress.

9 Preliminary results

9.1 Hydrographic and chemical data

9.1.1 The equatorial section

The first cruise leg started in 20th March in Las Palmas. The way to Luanda was used for several calibration measurements:

- maintenance and repair of devices of the ships weather station and the ships thermosalinograph,
- VMADCP calibration,
- calibration of oxygen, nitrate, nitrite, phosphate and silicate methods

After leaving the 200 n.m. economic zone CTD stations at a distance of about 60 n.m. have been worked in combination with underway measurements of the VMADCP and the thermosalinograph. Additionally Multinet and neuston samples have been taken after the CTD stations.

This equatorial section provides a typical view on the equatorial current system which should be of great value for a more detailed discussion of the measurements in the Angola Dome area. The upper 25 m are influenced by the ship and should be discarded. A discussion of the surface flow and the flow below 400 m depth will follow elsewhere after the geostrophic analysis of the CTD data is complete.

The main current signal is confined to the upper 300 m, however the water below this level is far from beeing quiescent. The most prominent signal is the eastward Equatorial Under Current. The core is in 70 m depth, its maximum velocity is about $1\,\mathrm{m\,s^{-1}}$. It is not symmetric with respect to the equator but slightly shifted to the south. The EUC is flanked to the north and to the south by westward currents with the core located at 2°N and 2°S respectively and a vertical extension from 100 m to 200 m depth. Below about 300 m depth the flow is eastward again and there is indication for a North and South Equatorial Under Current, (NEUC, SEUC).

At 4°S another eastward flowing stream band with a maximum velocity of about $50\,\mathrm{cm\,s^{-1}}$ could be detected, which can be interpreted as South Equatorial Counter Current. There is indication for a similar pattern between $3° - 4°$N.

The SECC seems to be embedded in a general eastward flow in the upper 150 m which continues to the Angolan coast and merges with a southward coastal surface current off Angola.

Temperature and salinity reflect the equatorial current system. The EUC can be seen as a strong faning out of the isotherms and has salinity 36.4 which is about 2 PSU more than the sea surface salinity. A second salinity maximum at about 4°S seems to be related with the SECC. From about 8°E to the Angolan coast the influence of the river outflow from the large African rivers, mainly the Zaire river, decreases the surface salinity well below 33. This is more than 200 n.m. off the coast.

Remarkably, the EUC cannot be seen clearly neither in the oxygen content nor in the fluorescence. Near the equator fluorescence is confined to a thin (20 m) layer at about 60 m depth. In the river plume the fluorescent water column is immidiately below the sea surface. Correlations with nutrient concentration will be discussed later. Oxygen content reveals a minimum at 300 m depth. Near the equator the minimum concentration is confined to a thin layer which broadens towards the Angolan coast to about 300 m. Especially below the river plume the minimum concentration is near zero.

9.1.2 Surveying the Angola Dome

The Angola Dome can be detected from the horizontal temperature distribution in 20 m depth since its temperature is decreased by about 4 °K. The temperature minimum was met at 8°E and 8°S. This is about 2 degree north from the position reported by other authors. There is no temperature minimum in the SST, neither in the CTD data nor in remote sensing data. This indicates a permanent upwelling so that the turbulent heat flux between the sea surface and the 20 m level, which should be much higher than the heat exchange with the layers below, cannot equilibrate the substantially lower temperature in the center of the Dome.

The salinity in 20 m depth does not reflect the dome structure but is strongly influenced by low salinity water masses from the river plumes. The near surface currents from the VMADCP are cyclonic as it could be expected from the temperature distribution.

The horizontal temperature and salinity distribution in 200 m depth indicates the continuation of the doming of isotherms below the thermocline.

The VMADCP data show cyclonic circulation around the Angola Dome area. The northern limb of the cyclonic cell seems to be related to the equatorial current system. The quasisynoptic picture can be interpreted as the SECC bending southward at the Angolan coast forming the surface branch of the Angola current. However, below the 100 m level the flow near the coast is directed northward. There is indication for a band of northward flow streching along the Namibian and the Angolan coast from the Angola-Benguela Frontal Zone to about 8°S. Possibly, this current structure is related to the huge amount of freshwater off the Angolan coast. This hypothesis has to be checked from the analysis of the geostrophic currents.

Increasing silicate concentrations from 12°S northwards can be understood as consequence of the freshwater input from the Zaire river. These water masses are normally characterized by a higher silicate content.

9.1.3 The Angola-Benguela Frontal Zone

The Angola-Benguela Frontal Zone was met at 16°S. It separates a band of relatively cold, i.e. 15°C upwelled water off the Namibian coast south of the front from warm, i.e. 29°C, water north of the front. In the light of hydrographic data it is a temperature front, only weak meridional salinity gradient is found. However, there are strong gradients in nutrients as well as in phytoplankton and zooplankton abundances and species. The front appears to be confined to the surface layer above the thermocline at about upper 50 m, there are only slight gradients below the thermocline. The meridional extent of the frontal zone is only 120 n.m. near the coast but it fans out in the open ocean to a smooth transition area.

The currents in the frontal area have a complex structure indicating the occurence of small eddies which, however, cannot be resolved properly by the relatively large distance of the sections. There is a jet like northward flow with a velocity of about $50\,\mathrm{cm\,s^{-1}}$ toward the front. The velocity of this jet becomes smaller with increasing depth and becomes very small below 200 m. At depth above the thermocline depth, i.e., where the front in the horizontal temperature distribution is visible, the jet stops within the frontal zone and cannot be observed at the northern side of the front. However, at the northern limb of the front there is a northward flow with a velocity increasing with depth. It's maximum speed is found below the 200 m level and it is still visible below 300 m.

The general nutrient distribution patterns are closely coupled to the upwelling processes. Thus, the whole upwelling area is characterized by high phosphate and nitrate concentrations reaching maximum values at 17°S at the coastal nearest stations with 1.7 $\mu\mathrm{mol\,dm^{-3}}$ and 25 $\mu\mathrm{mol\,dm^{-3}}$ respectively. The offshore extension of these nutrient enriched water masses is around 100 n.m. whereby the concentrations are decreasing due to the uptake phytoplankton organisms. In the upwelling centre silicate concentrations of around 13 $\mu\mathrm{mol\,dm^{-3}}$ are measured. In offshore direction a rapid reduction is observed and concentrations below 1 $\mu\mathrm{mol\,dm^{-3}}$ a were found possibly indicating a silicate limitation.

North of the Angola-Benguela Frontal Zone, very low phosphate and nitrate values are observed in the surface water as expected. Remarkable are increasing silicate concentrations from 12°S northwards. This is an evidence for freshwater input from the Zaire river. These water masses are normally characterized by a higher silicate content.

In deeper water layers (135 to 165 m) below the upwelling zone again high phosphate and nitrate concentrations could be detected. These are resulting from the current regime and the enhanced degradation of sedimenting organic material.

Oxygen depleted water with less than 2 $\mathrm{ml\,l^{-1}}$ was observed normally in the depth range between 600 m and the lower rim of the thermocline. Water with oxygen concentrations below 1 $\mathrm{ml\,l^{-1}}$ was found between 500 m depth and at least 200 m depth. South of the Angola-Benguela Frontal Zone patches of water were observed at the coast containing oxygen concentration below 0.5 $\mathrm{ml\,l^{-1}}$. North of the front the upper bound of the 1 $\mathrm{ml\,l^{-1}}$ was found significantly deeper. Normally oxygen concentrations below 1 $\mathrm{ml\,l^{-1}}$ were measured only at the 400 m level. Taking into account the observed current pattern it seems to be that oxygen depleted water is advected polward along the coast from the pool of oxygen depleted water located in the area of the Angola Dome.

The oxygen distribution in the upwelling area south of the Angola-Benguela Frontal Zone suggests that oxygen consumption by remineralization of sinking particulate organic material is intensified here due to the higher productivity.

9.1.4 The 8°E section

The outmost stations of each section are aligned at 8°E to a long meridional section from 6°S to 20°S. The temperature shows an overall north-south gradient in the surface water from 30 °C off Angola and 18 °C at 20°S. Well off the coast the Angola-Benguela Front appears as an smooth transition. Below the thermocline the meridional temperature gradients are generally weak. The only large scale signal is a southward decreasing temperature of the water below the core of the AAIW. There are several dome like elevations of isotherms (and isohalines) with horizontal scales of about 100 n.m. The most prominent one is located at 16°S. The VMADCP data show an eddy like current pattern in this area. The comparison with climatological data sets will show whether theses features are transient phenomena or are found repeatedly at similar positions.

The meridional salinity gradients are maintained by the huge river plumes in the north and the Benguela upwelling zone in the south which injects water from deeper layers with a lower salinity into the Ekman surface current. There is a salinity maximum of about 36.6 at 13°S from open ocean SACW.

The core of AAIW is found at 800 m depth, the minimum salinity is 34.4 slightly decreasing southward.

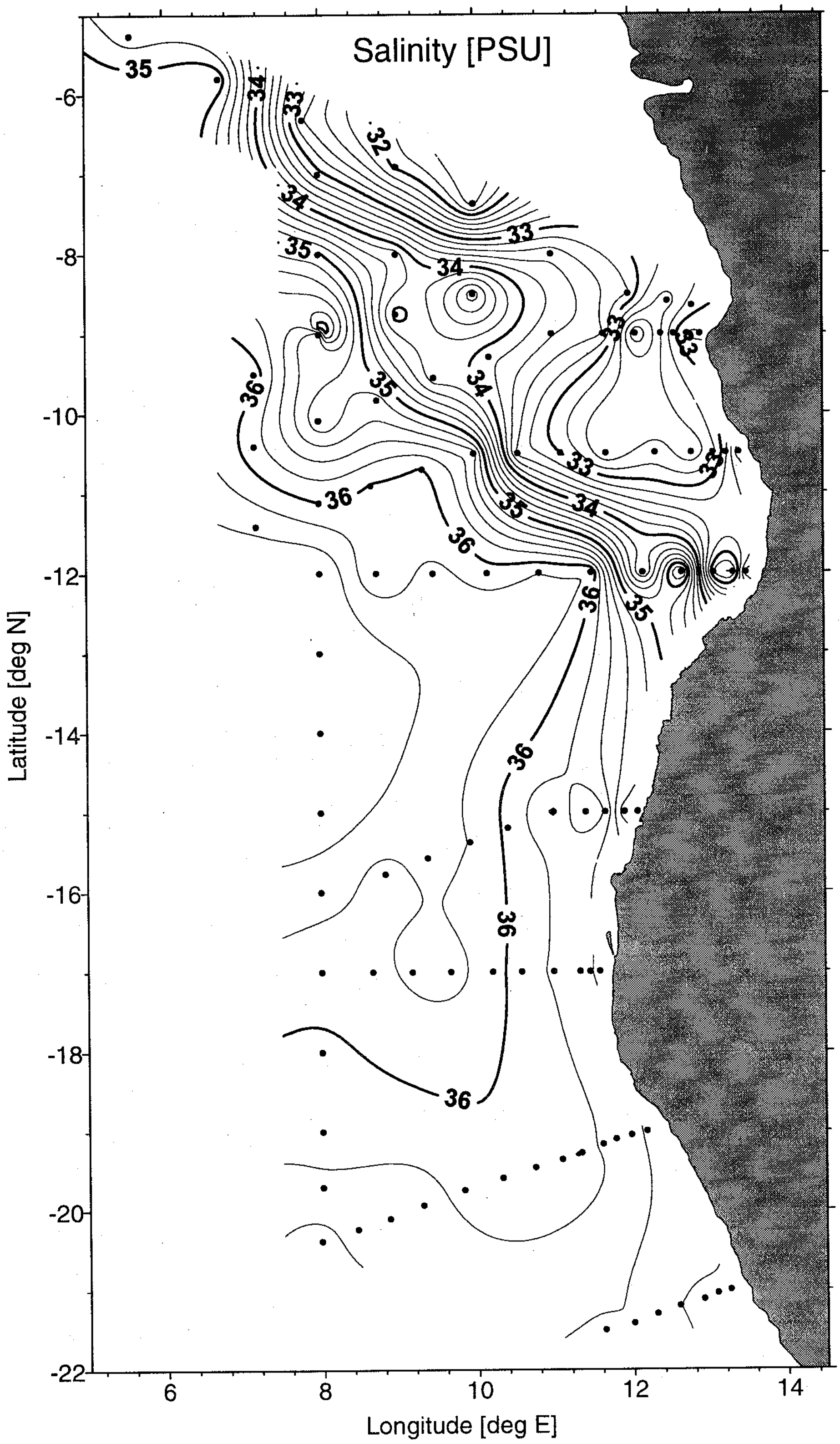

Figure 9.1: Sea surface salinity on the cruise POS250 (02. - 28. April 1999)

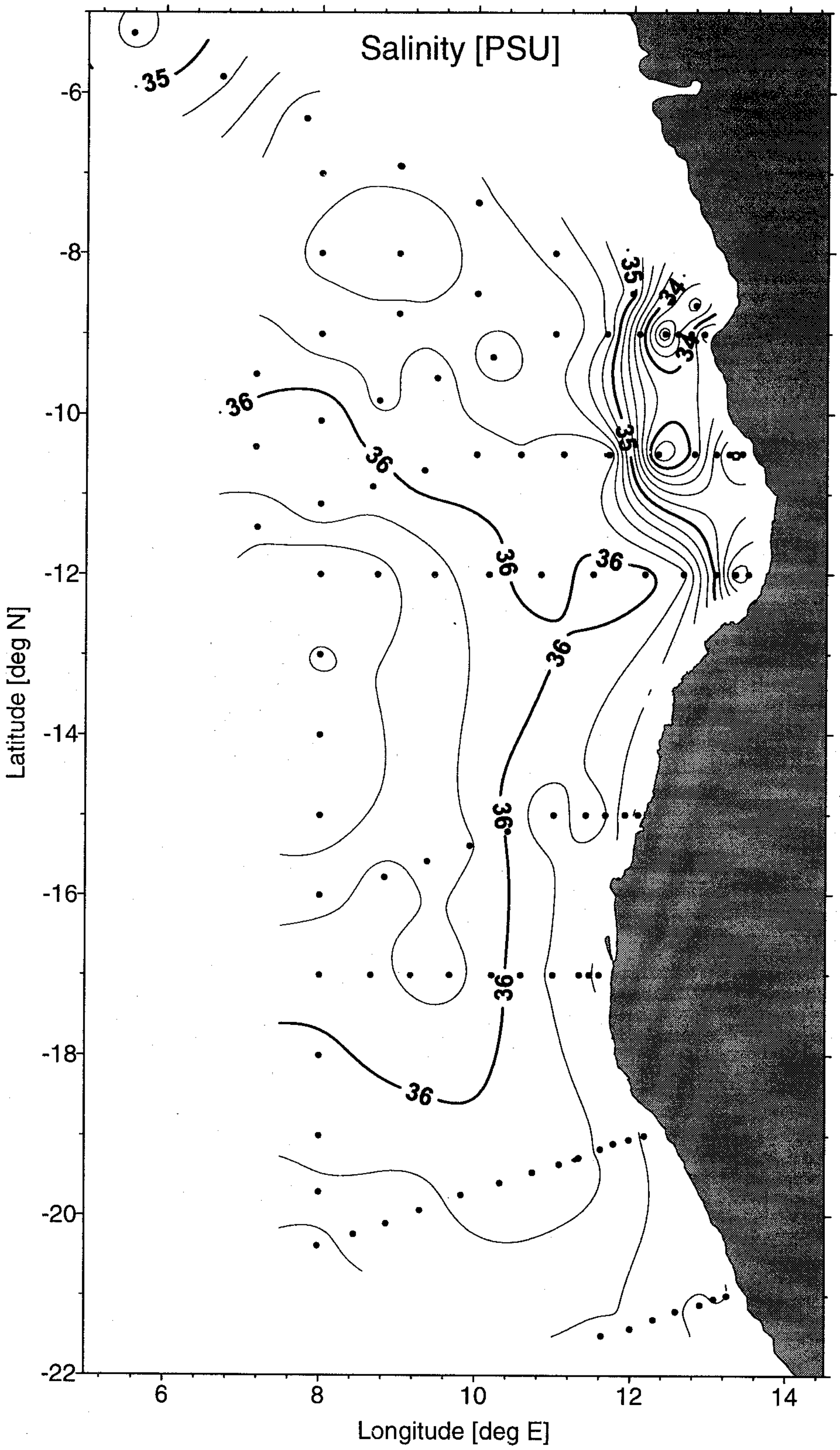

Figure 9.2: Salinity in 20 m depth on the cruise POS250 (02. - 28. April 1999)

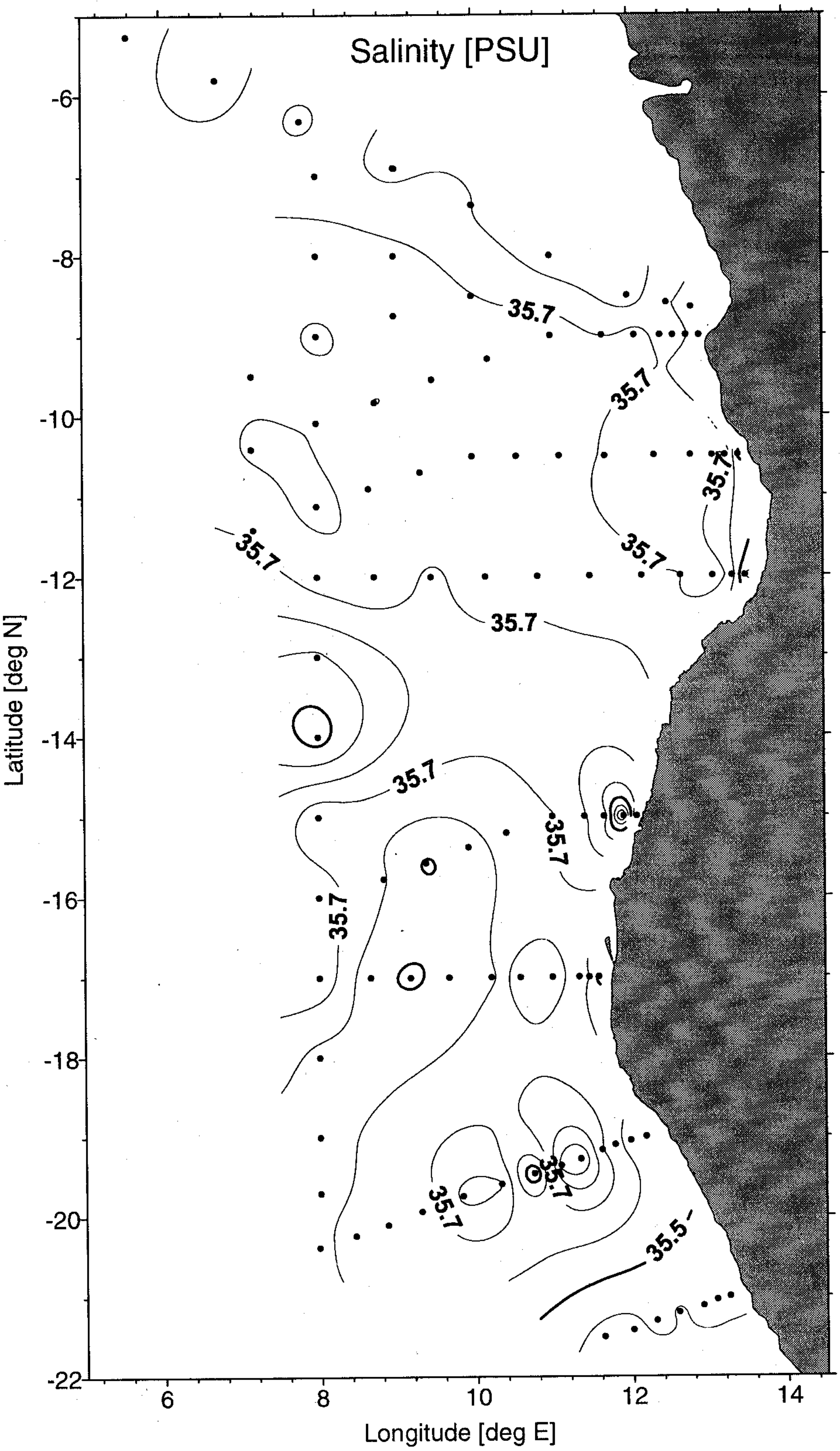

Figure 9.3: Salinity in 50 m depth on the cruise POS250 (02. - 28. April 1999)

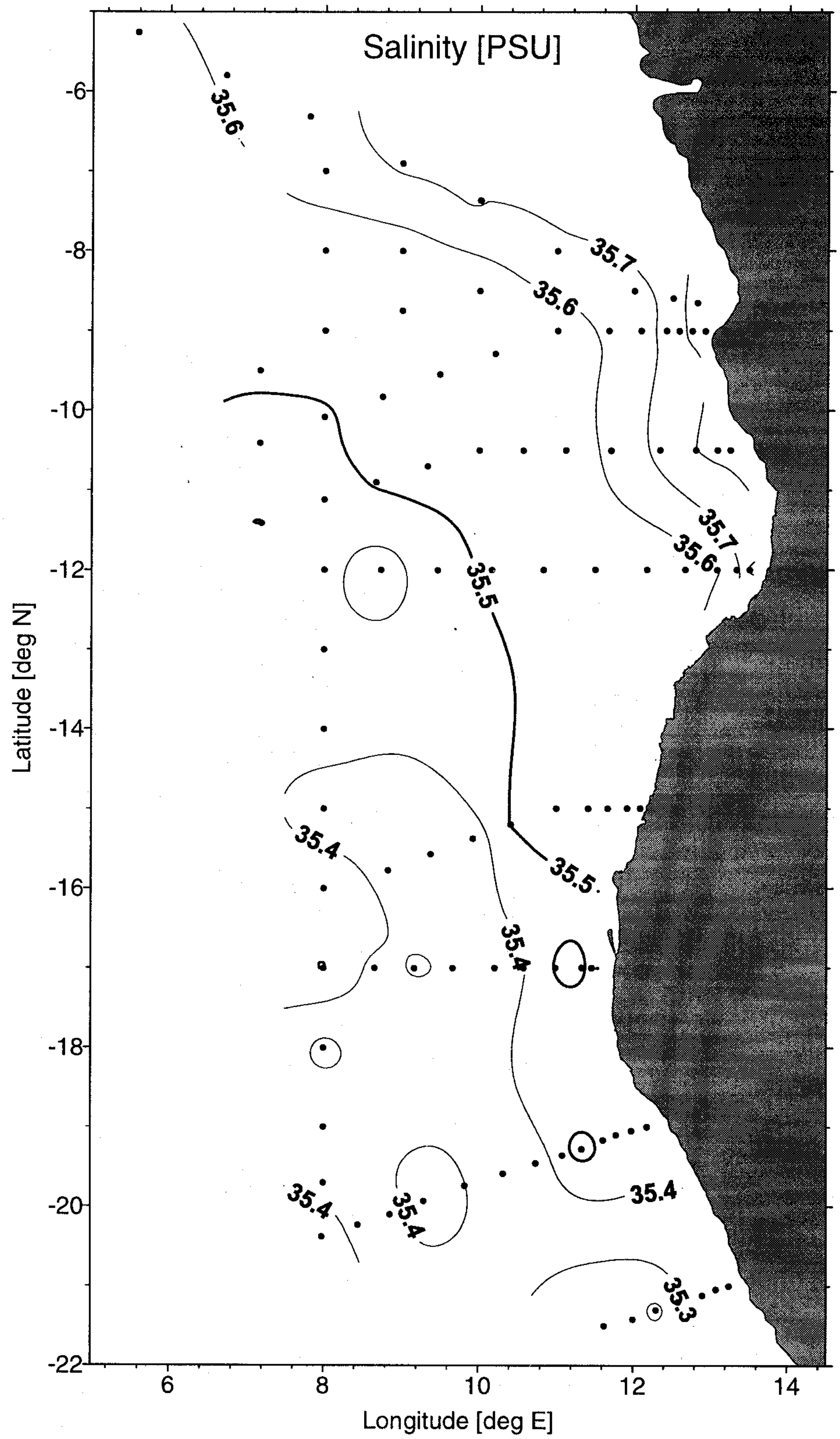

Figure 9.4: Salinity in 100 m depth on the cruise POS250 (02. - 28. April 1999)

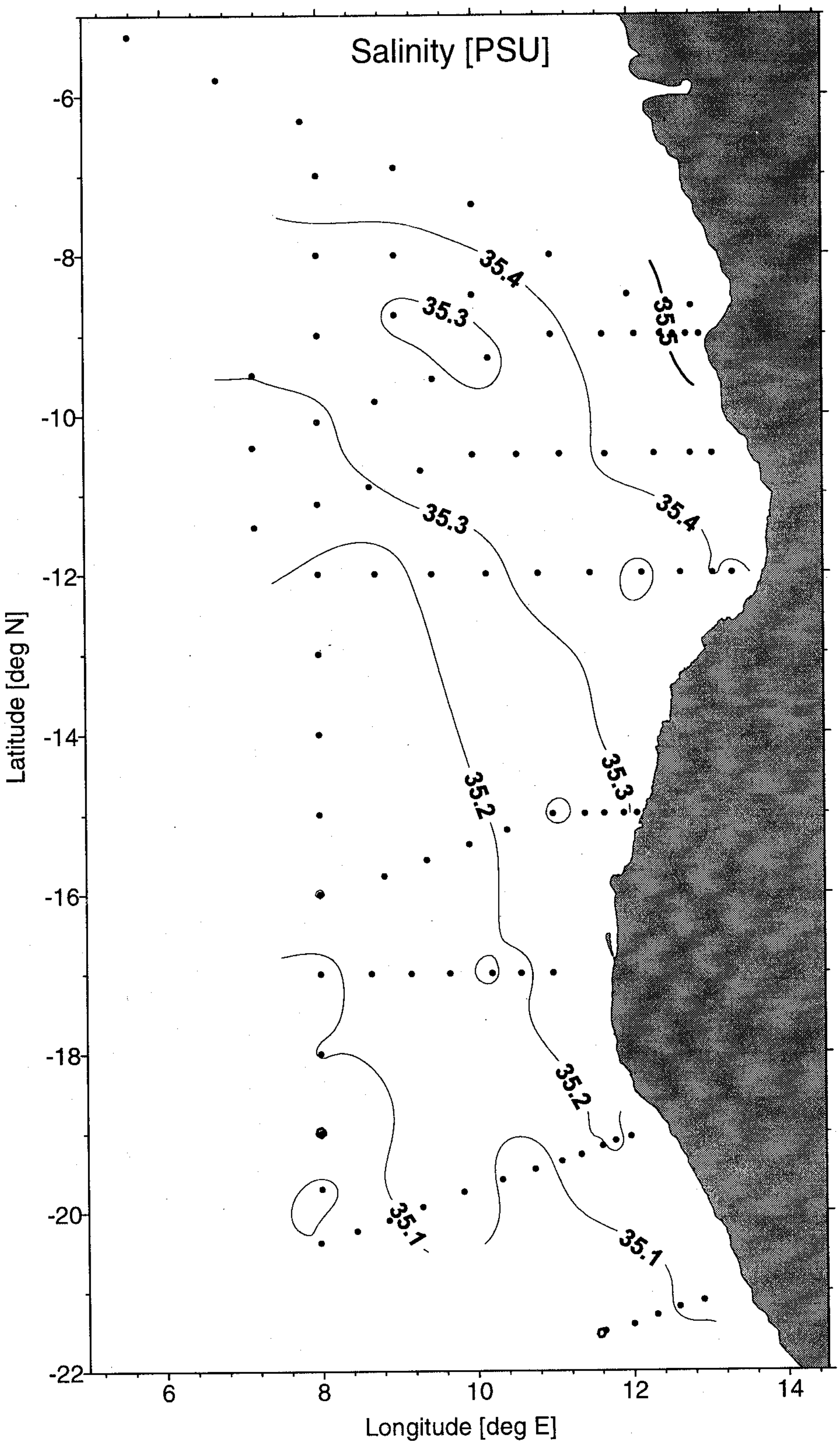

Figure 9.5: Salinity in 200 m depth on the cruise POS250 (02. - 28. April 1999)

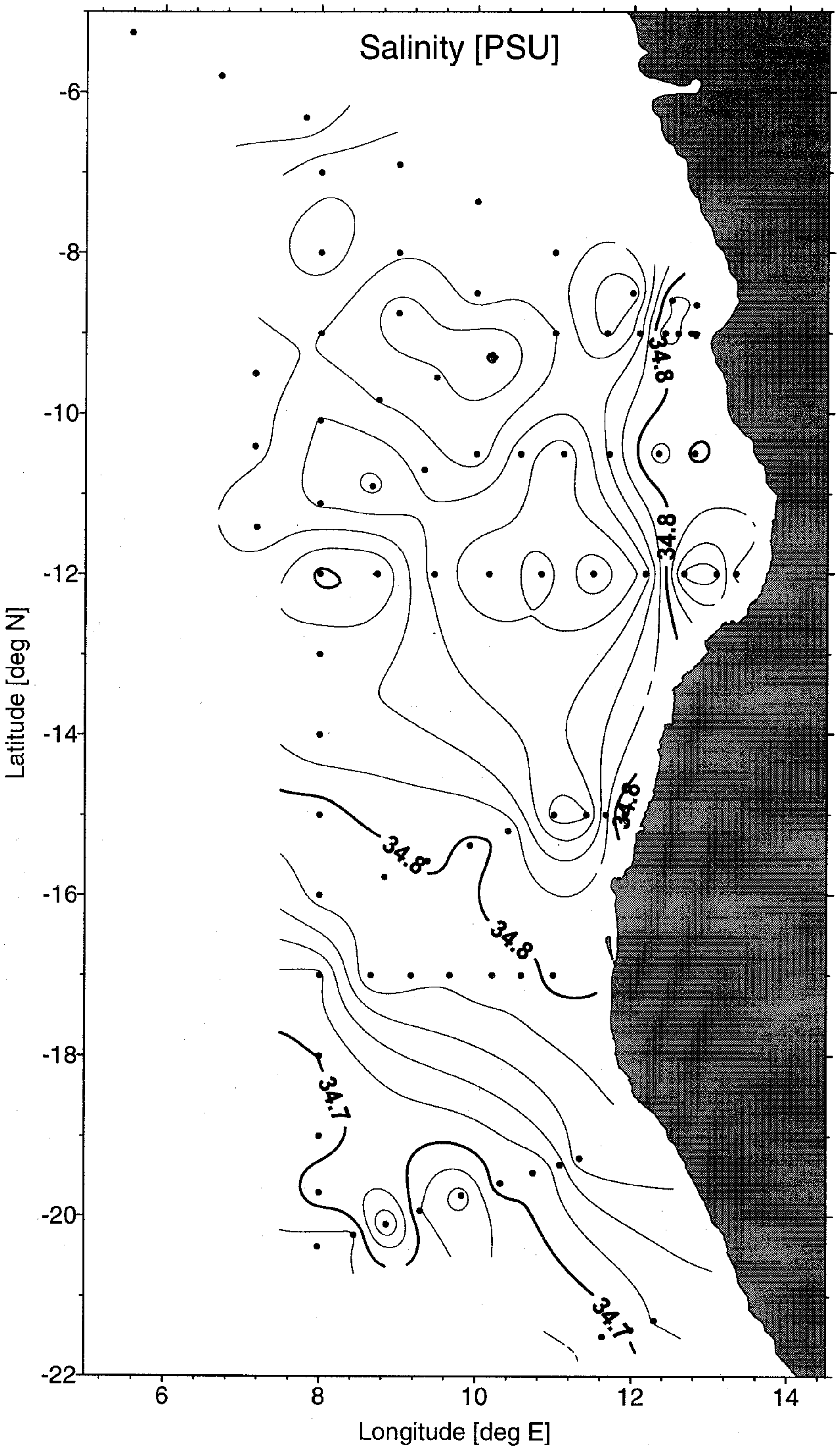

Figure 9.6: Salinity in 400 m depth on the cruise POS250 (02. - 28. April 1999)

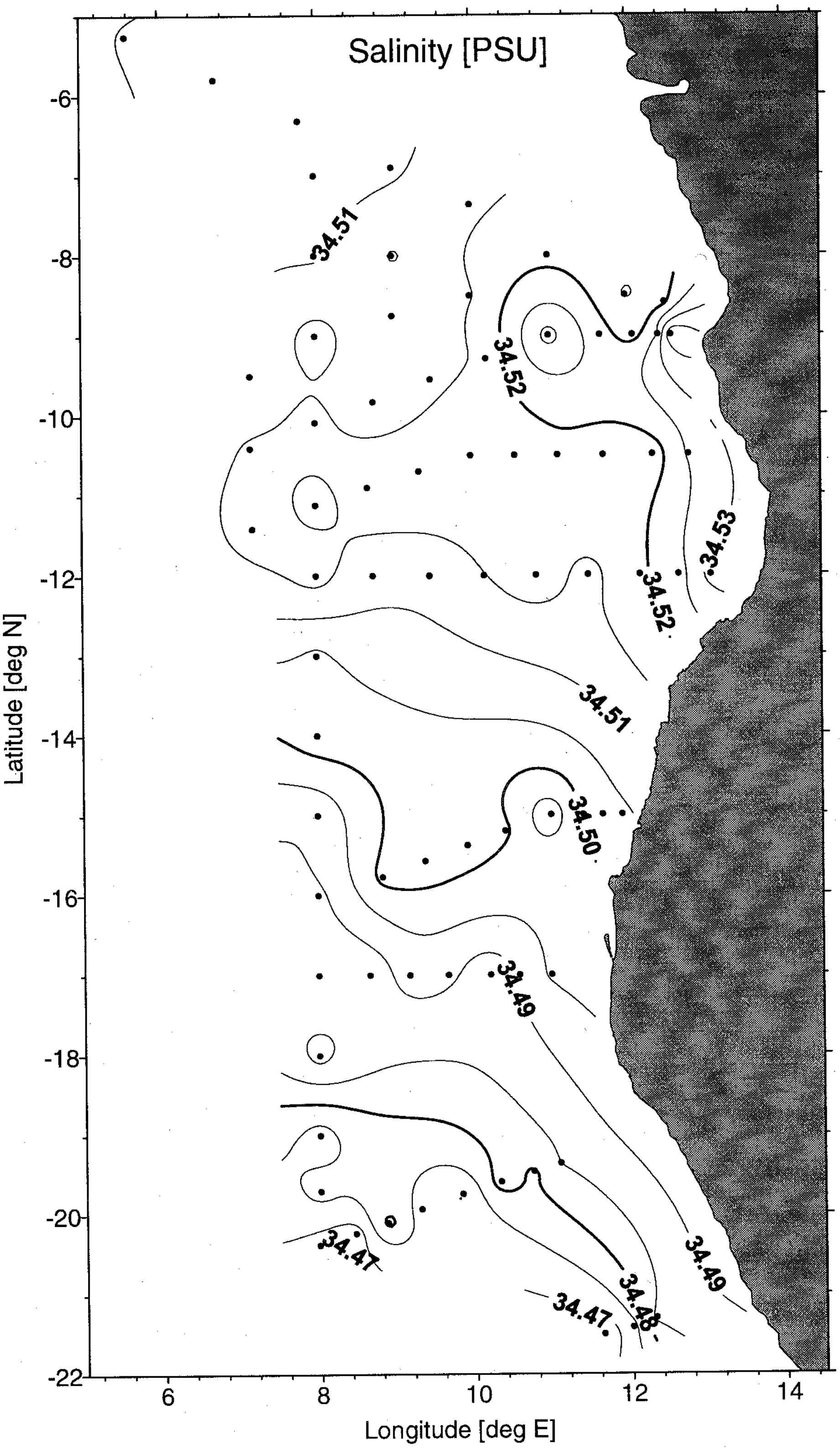

Figure 9.7: Salinity in 800 m depth on the cruise POS250 (02. - 28. April 1999)

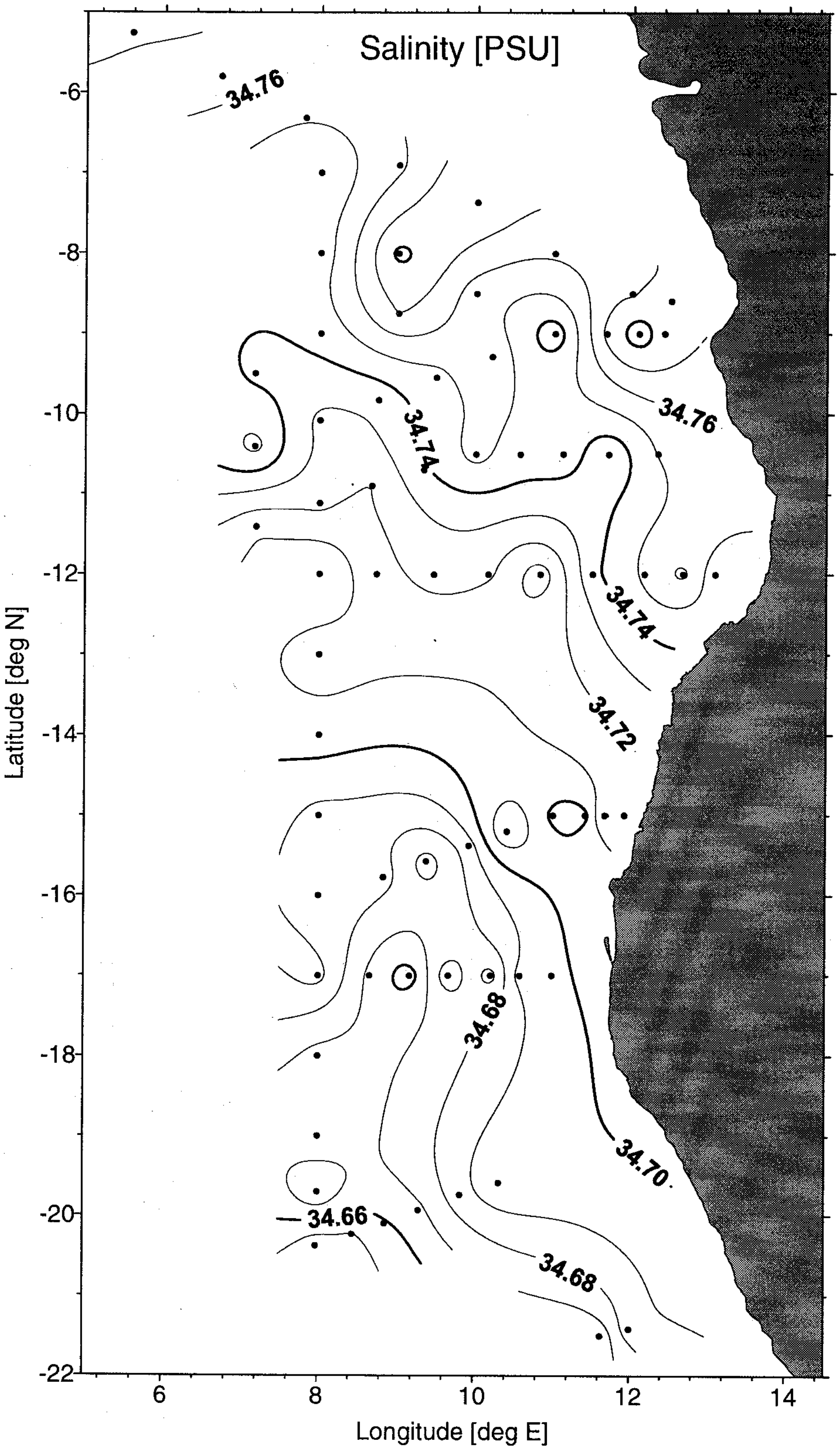

Figure 9.8: Salinity in 1200 m depth on the cruise POS250 (02. - 28. April 1999)

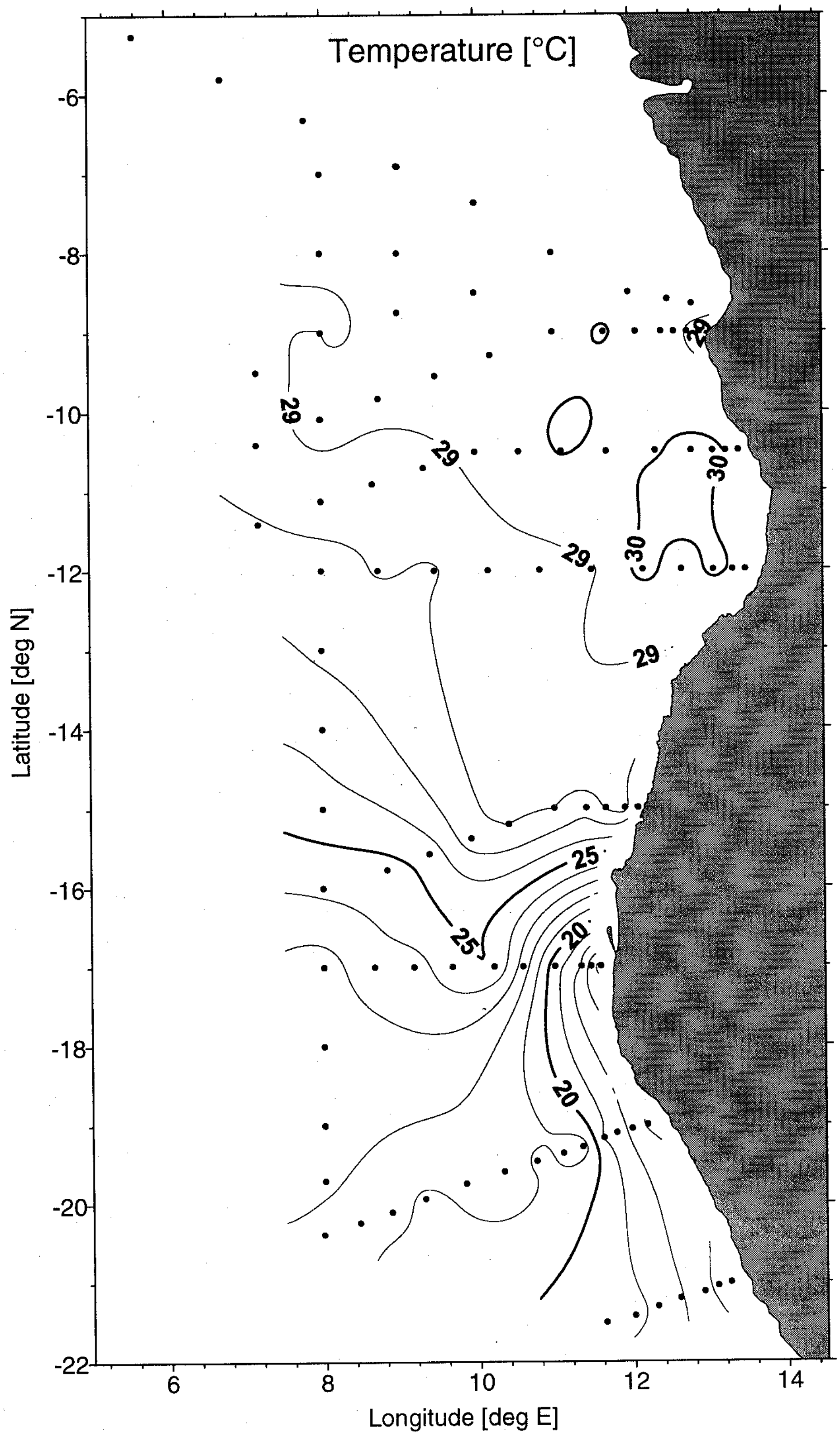

Figure 9.9: Sea surface temperature on the cruise POS250 (02. - 28. April 1999)

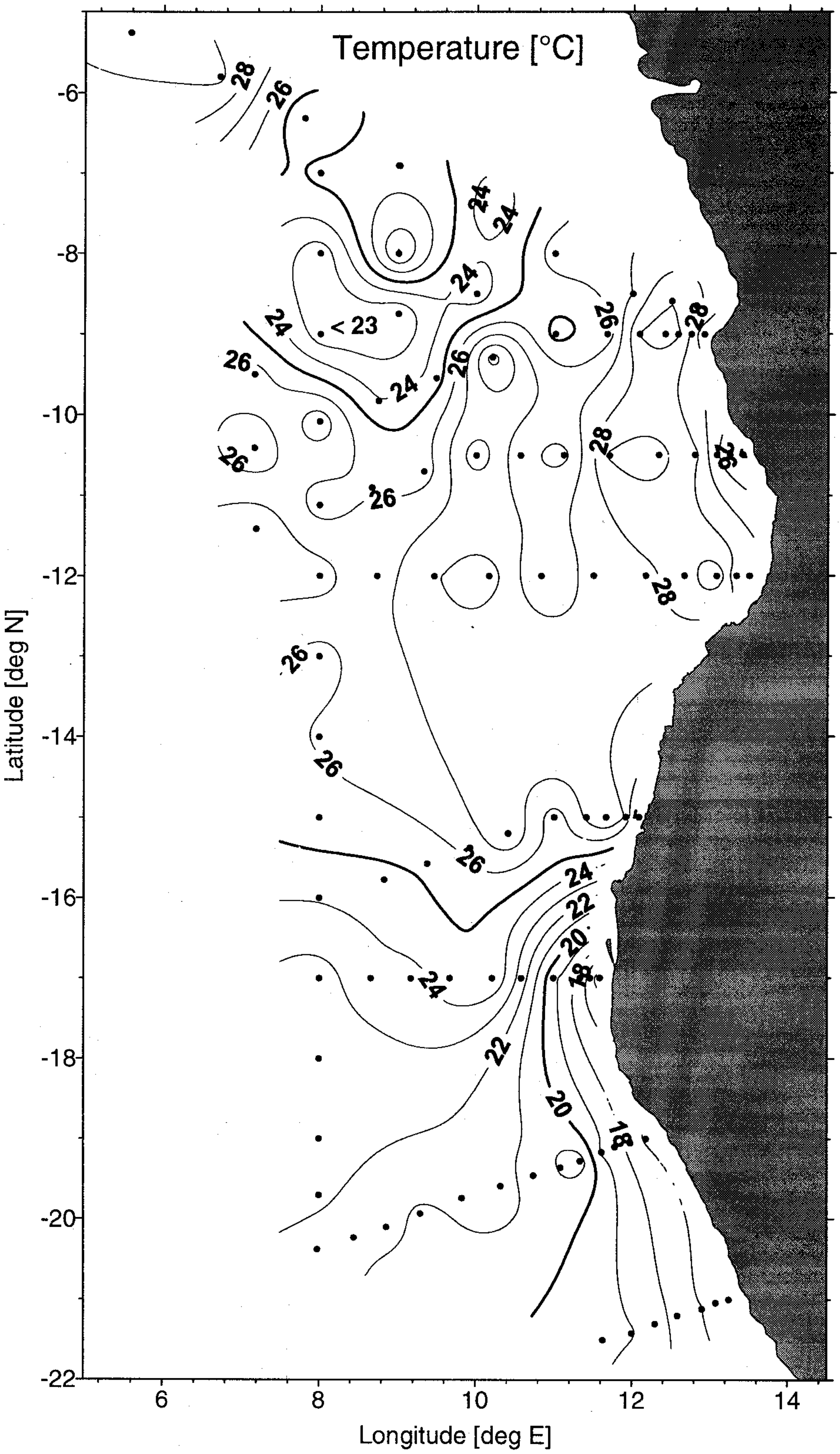

Figure 9.10: Temperature in 20 m depth on the cruise POS250 (02. - 28. April 1999)

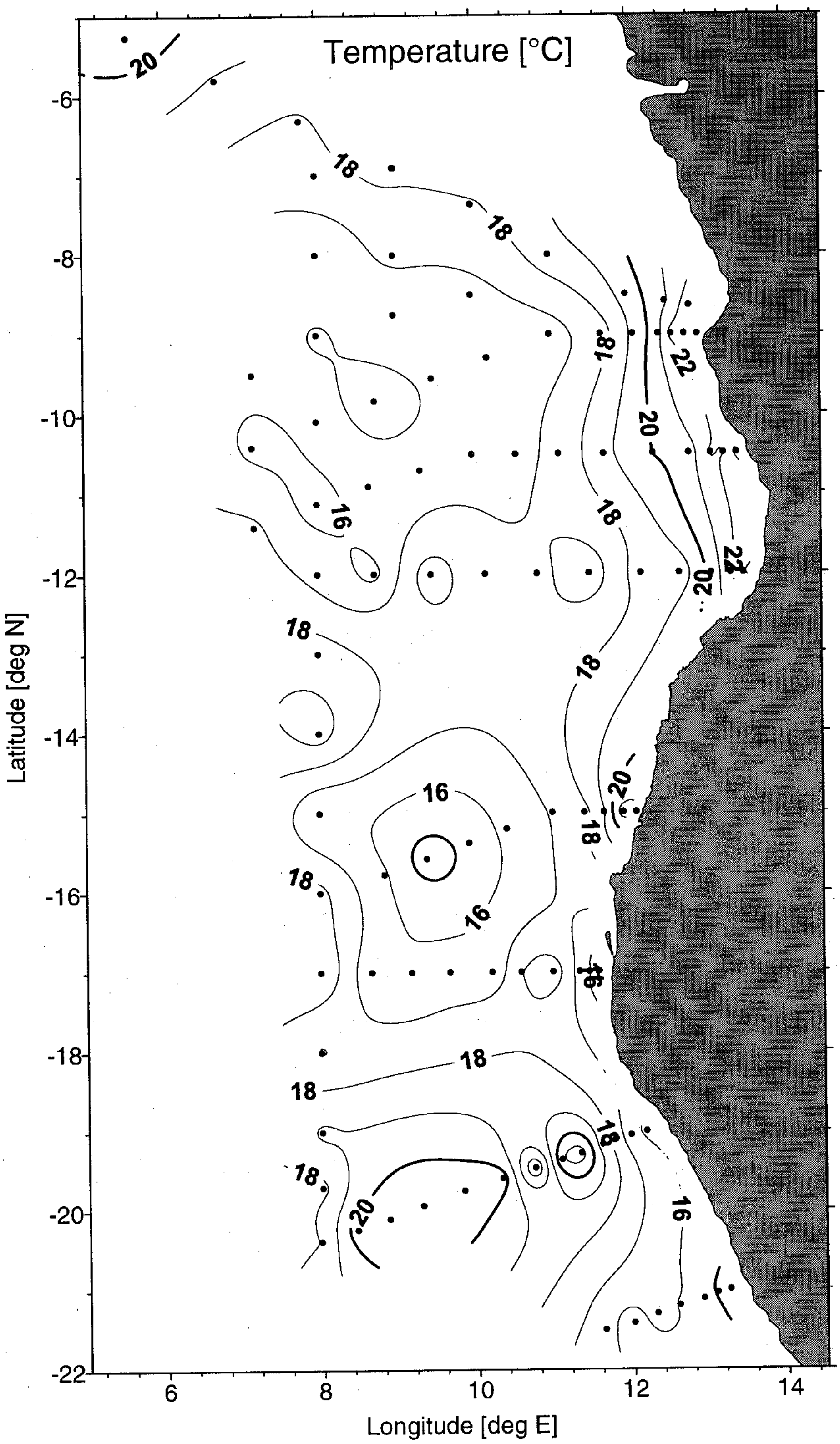

Figure 9.11: Temperature in 50 m depth on the cruise POS250 (02. - 28. April 1999)

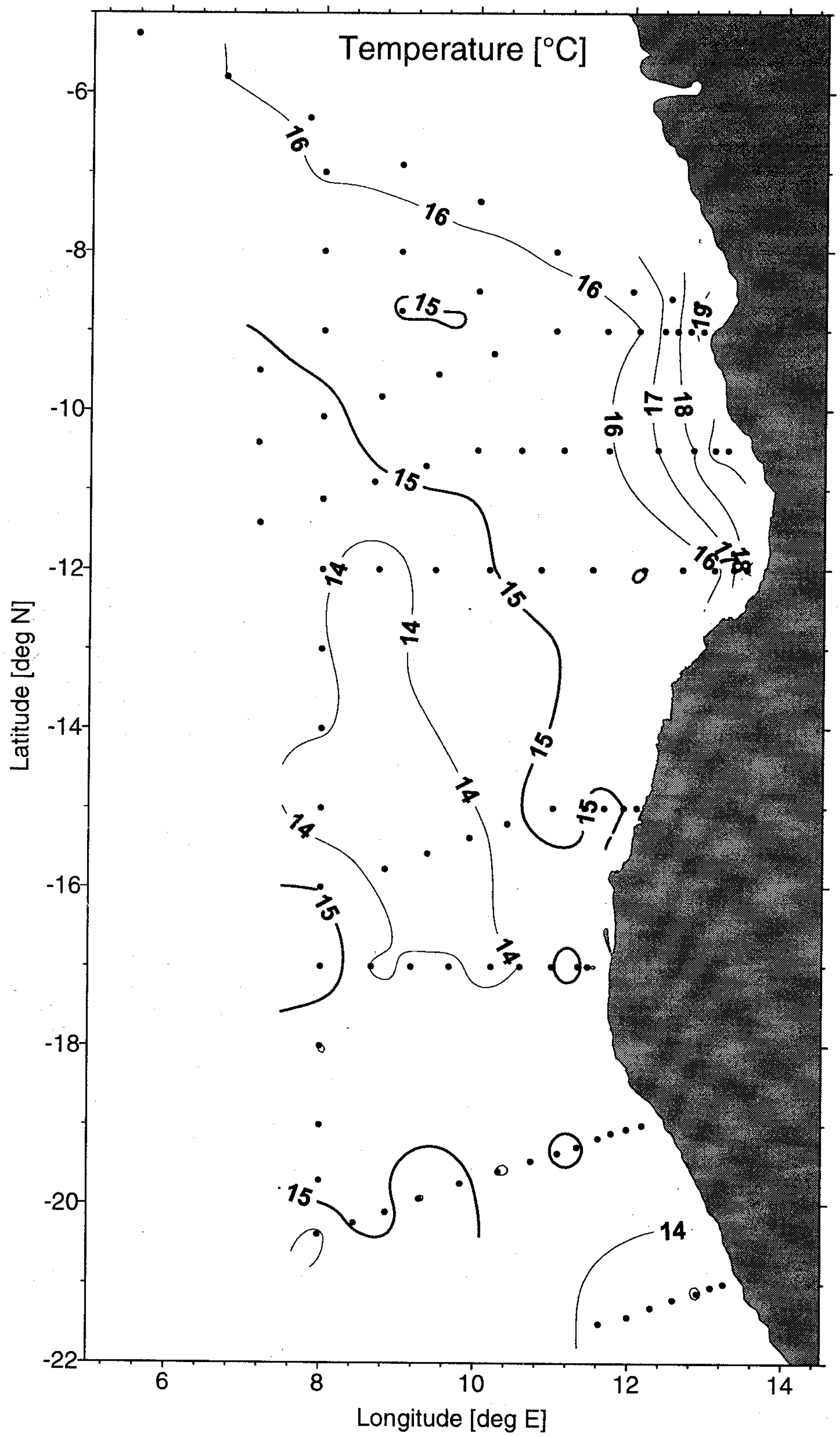

Figure 9.12: Temperature in 100 m depth on the cruise POS250 (02. - 28. April 1999)

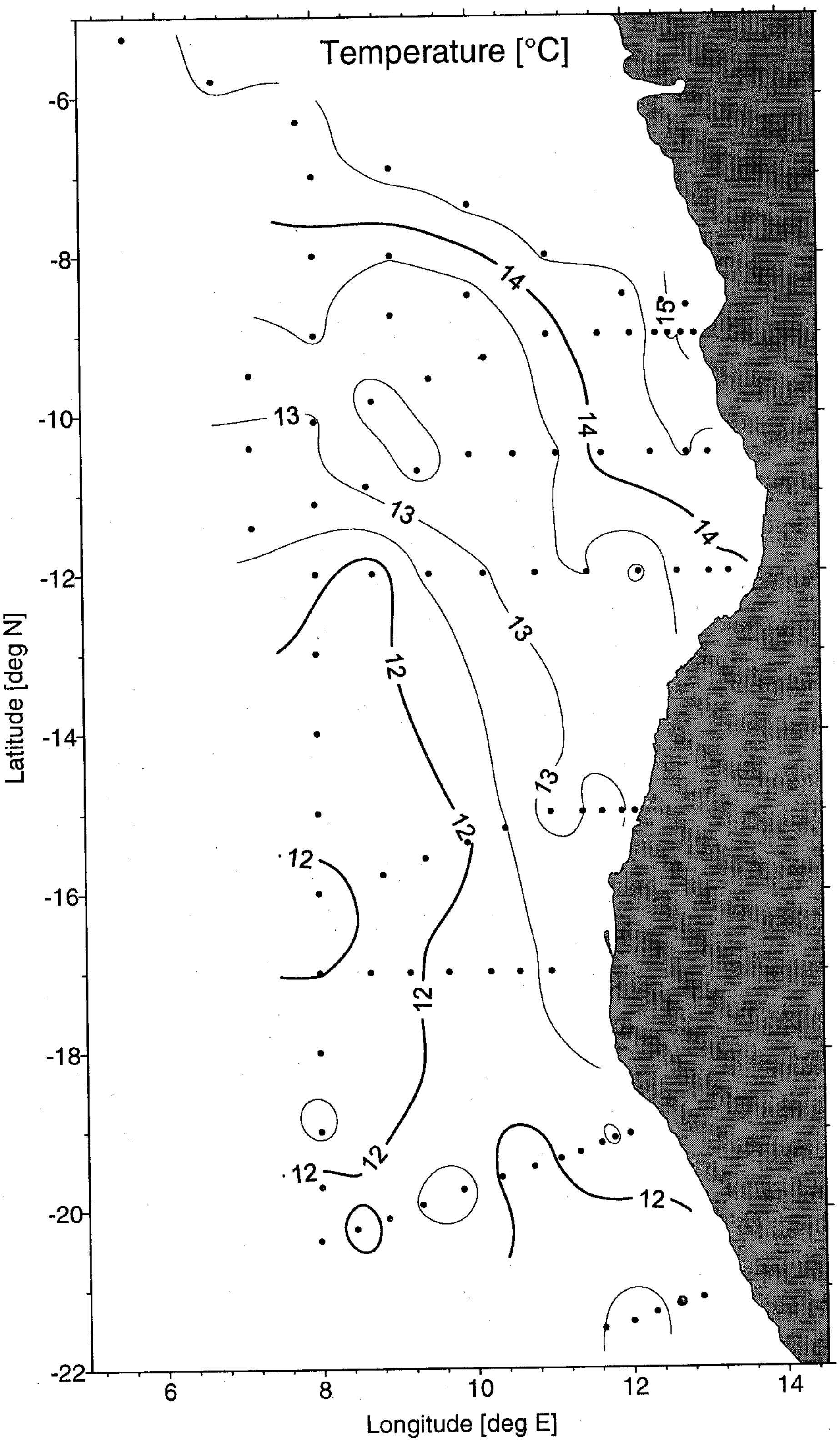

Figure 9.13: Temperature in 200 m depth on the cruise POS250 (02. - 28. April 1999)

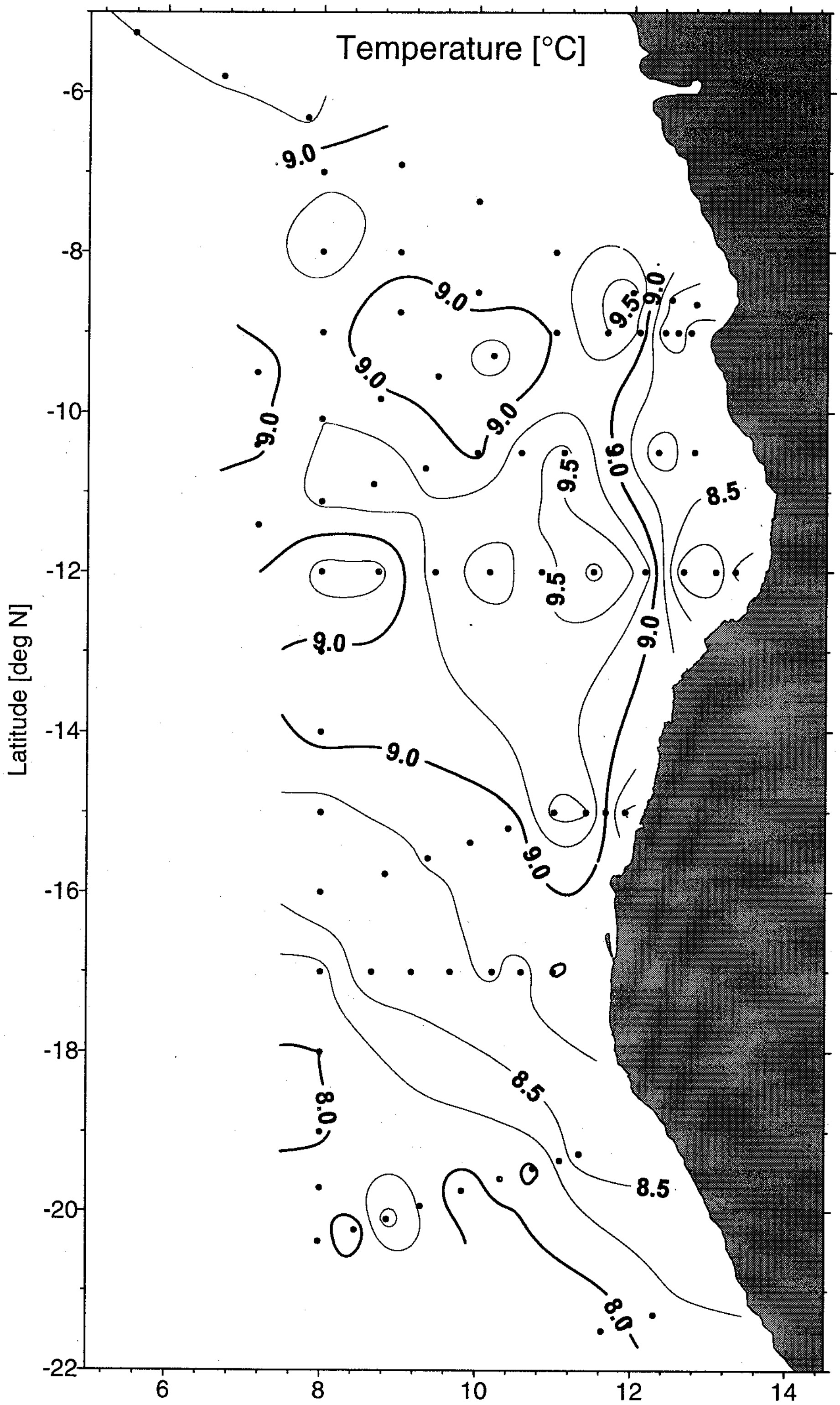

Figure 9.14: Temperature in 400 m depth on the cruise POS250 (02. - 28. April 1999)

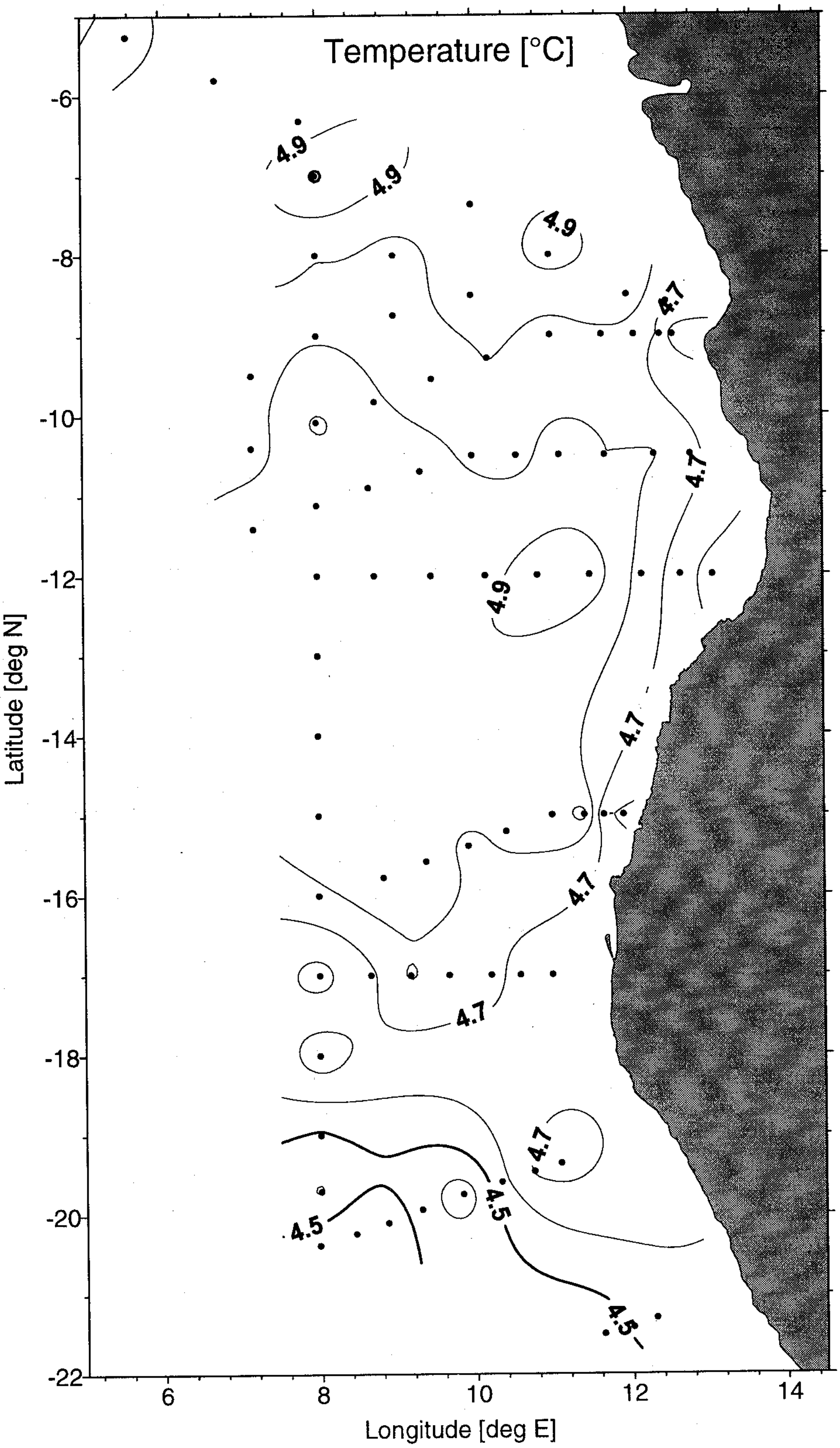

Figure 9.15: Temperature in 800 m depth on the cruise POS250 (02. - 28. April 1999)

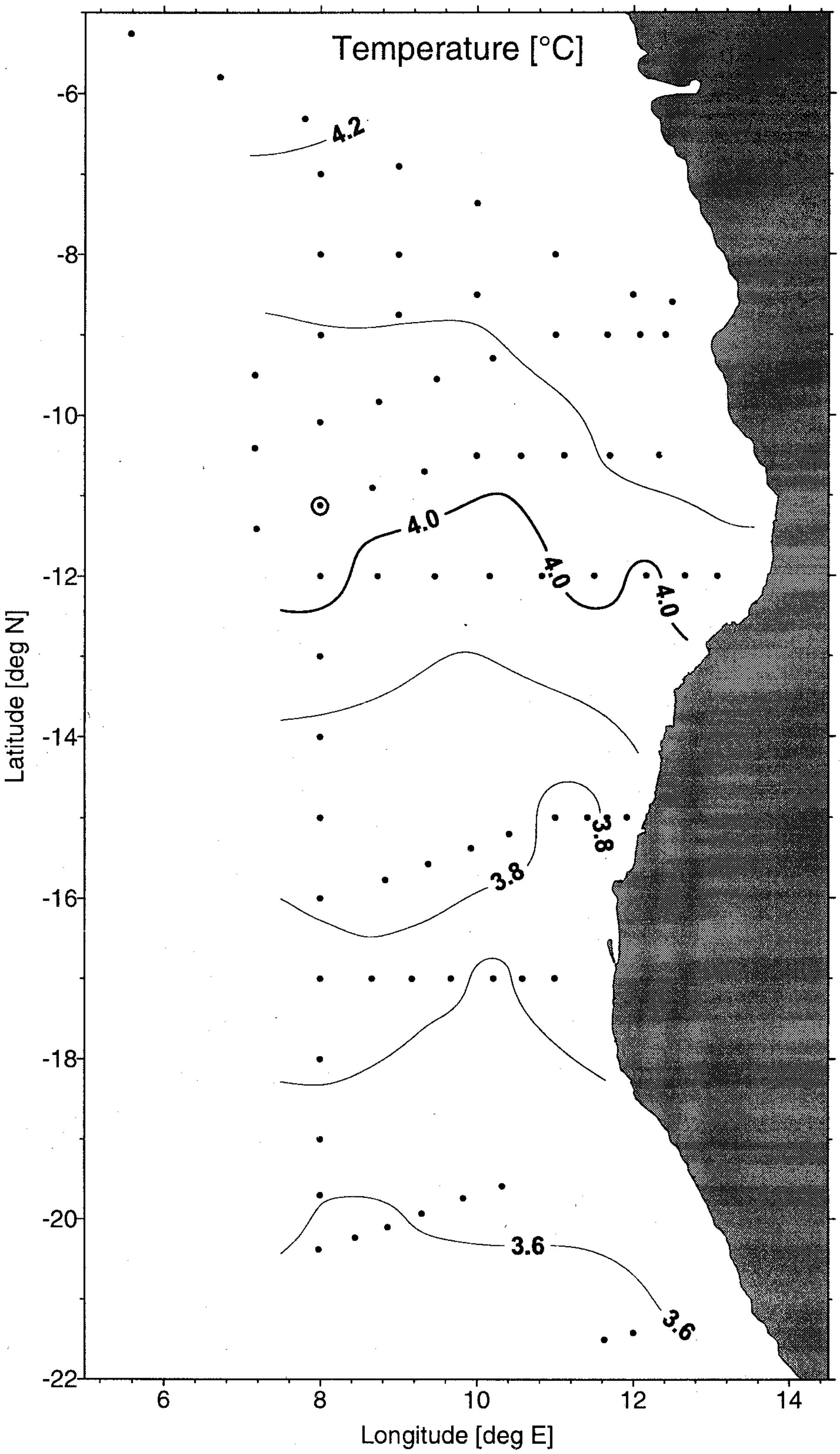

Figure 9.16: Temperature in 1200 m depth on the cruise POS250 (02. - 28. April 1999)

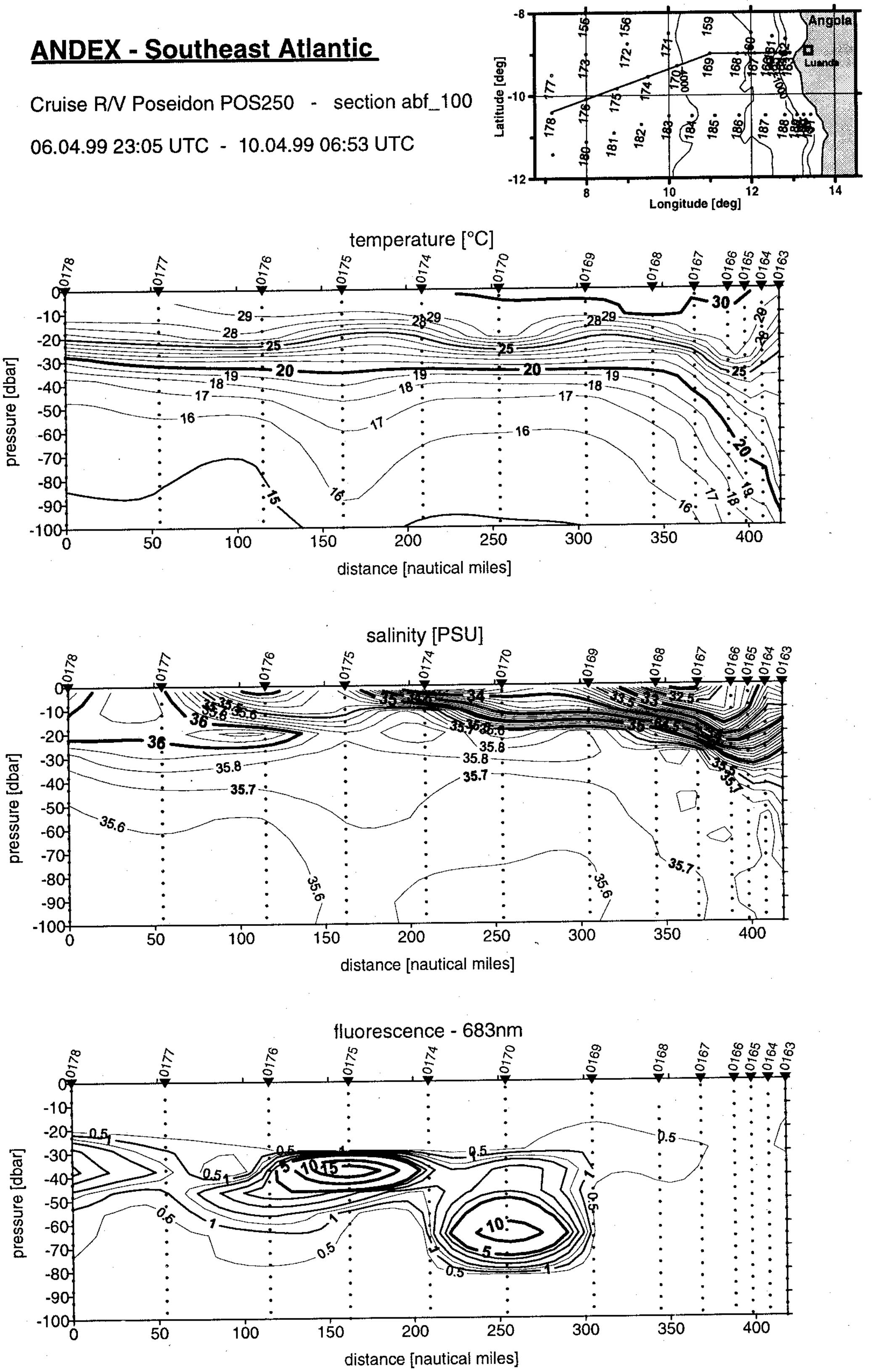

Figure 9.17: Vertical section of temperature, salinity and fluorescence at transect abf_100

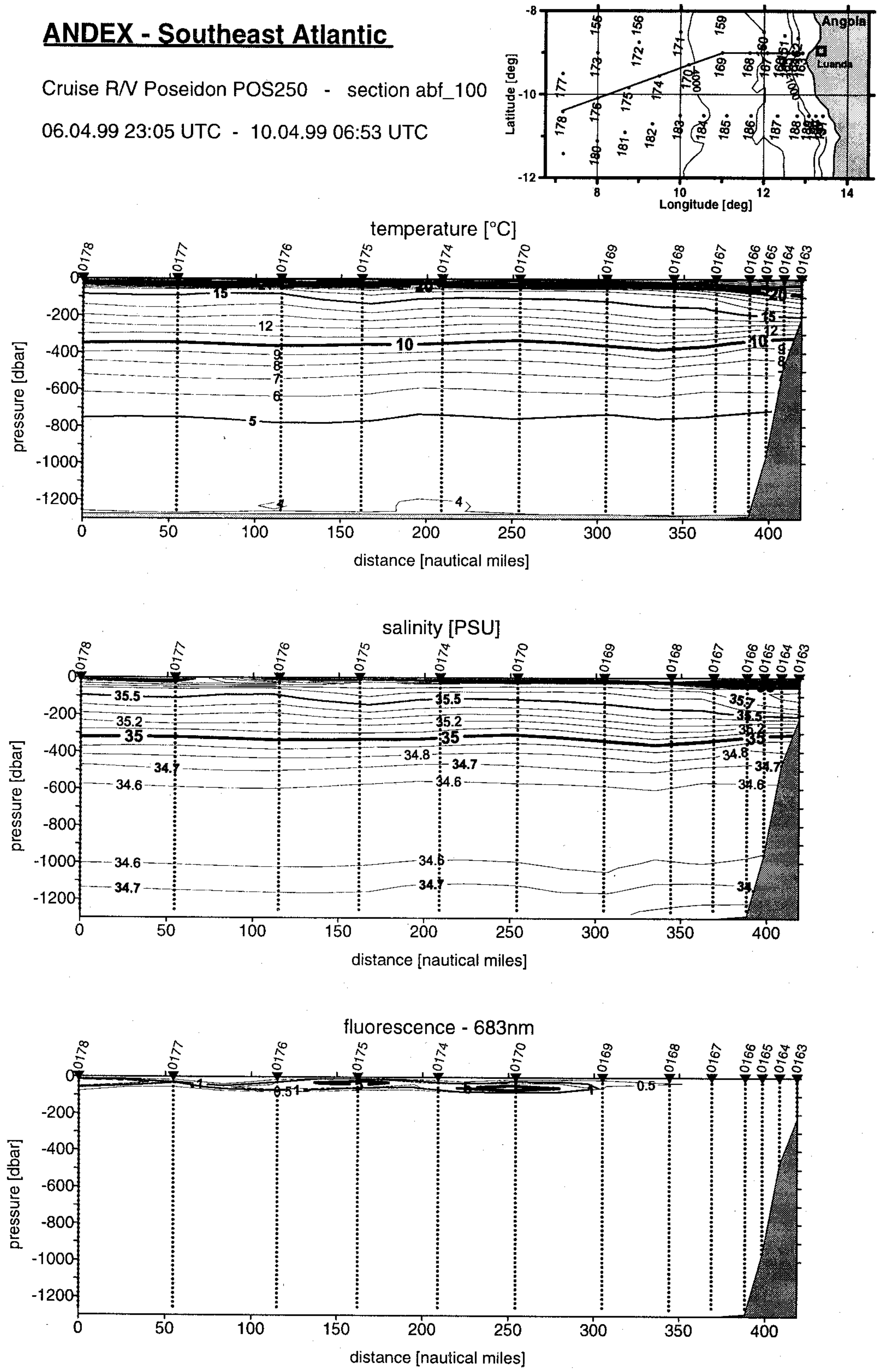

Figure 9.18: Vertical section of temperature, salinity and fluorescence at transect abf_100

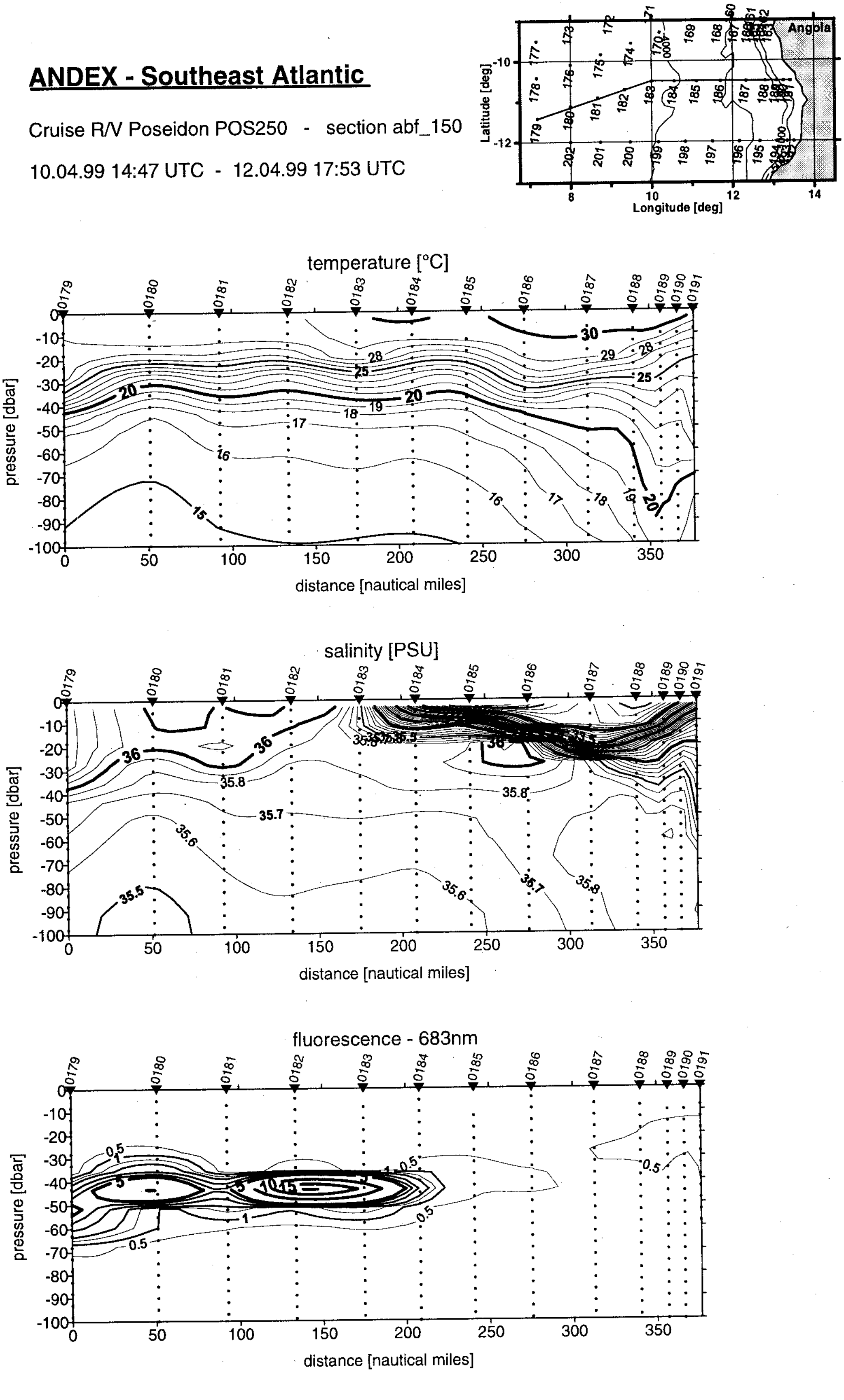

Figure 9.19: Vertical section of temperature, salinity and fluorescence at transect abf_150

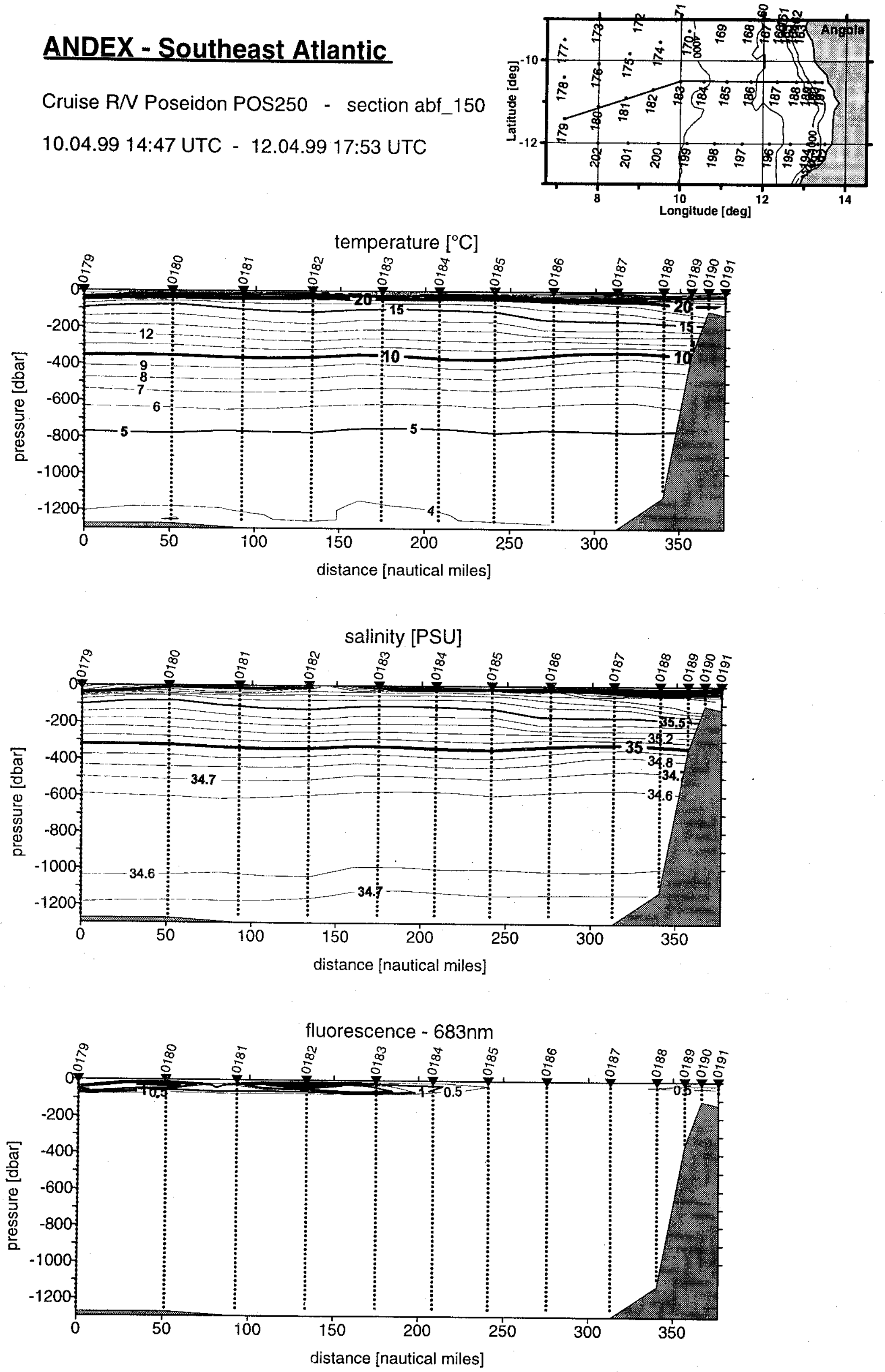

Figure 9.20: Vertical section of temperature, salinity and fluorescence at transect abf_150

ANDEX - Southeast Atlantic

Cruise R/V Poseidon POS250 - section abf_250

13.04.99 03:33 UTC - 14.04.99 20:47 UTC

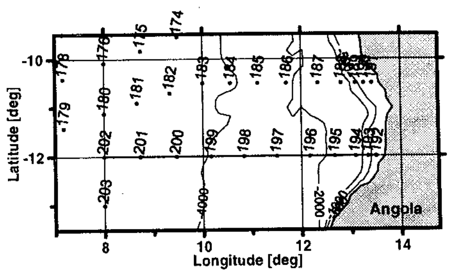

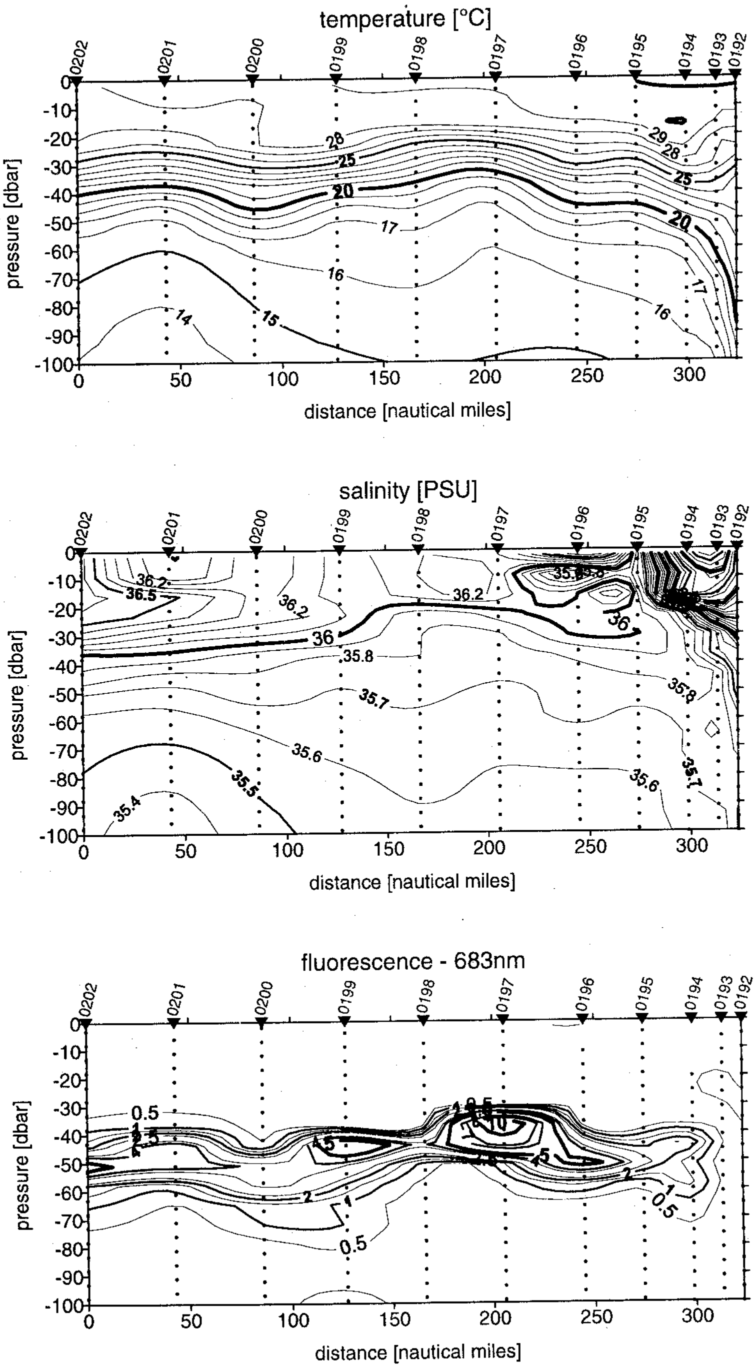

Figure 9.21: Vertical section of temperature, salinity and fluorescence at transect abf_250

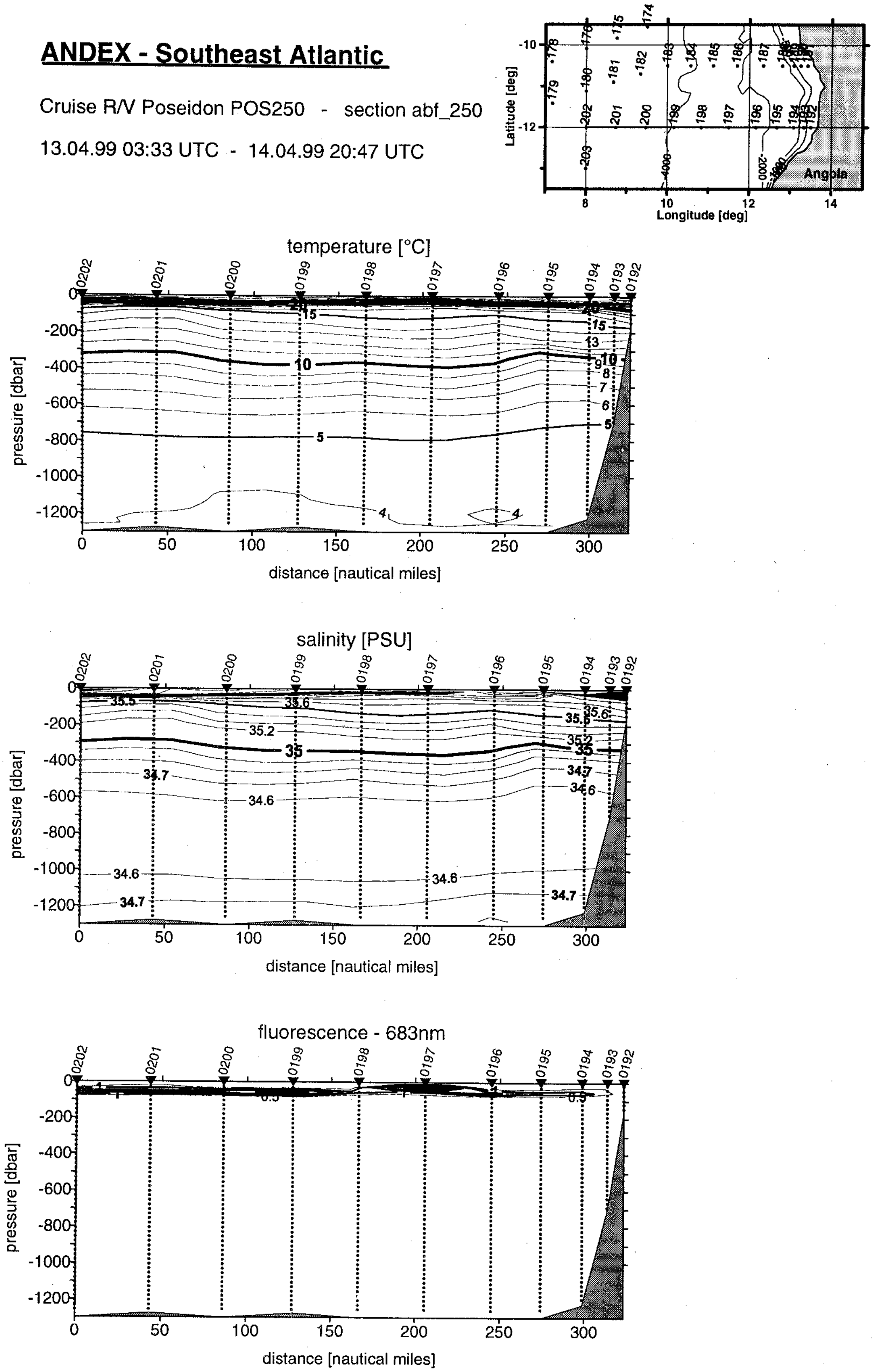

Figure 9.22: Vertical section of temperature, salinity and fluorescence at transect abf_250

ANDEX - South-east Atlantic

Cruise R/V Poseidon POS250 - section abf_400

16.04.99 09:23 UTC - 18.04.99 11:47 UTC

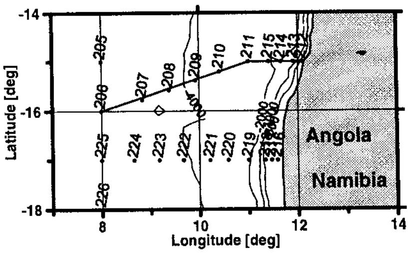

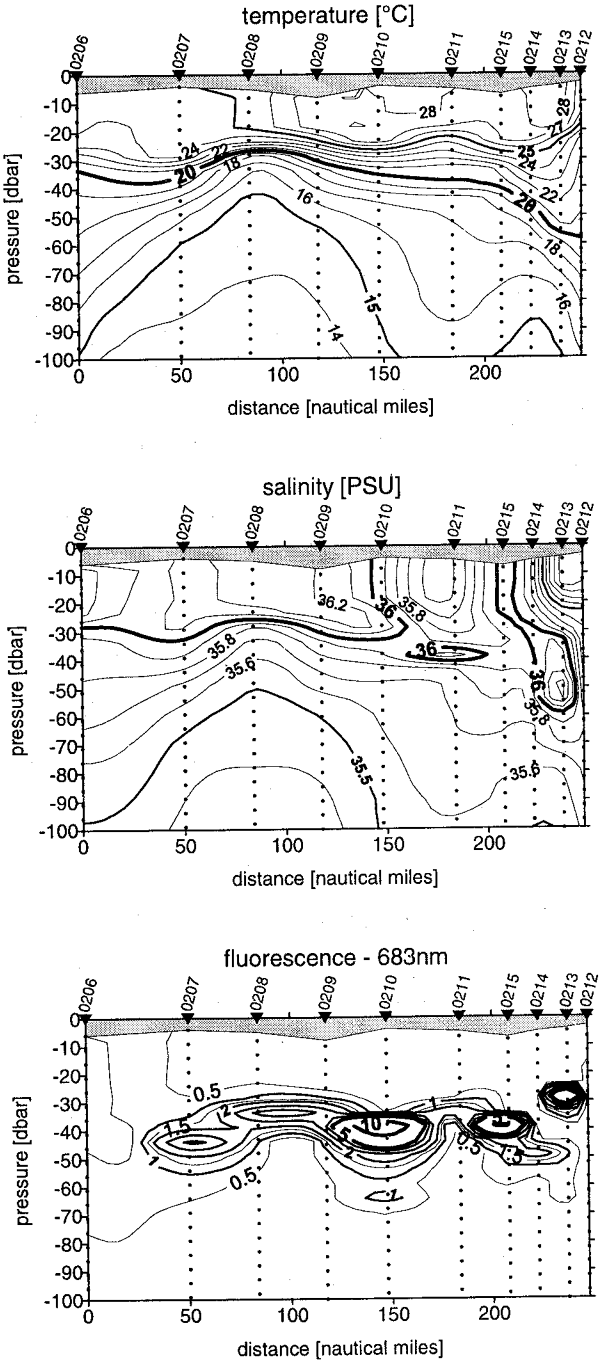

Figure 9.23: Vertical section of temperature, salinity and fluorescence at transect abf_400

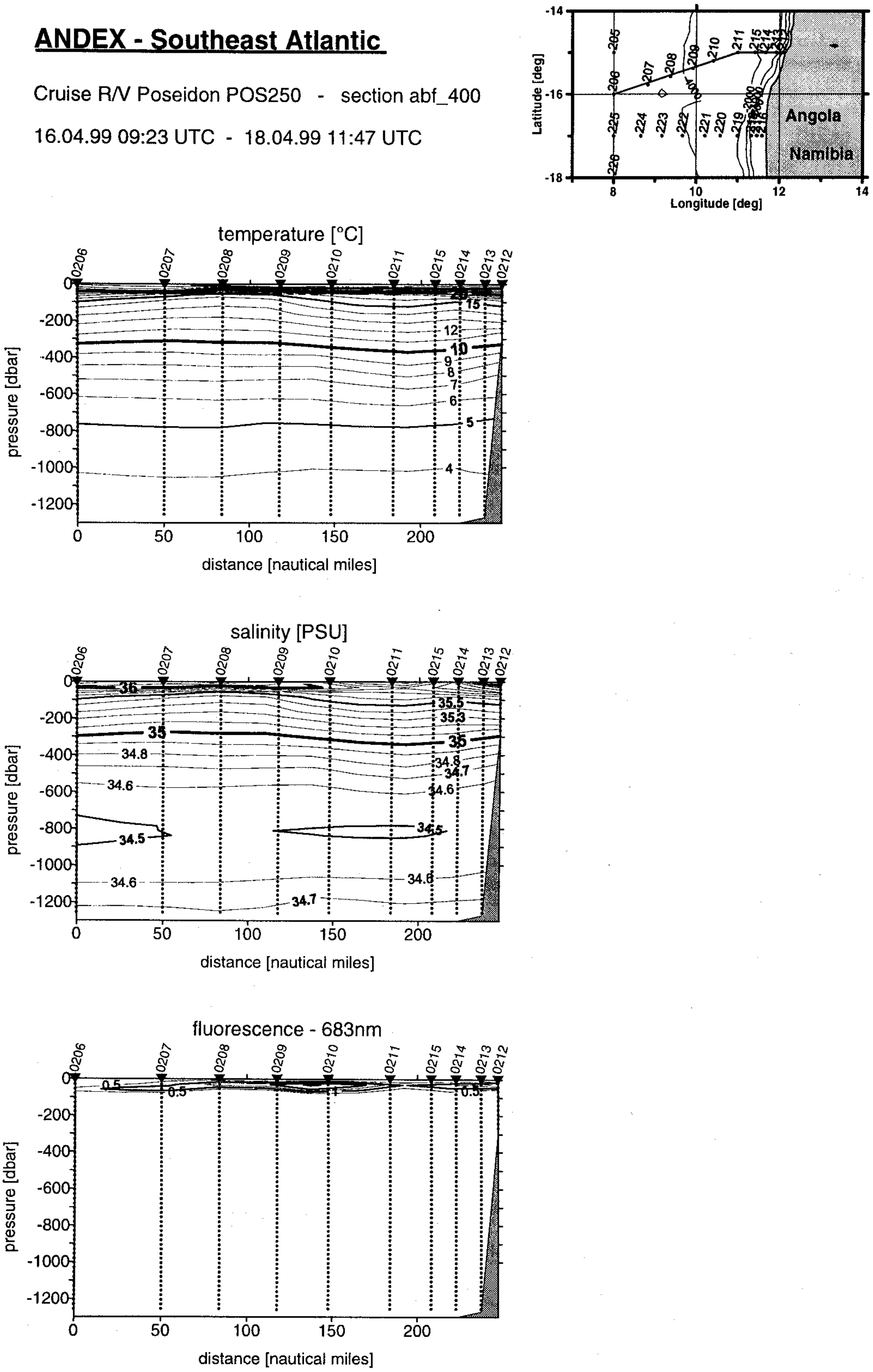

Figure 9.24: Vertical section of temperature, salinity and fluorescence at transect abf_400

ANDEX - Southeast Atlantic

Cruise R/V Poseidon POS250 - section abf_600

19.04.99 14:25 UTC - 21.04.99 02:22 UTC

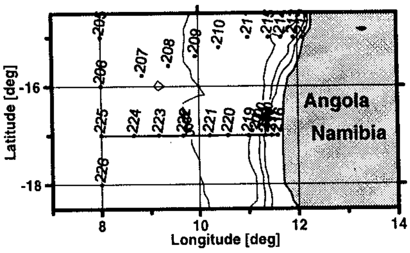

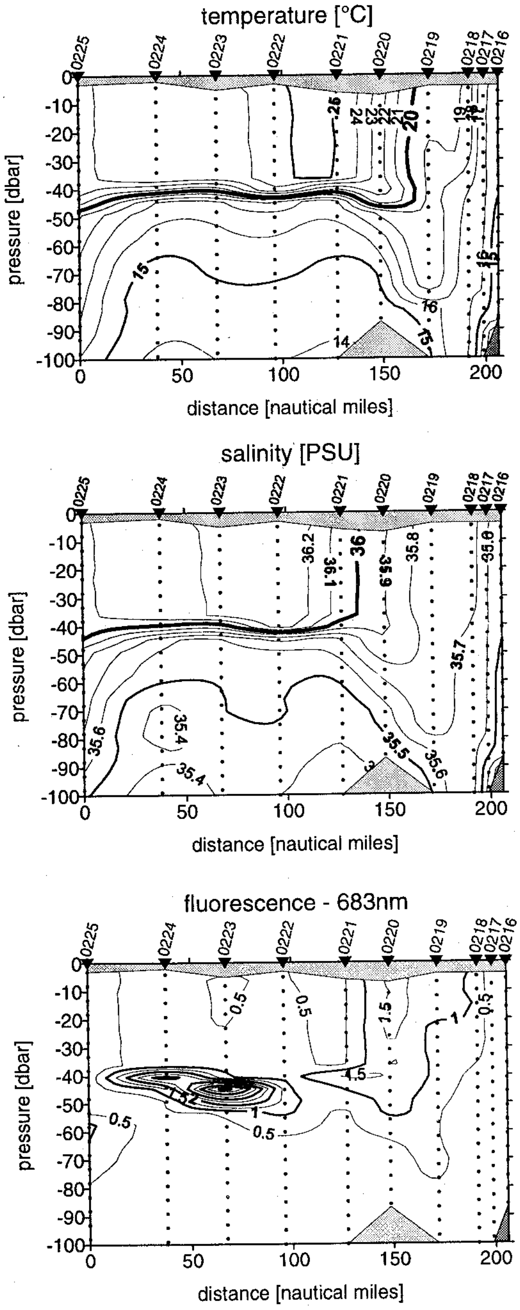

Figure 9.25: Vertical section of temperature, salinity and fluorescence at transect abf_600

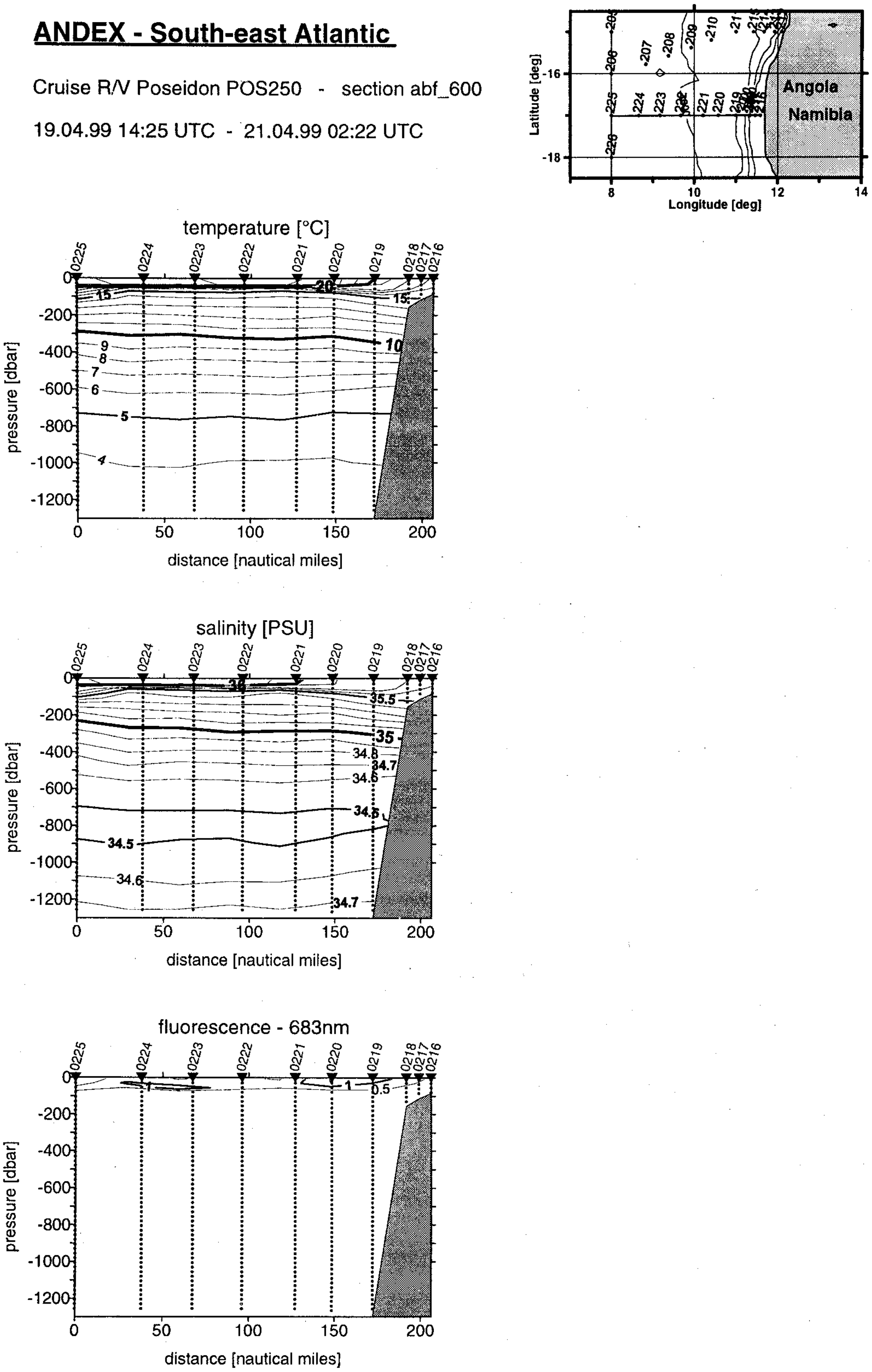

Figure 9.26: Vertical section of temperature, salinity and fluorescence at transect abf_600

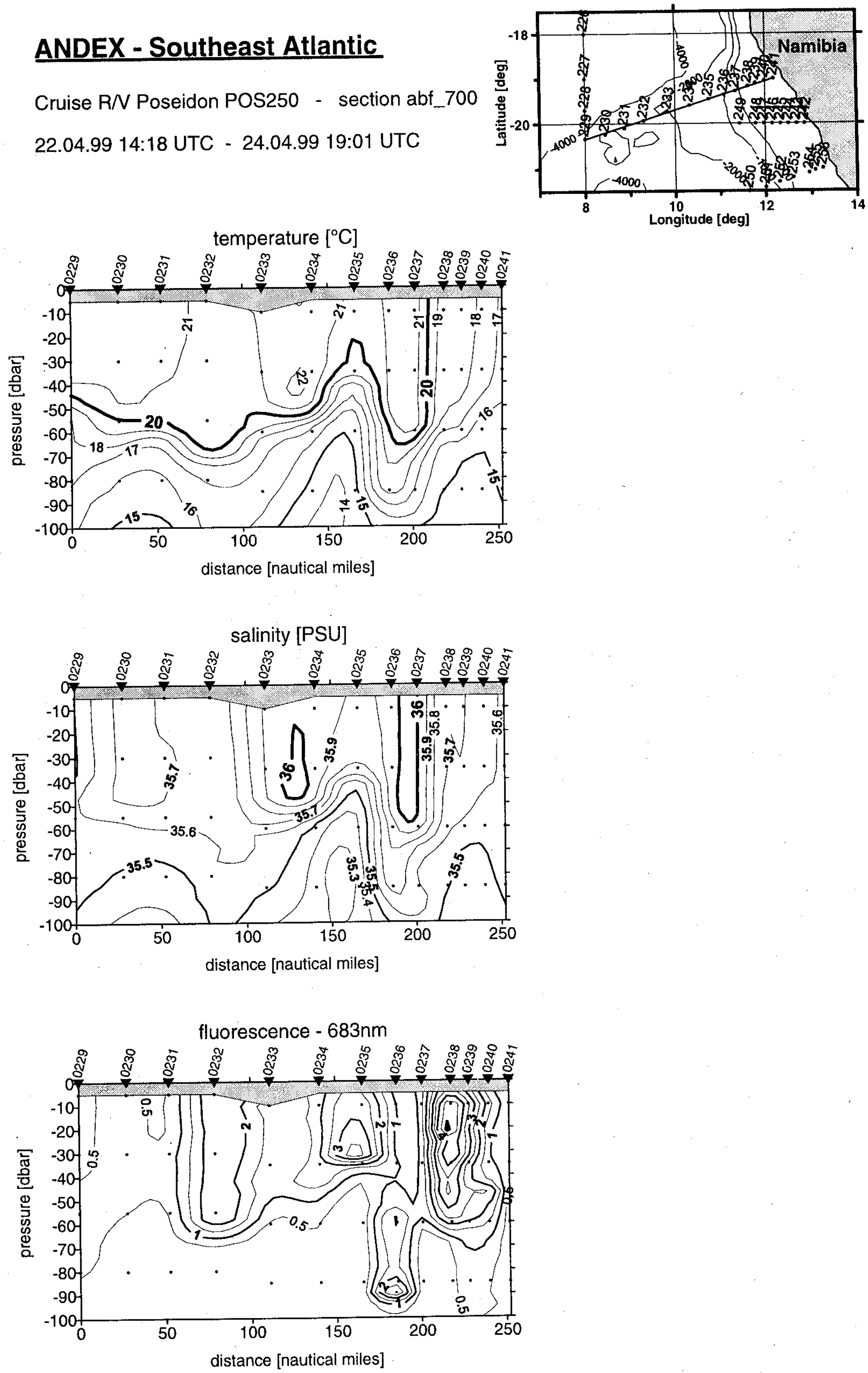

Figure 9.27: Vertical section of temperature, salinity and fluorescence at transect abf_700

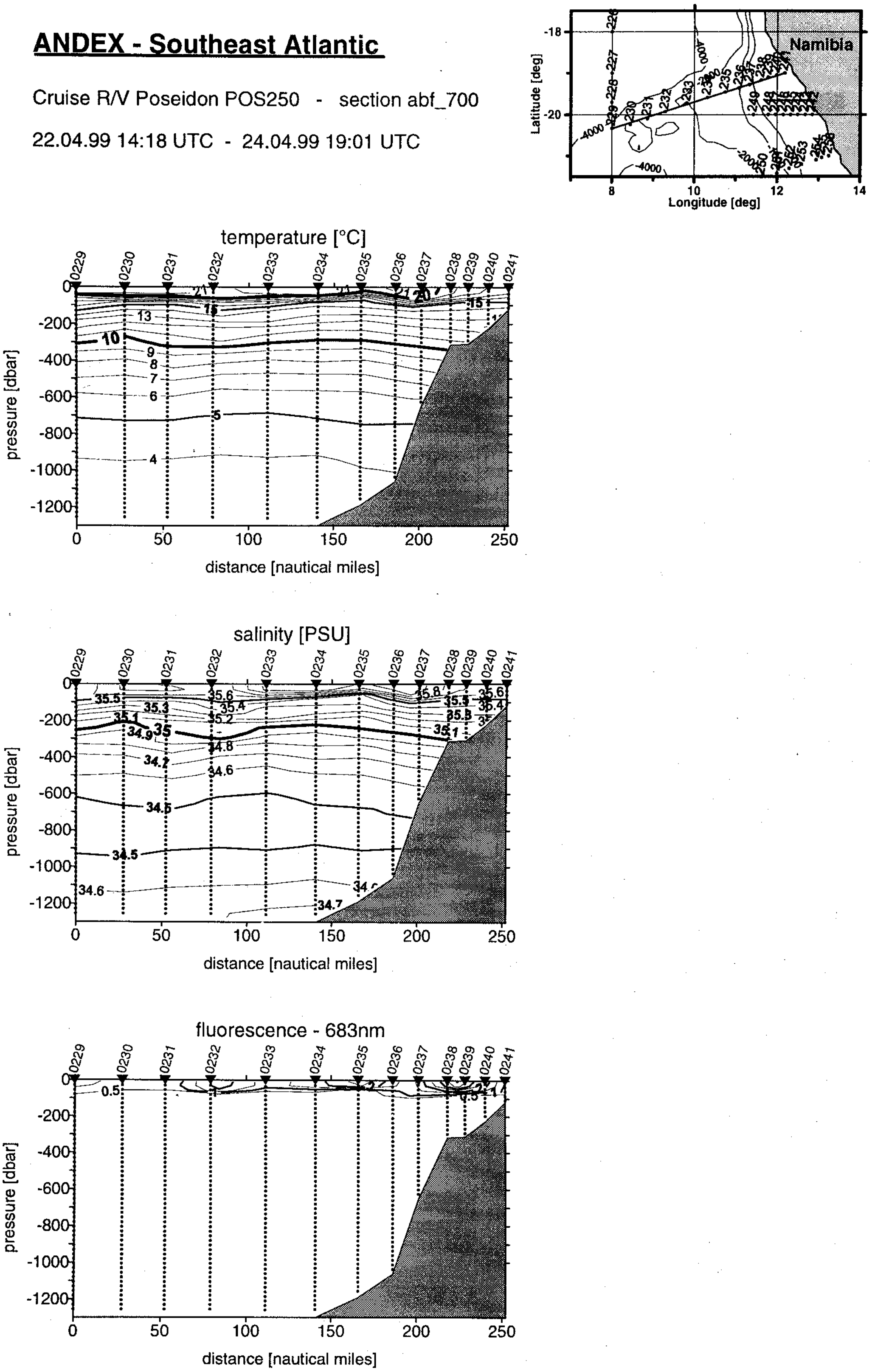

Figure 9.28: Vertical section of temperature, salinity and fluorescence at transect abf_700

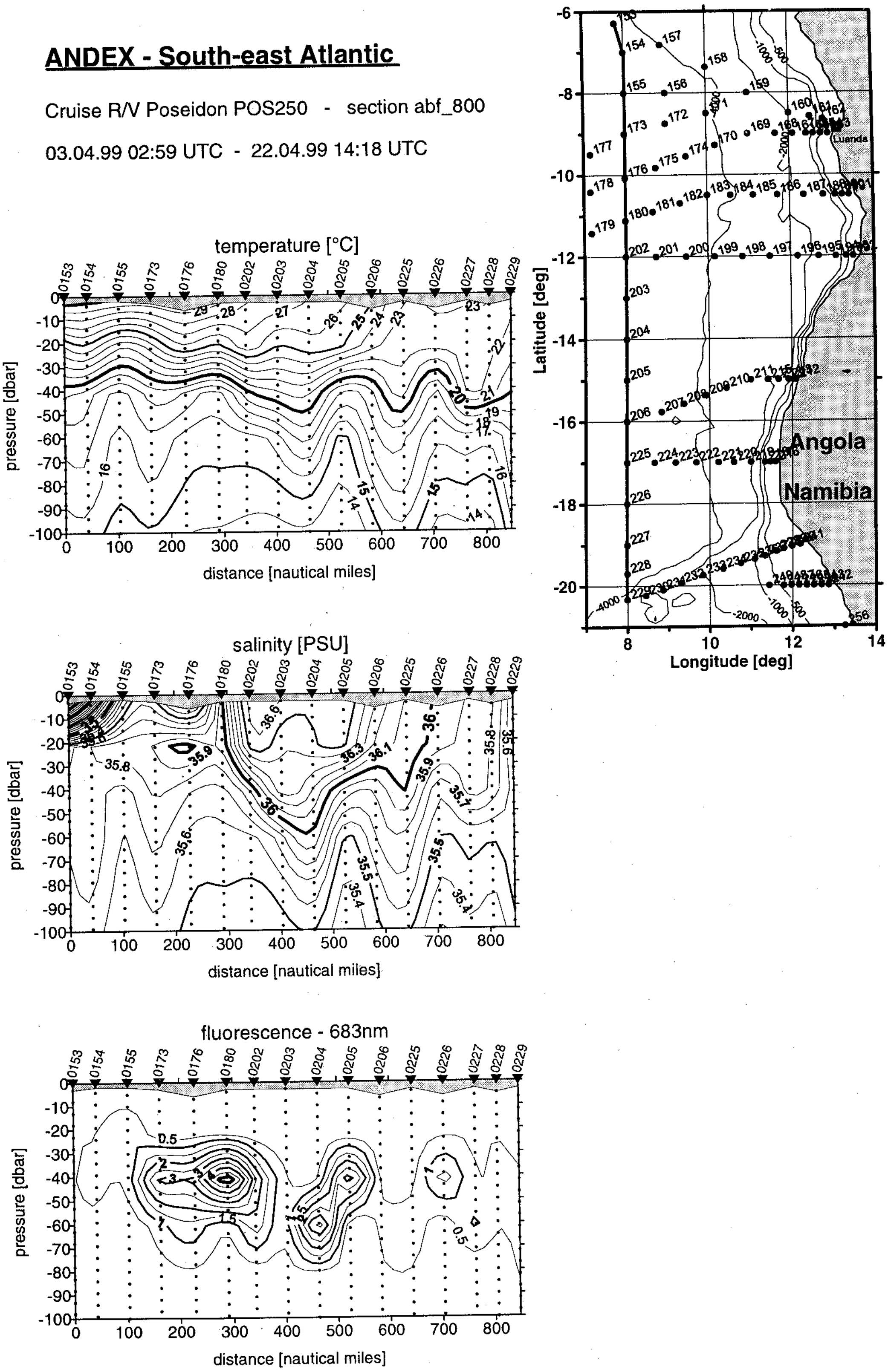

Figure 9.29: Vertical section of temperature, salinity and fluorescence at transect abf_800

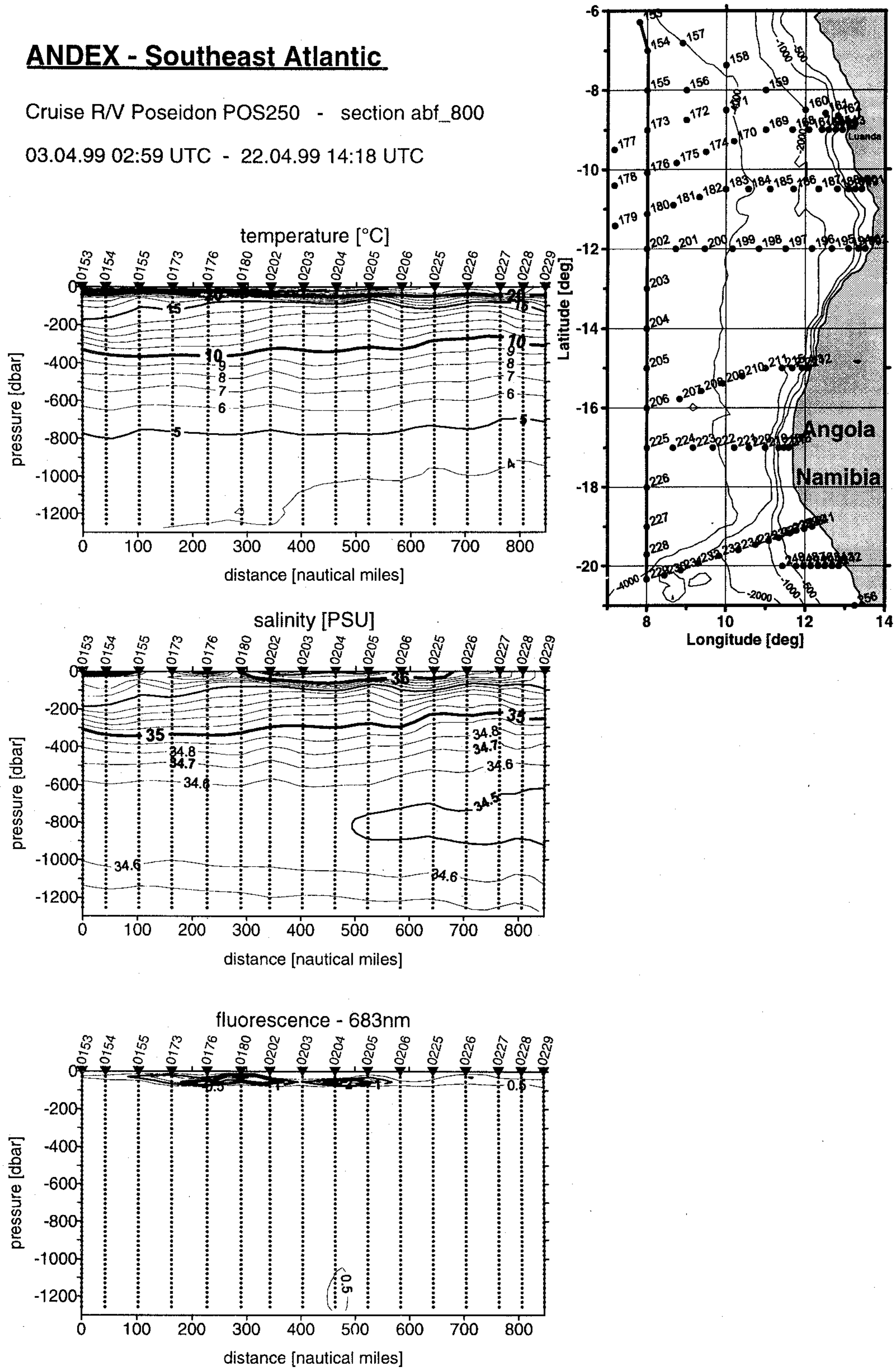

Figure 9.30: Vertical section of temperature, salinity and fluorescence at transect abf_800

ANDEX - Southeast Atlantic

Cruise R/V Poseidon POS250 - section abf_900

26.04.99 07:13 UTC - 26.04.99 21:57 UTC

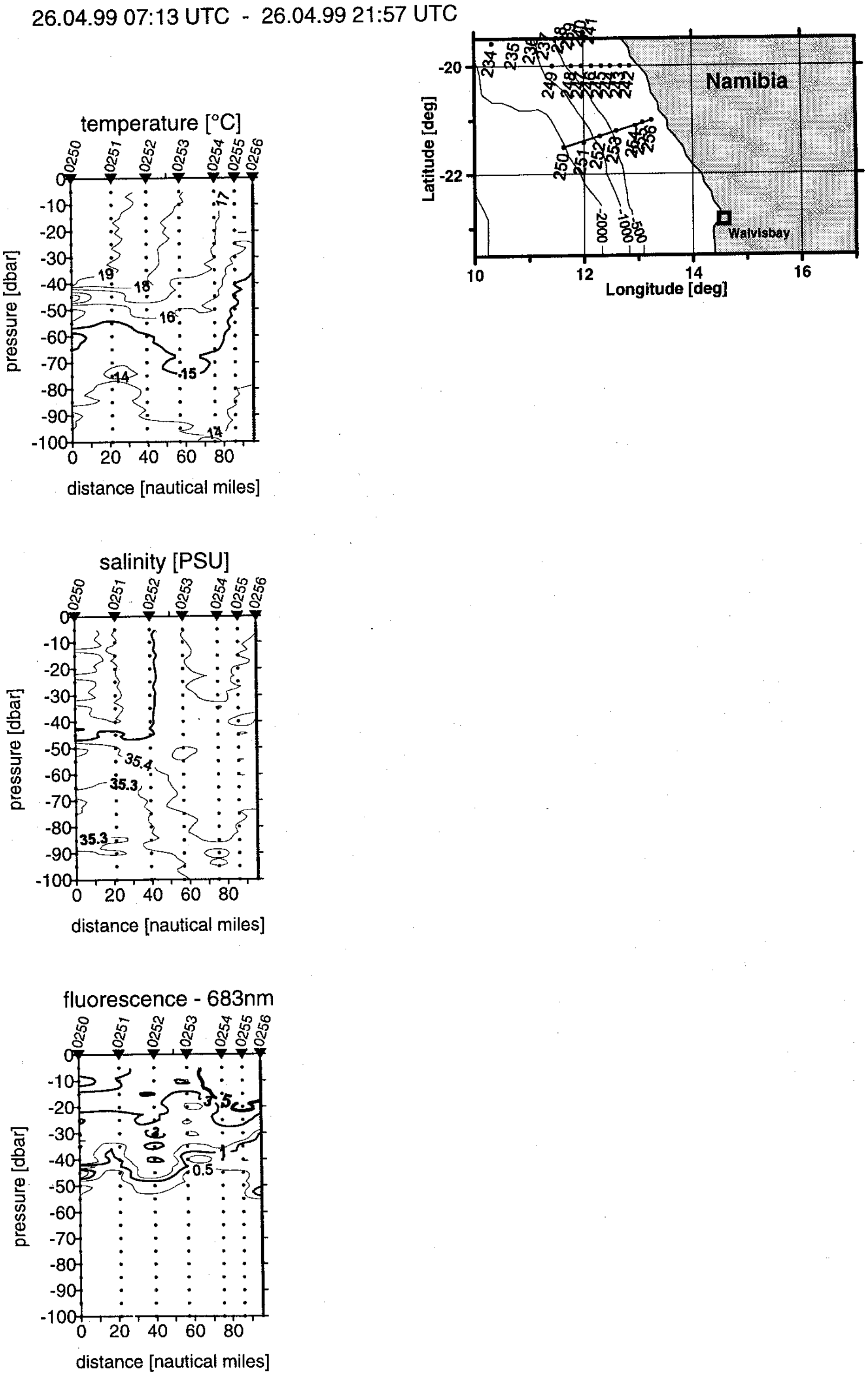

Figure 9.31: Vertical section of temperature, salinity and fluorescence at transect abf_900

ANDEX - Southeast Atlantic

Cruise R/V Poseidon POS250 - section abf_900

26.04.99 07:13 UTC - 26.04.99 21:57 UTC

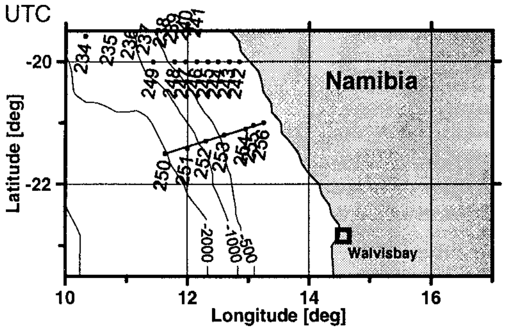

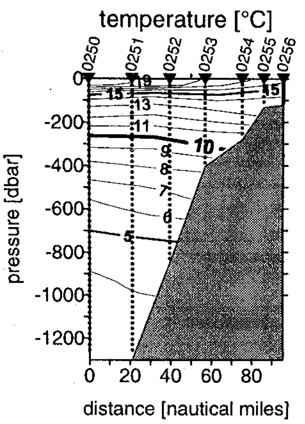

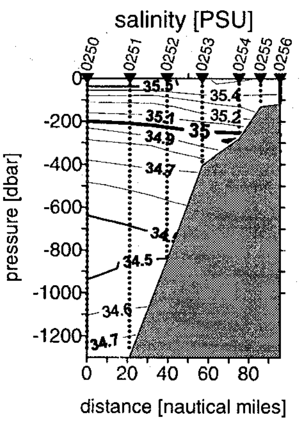

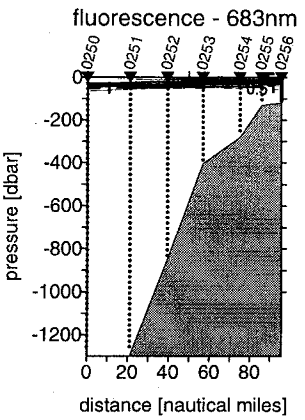

Figure 9.32: Vertical section of temperature, salinity and fluorescence at transect abf_900

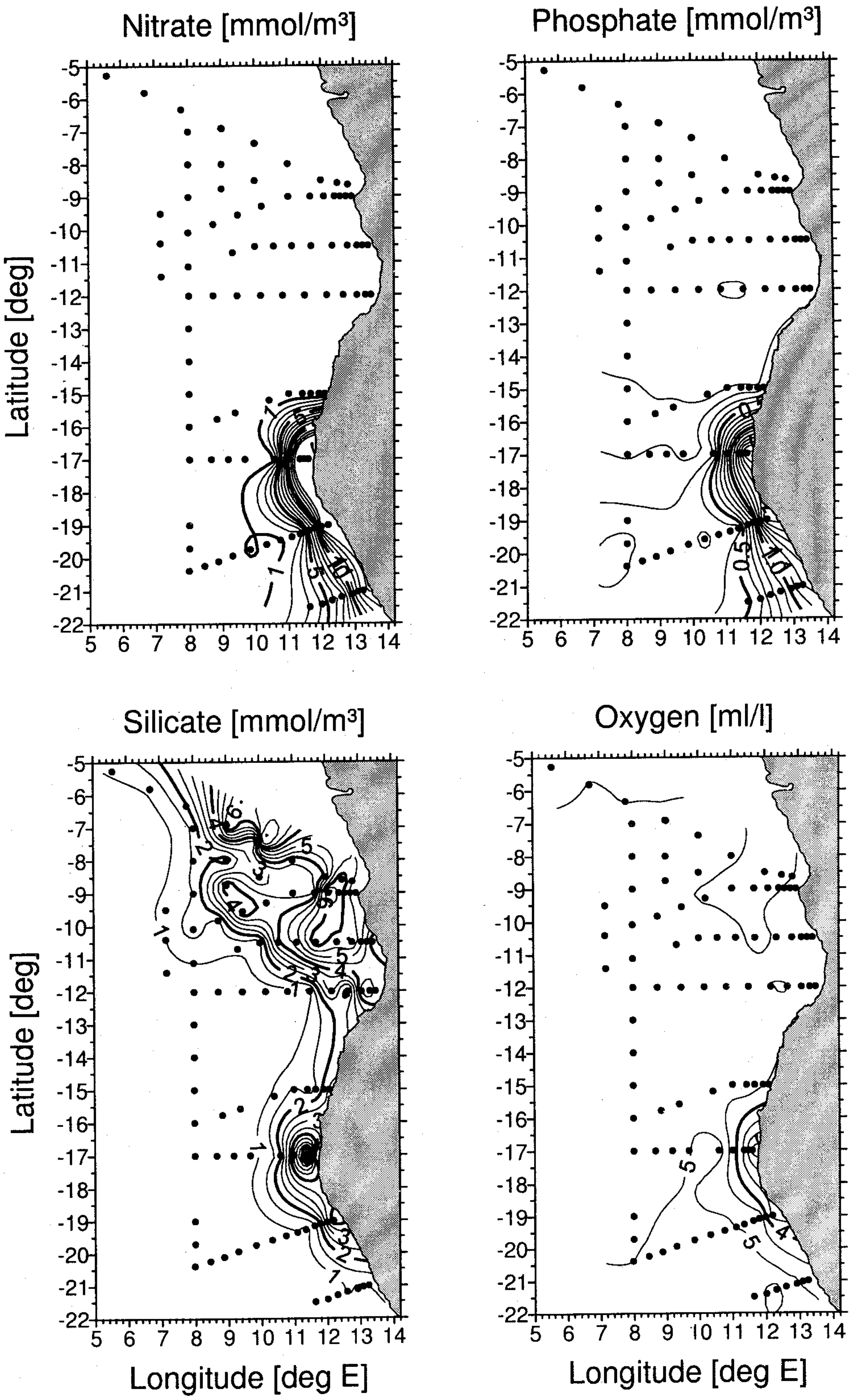

Figure 9.33: Horizontal distribution of nutrients and oxygen near the surface on the cruise POS250 (02. - 28. April 1999)

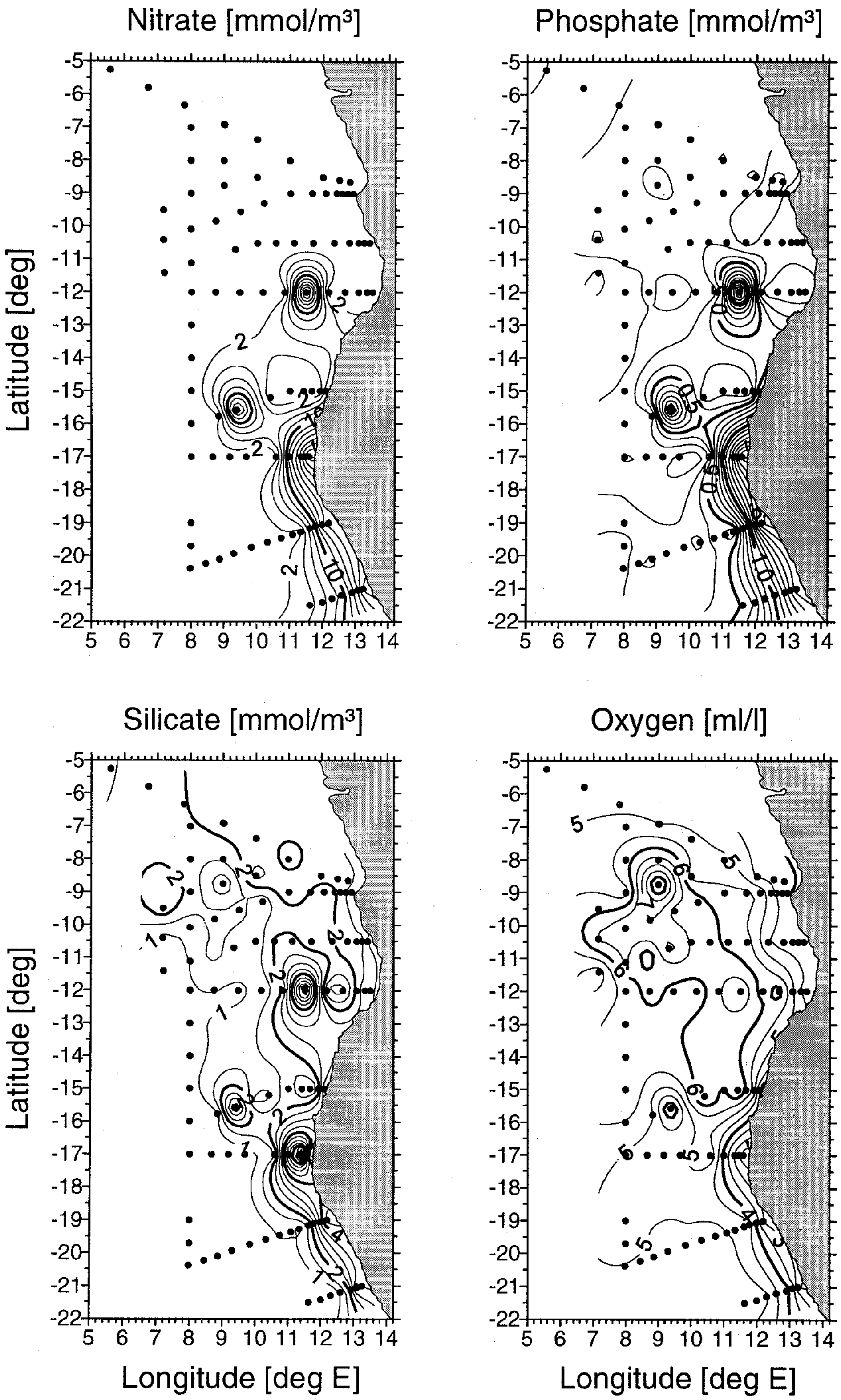

Figure 9.34: Horizontal distribution of nutrients and oxygen in 28 m depth on the cruise POS250 (02. - 28. April 1999)

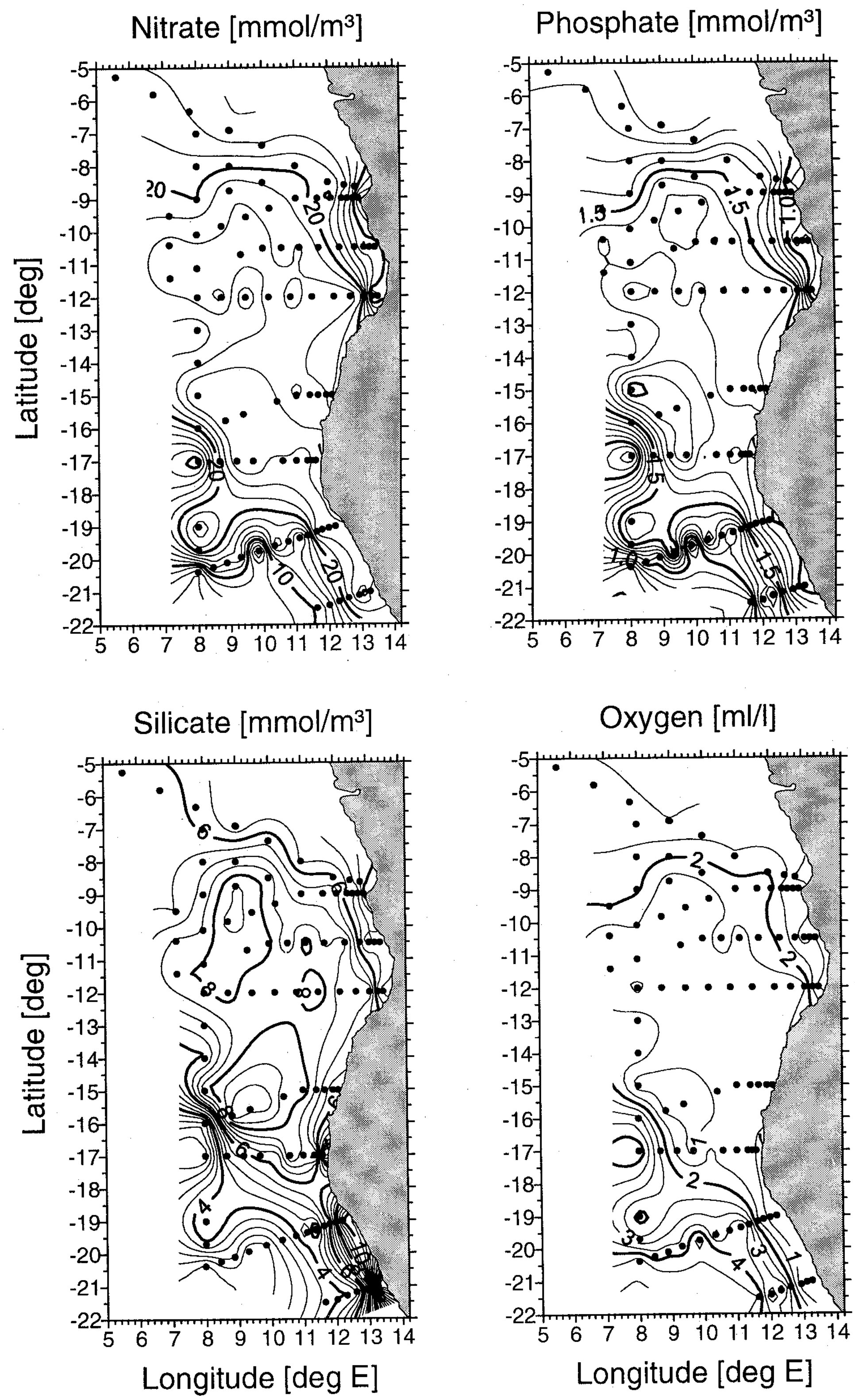

Figure 9.35: Horizontal distribution of nutrients and oxygen in 85 m depth on the cruise POS250 (02. - 28. April 1999)

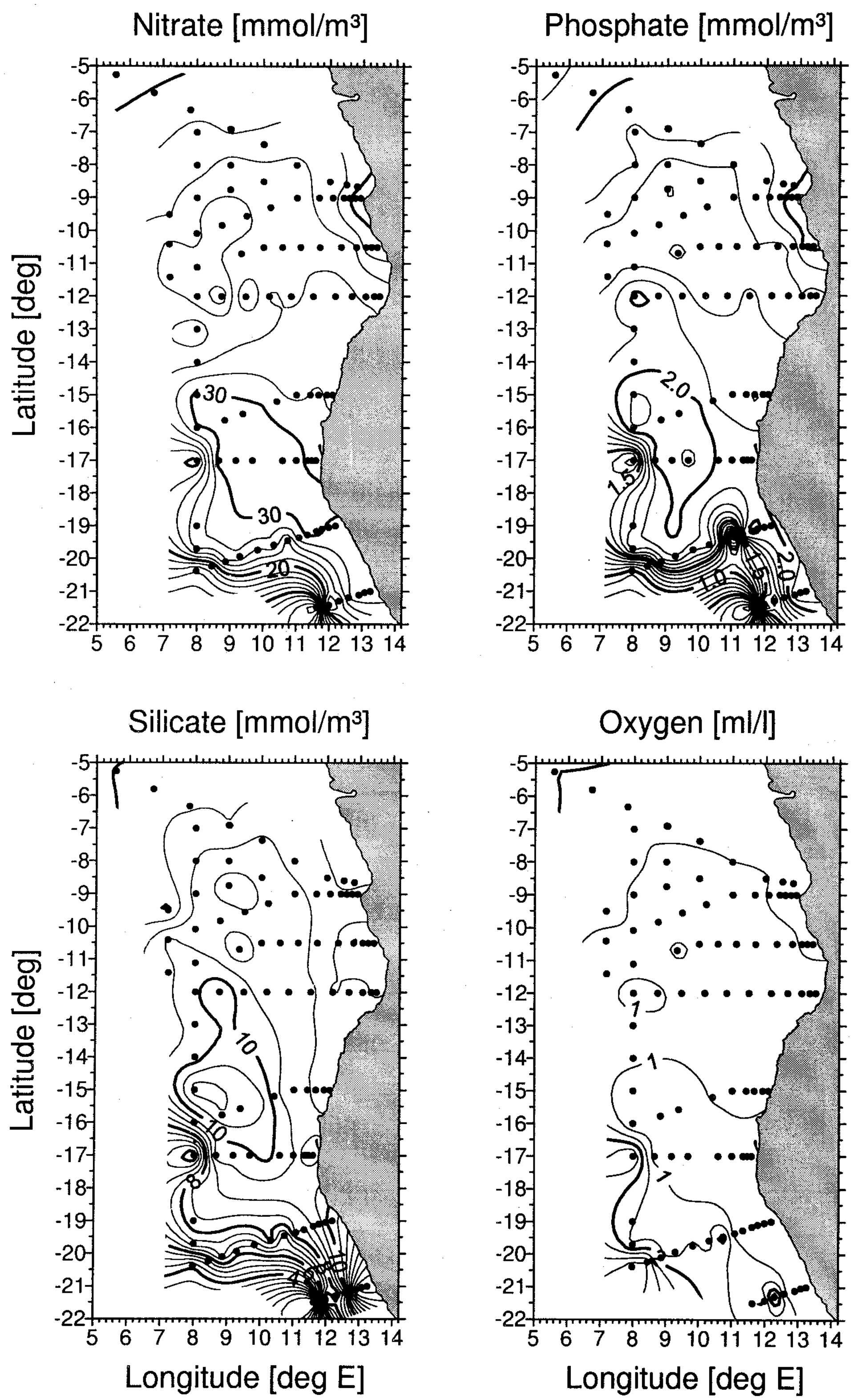

Figure 9.36: Horizontal distribution of nutrients and oxygen in 150 m depth on the cruise POS250 (02. - 28. April 1999)

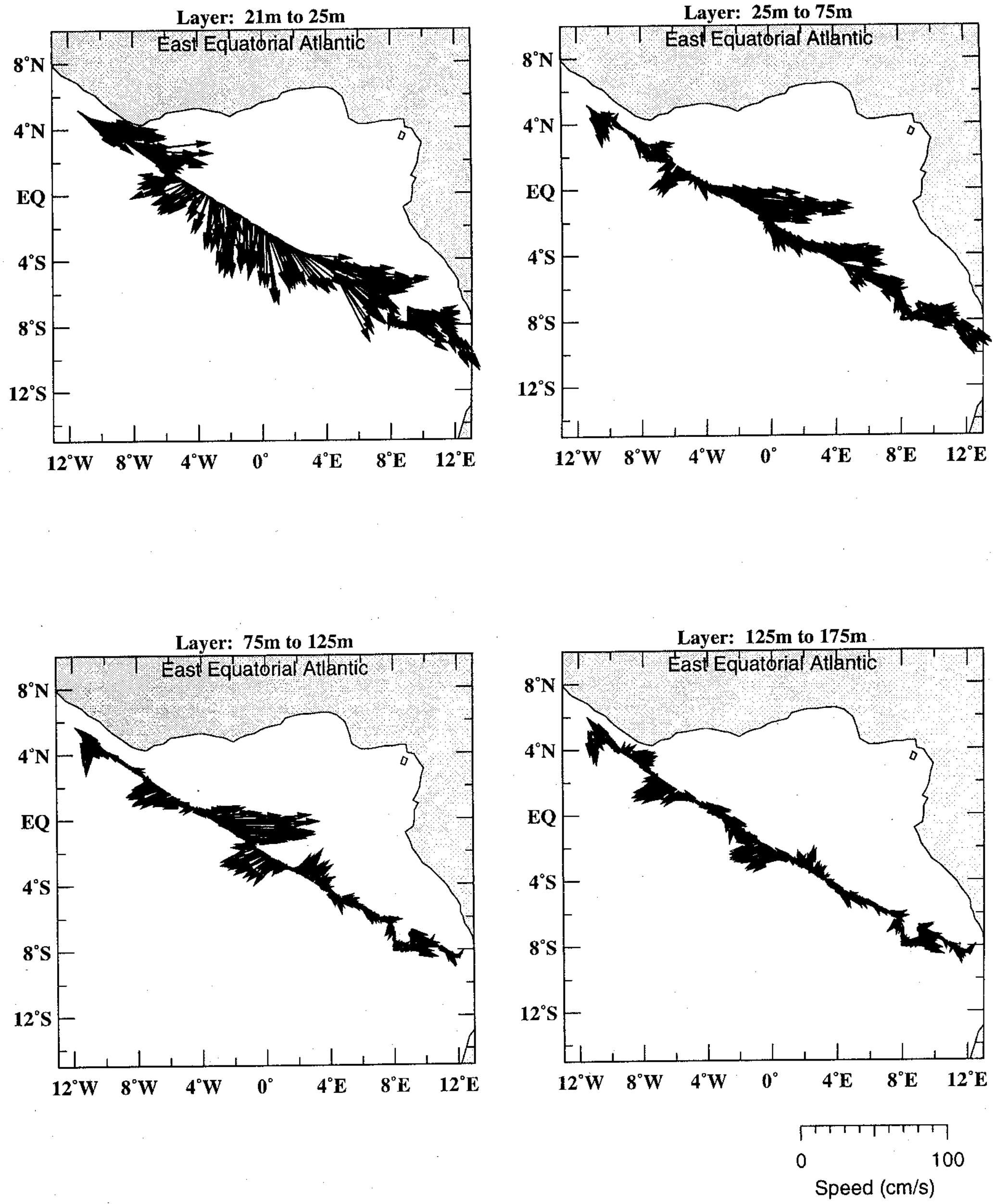

Figure 9.37: Current vectors in at levels 21-25 m, 25-75 m, 75-125 m and 125-175 m estimated from vessel mounted ADCP measurements. (02. - 28. April 1999)

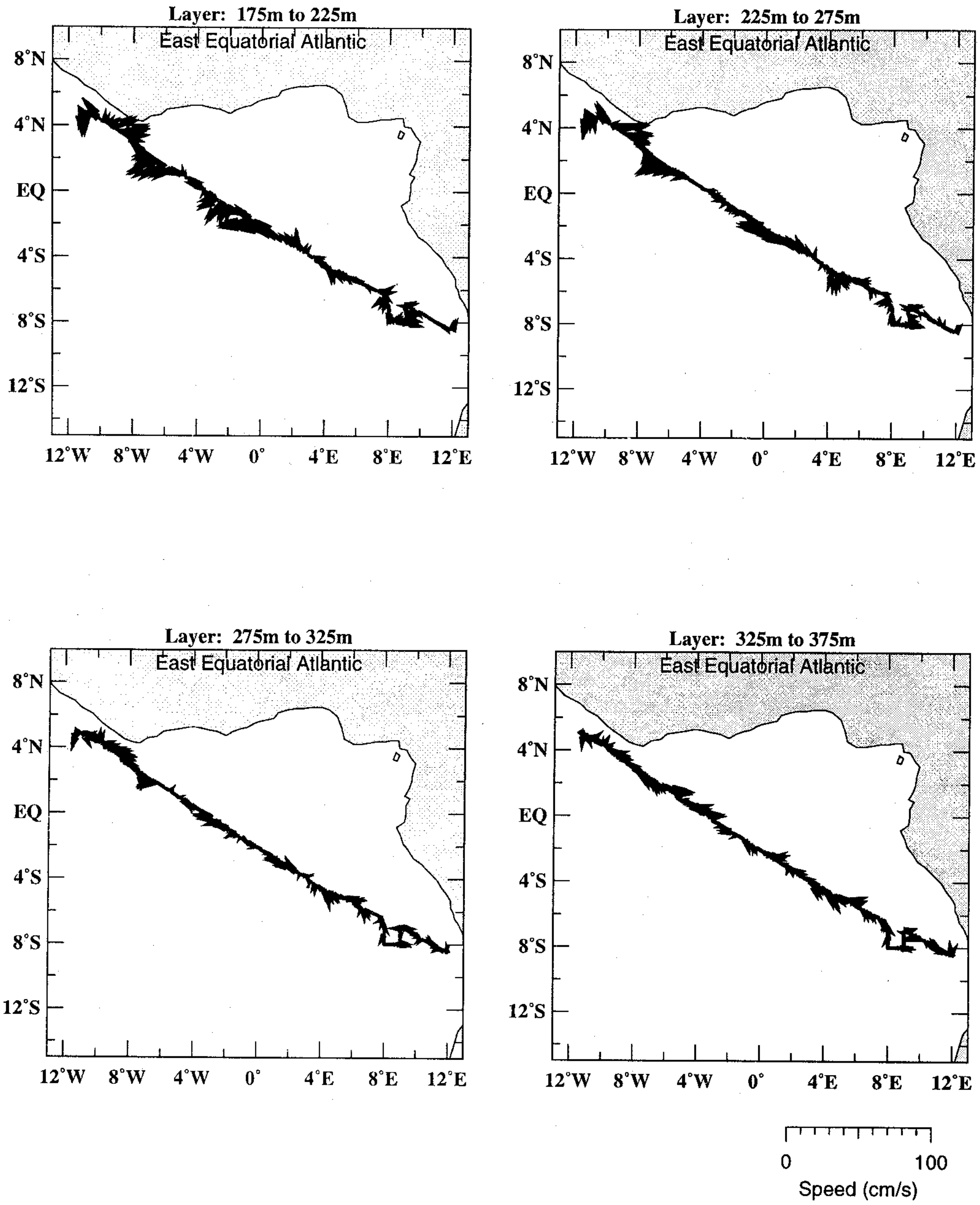

Figure 9.38: Current vectors at levels 175-225 m, 225-275 m, 275-325 m and 325-375 m estimated from vessel mounted ADCP measurements. (02. - 28. April 1999)

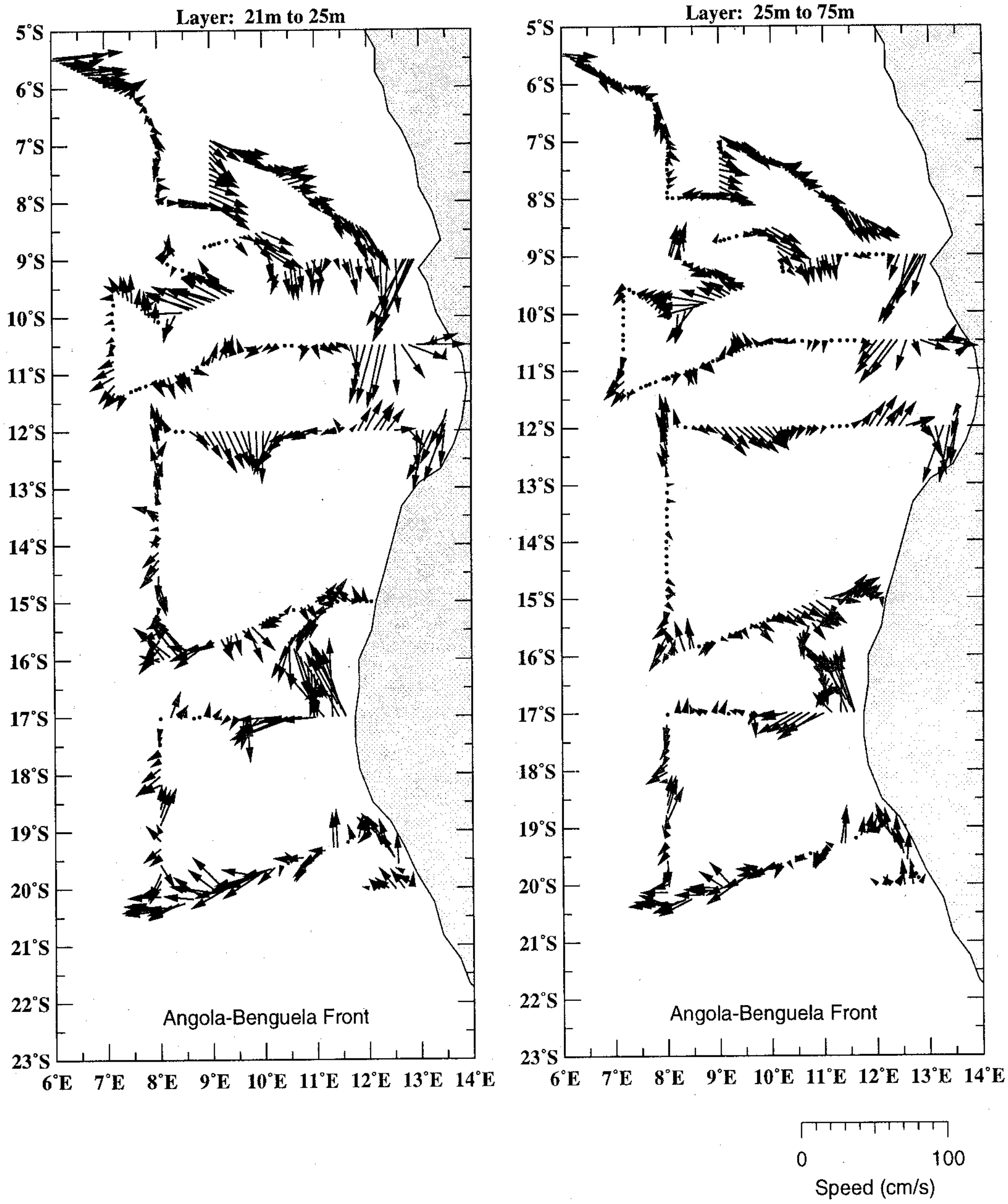

Figure 9.39: Current vectors at 21-25 m level and 25-75 m level, estimated from vessel mounted ADCP measurements. (02. - 28. April 1999)

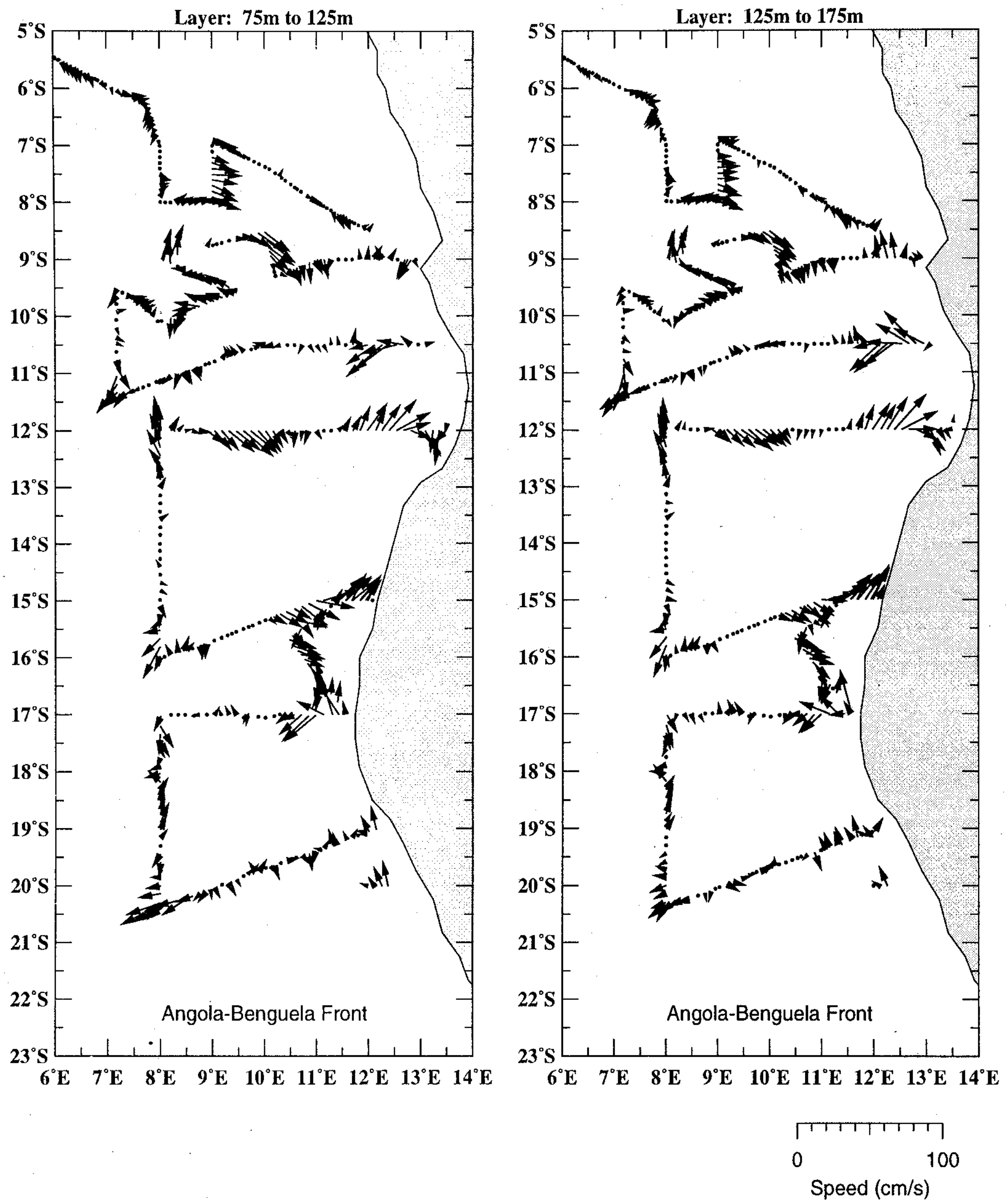

Figure 9.40: Current vectors at 75-125 m level and 125-175 m level, estimated from vessel mounted ADCP measurements. (02. - 28. April 1999)

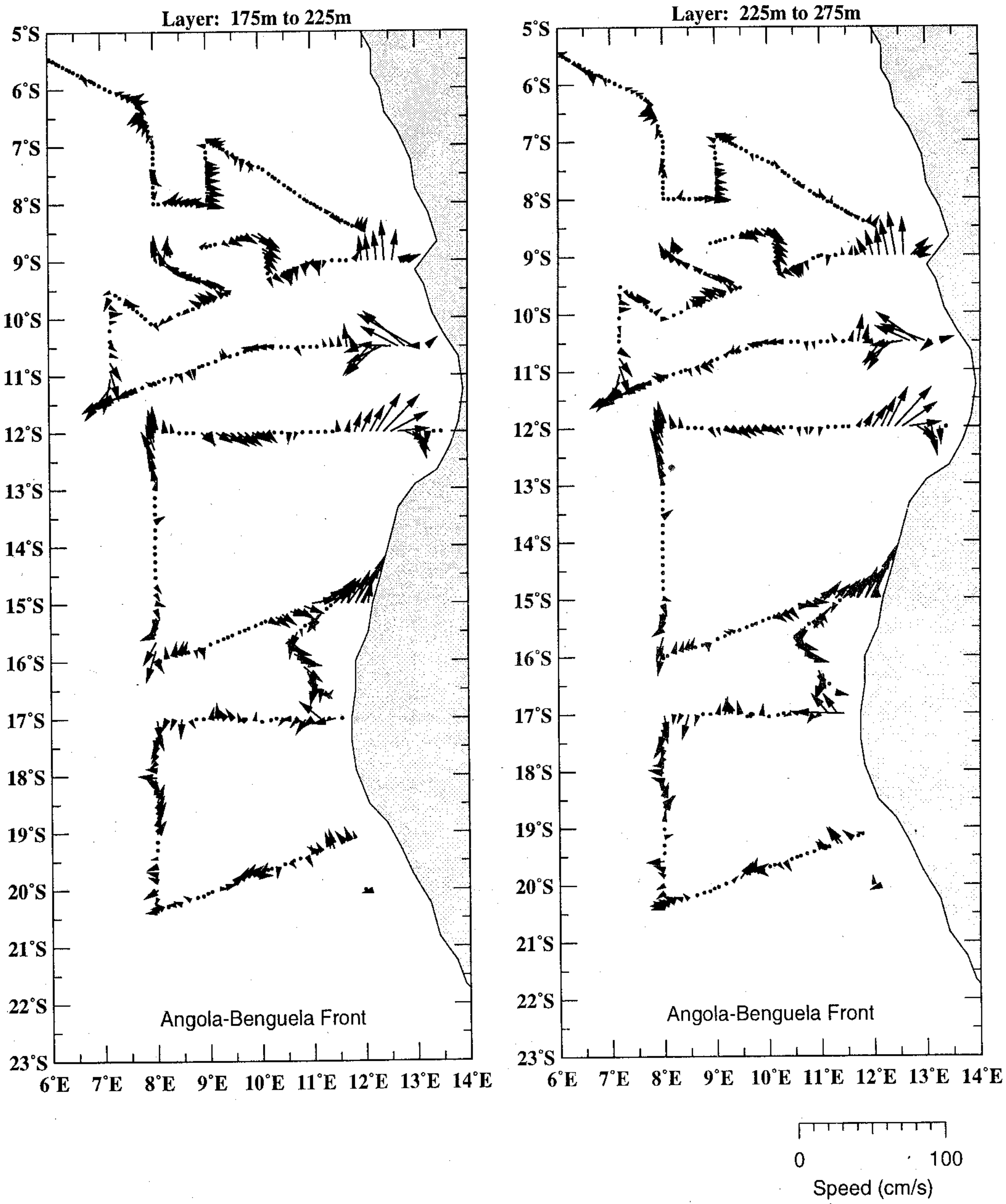

Figure 9.41: Current vectors at 175-225 m level and 225-275 m level, estimated from vessel mounted ADCP measurements. (02. - 28. April 1999)

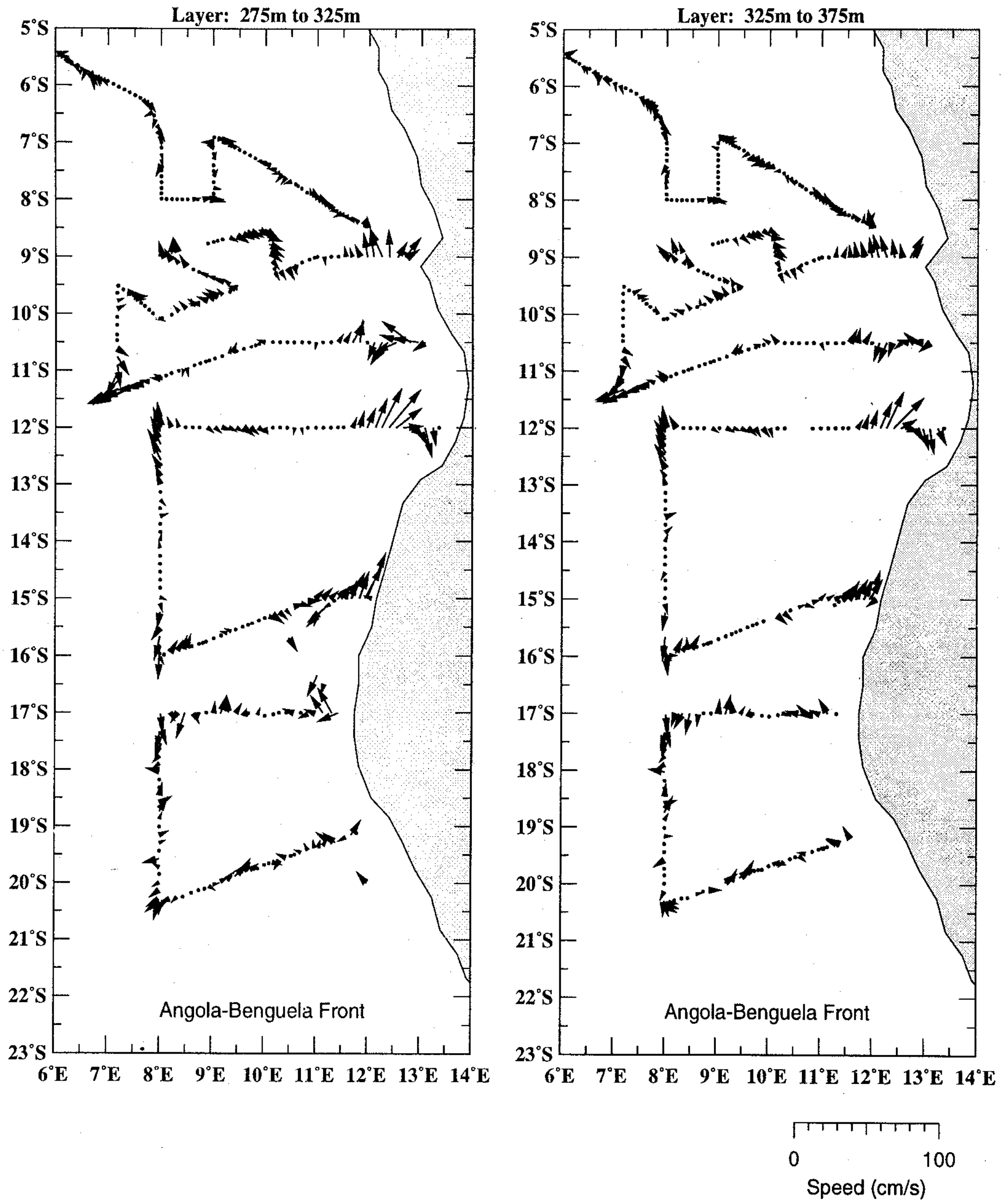

Figure 9.42: Current vectors at 275-325 m level and 325-375 m level, estimated from vessel mounted ADCP measurements. (02. - 28. April 1999)

9.2 Meteorological data

9.2.1 Air pressure and wind fields

Wind and air pressure are shown in Figure 9.43. The air pressure is permanently below 1015 hPa. This coincides well with climatological data. The zonal wind component is generally weak (well below 5 m/s) and comes from west on northern hemishere and oscillates on the southern hemisphere.

The meridional wind component is negative (from north) on the northern hemishpere and positive(from south) on the southern hemisphere reflecting mostly the trade winds. The meridional wind speed is generally mild except one strong wind event from 17th April to 21th April.

Figure 9.44 shows the air temperature, the relative humidity and the global solar radiation.

The cloud observations are summarized in Table 9.1.

One should keep in mind that the figures 9.43 to 9.44 show neither a time series nor a synoptic view. Thus for a better orientation with the plots figure 9.45 shows ships latitude and longitude as function of time.

9.3 Thermosalinograph

Figure 9.46 shows a quasisynoptic view of sea surface salinity (SSS) and sea surface temperature (SST) measured with the thermosalinograph. The most obvious structure in SSS are the strong salinity fronts at the equatorial transect, at 8° S and $10 - 12°$ S. SSS varies horizontally over about 4 PSU from 32 PSU in the north-east to more than 36 PSU in the south west of the area of investigation. The salinity minima correspond to the observed river plumes at the equatorial transect with significantly different water colour and that one observed off Angola with lots of drifting plants and waste.

The SST pattern is obviously correlated with the SSS pattern. The less saline water is significanly warmer than the water in the south-west with SACW characteristics. This indicates the important role of advection in the water mass formation. The correspondence with the VMADCP data is not clear since no surface data are available and the strong stratification below the surface mixed layer may correspond to a large vertical shear of the horizontal flux.

The Angola-Benguela front can be seen in the SST at about 16° S near the Namibian coast.

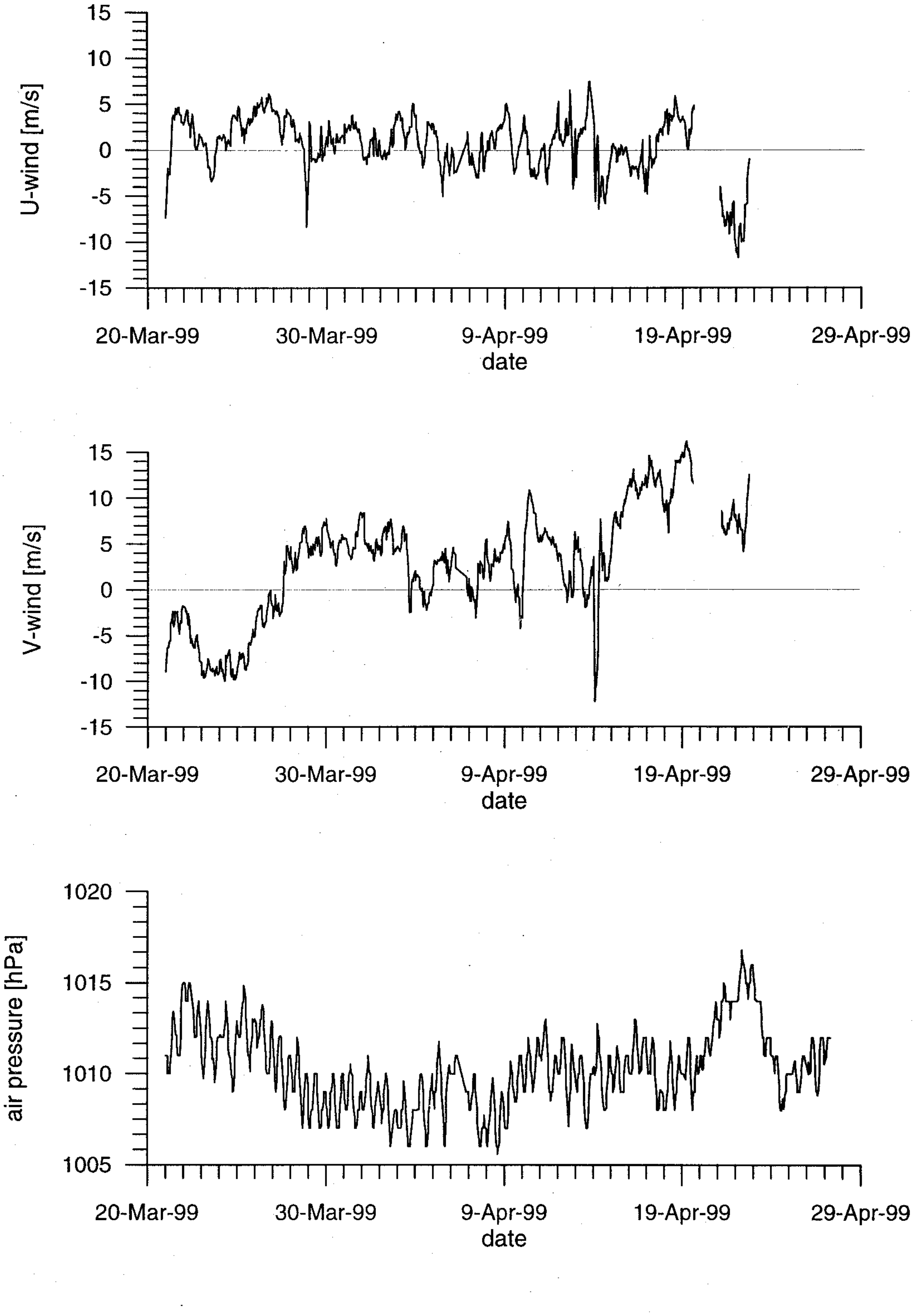

Figure 9.43: Zonal and meridional wind component and air pressure as function of time on the cruise POS250 (02. - 28. April 1999)

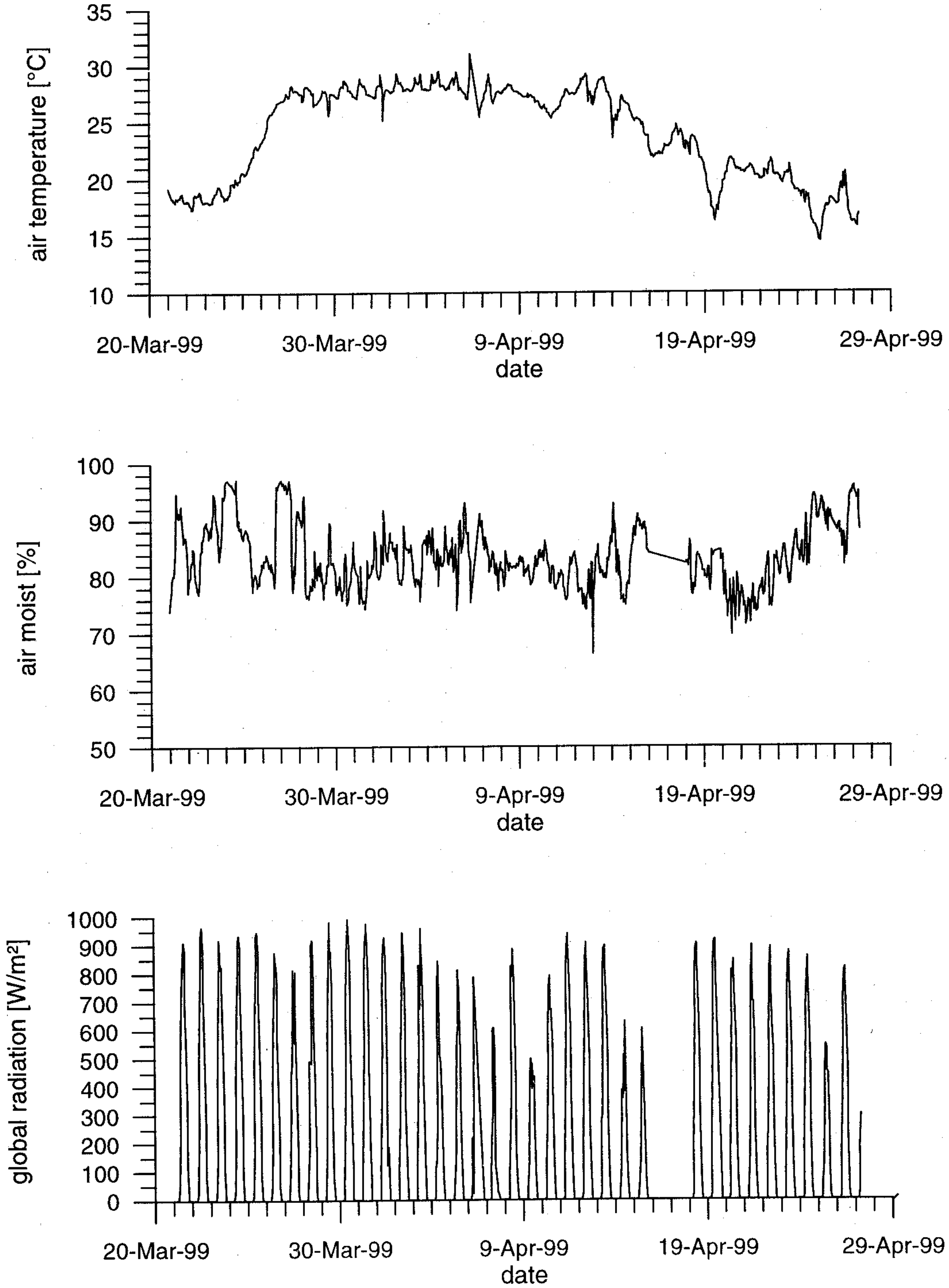

Figure 9.44: air temperature, relative air humidity and global radiation as function of time on the cruise POS250 (02. - 28. April 1999)

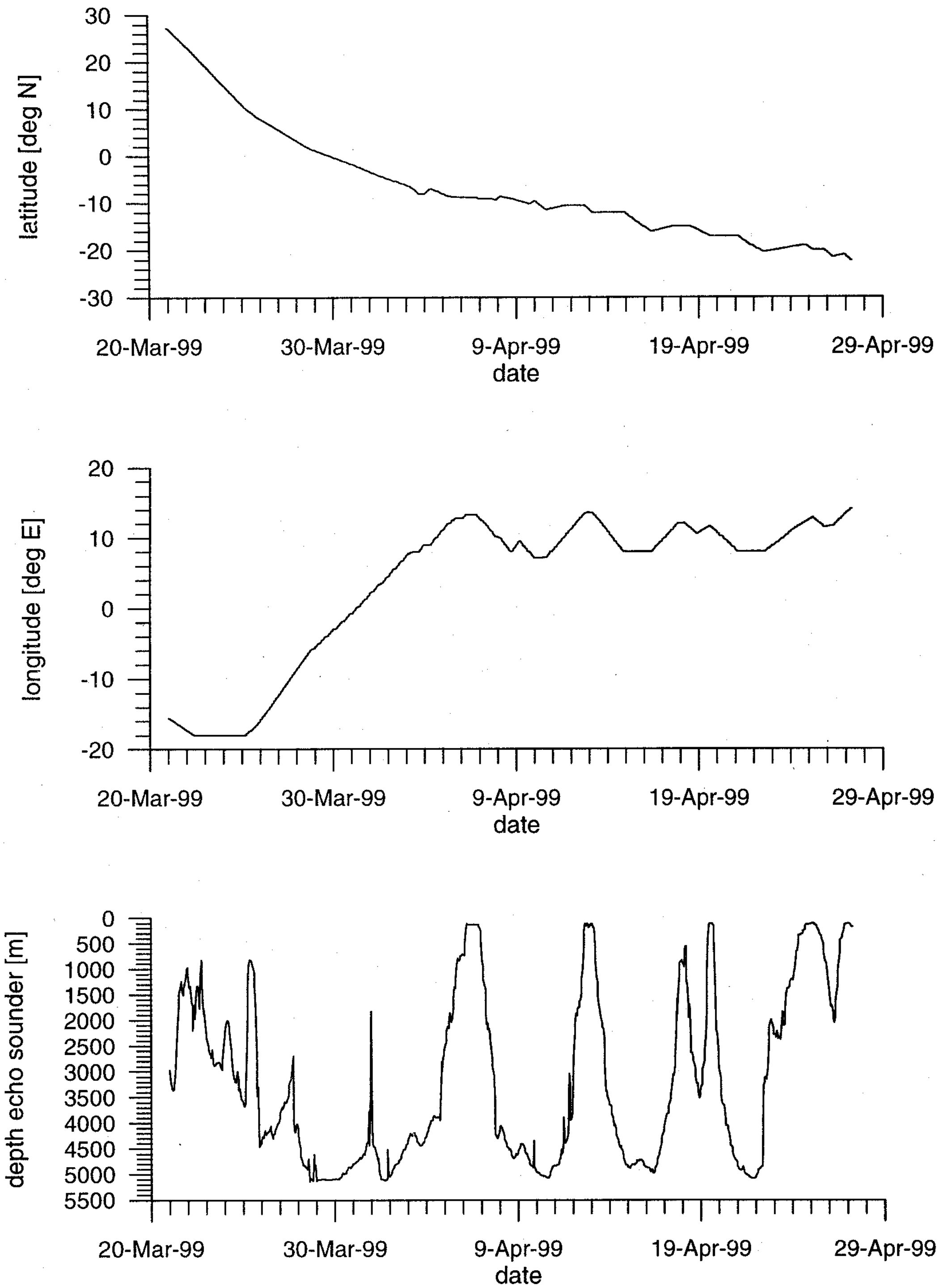

Figure 9.45: Ship's position as function of time on the cruise POS250 (02. - 28. April 1999)

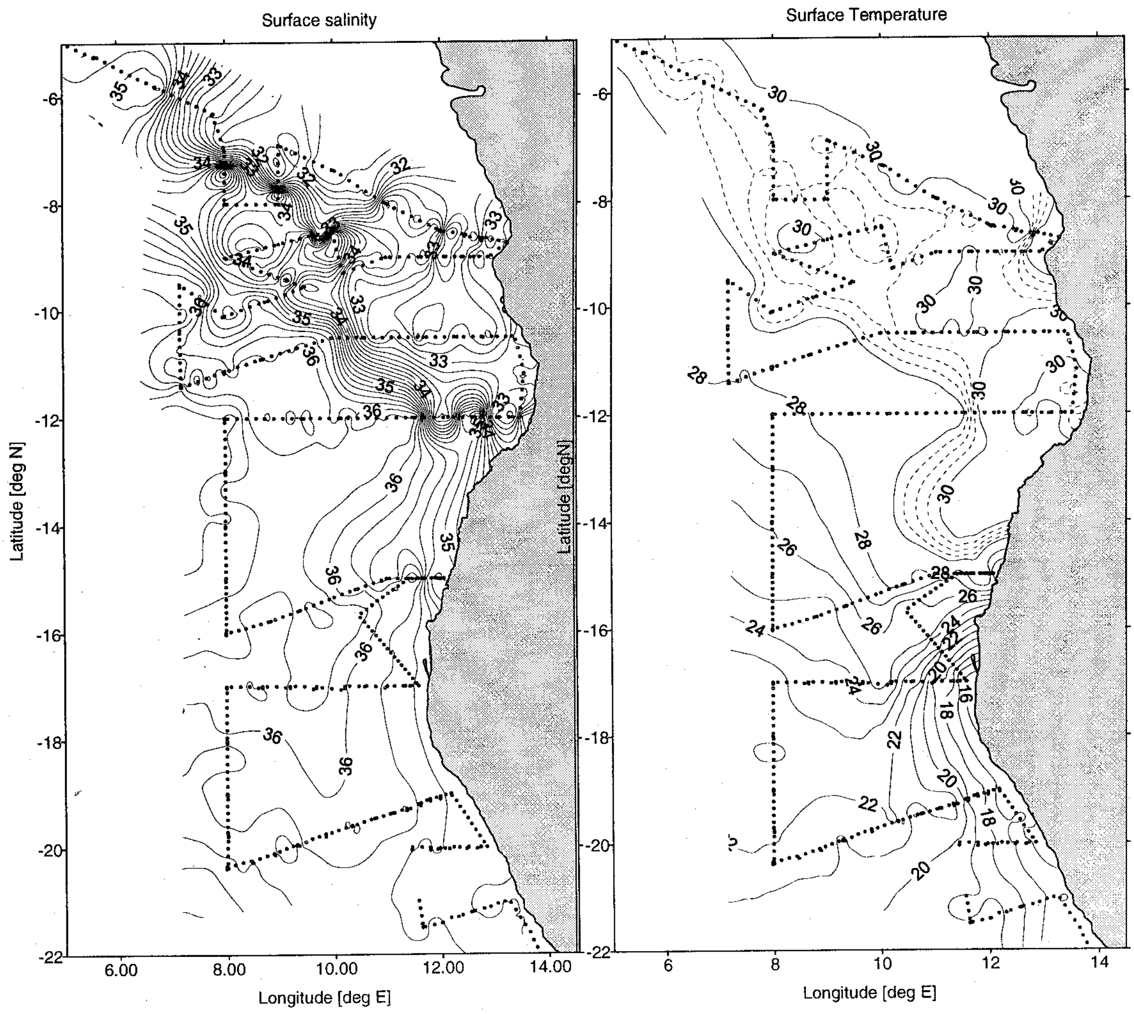

Figure 9.46: Quasisynoptic view of the sea surface salinity (left pannel) and sea surface temperature (right pannel) on cruise POS250 (02. - 28. April 1999)

Table 9.1: Cloud observation

date	time	latitude	longitude	ci	low_cl	mid_c	high_cl	comments
29.03.	06:50	0° 56.222	−4°-59.062	6	Cu		CI	
29.03.	12:00	0° 33.233	−4°-16.313	2	Cu		CI	
29.03.	18:00	0° 15.776	−3°-50.754	2	Cb		CI	shower
30.03.	06:00	0°-25.900	−2°-40.576	3	Cucon		CI,Cf	
30.03.	08:00	0°-34.147	−2°-24.661	1			Cf	vgv
30.03.	12:00	0°-54.834	−1°-51.923	2	Cuhum			vgv
30.03.	18:00	−1°-13.090	−1°-22.386	1	Cuhum			vgv
31.03.	06:00	−1°-59.502	0° -6.062	1	Cuhum			vgv
31.03.	12:00	−2°-22.147	0° 27.882	1	Cu			vgv
31.03.	18:00	−2°-51.853	1° 19.037	2	Cu			
01.04.	06:00	−3°-35.176	2° 29.042	2	Cucon	Actra		vgv
01.04.	12:00	−4° -7.424	3° 23.311	3	Cucon			gv
01.04.	18:00	−4°-18.806	3° 41.892	5	Cb	Actra		rainstorms
02.04.	08:00	−5°-15.581	5° 35.101	6	Cucon		Cc	vgv
02.04.	12:00	−5°-21.140	5° 50.287	3		Actra	Cispi	vgv
02.04.	18:00	−5°-47.858	6° 43.075	4	Cuhum		Cc	vgv
03.04.	06:00	−6°-30.410	7° 50.879	7		Actra		vgv
03.04.	14:00	−7°-37.700	8° 0.055	4	Cucon			vgv, haze
03.04.	18:00	−7°-59.803	8° 5.879	3	Cucon		Ciunc, Cc	vgv
04.04.	06:00	−7° -1.537	9° 0.187	7	Cucon	Actra		gv,calm, lightning
04.04.	12:00	−7° -8.985	9° 32.356	7	Cucon	AS,AC		gv,calm
04.04.	18:00	−7°-29.187	10° 12.734	4	Cucon	Actra		gv
05.04.	06:00	−8°-25.597	11° 51.447	6	Cucon, Cucap		Cf	gs, lightning
05.04.	12:00	−8°-33.341	12° 18.620	3	Cucon, Cucap		Cc	vgv
05.04.	18:00	−8°-39.717	12° 48.349	7				
06.04.	06:00	−8°-42.727	13° 9.317	6		Actra	CI	vgv
07.04.	06:00	−8°-59.991	12° 11.699	7	Cucon	AC	Cc	gv
07.04.	12:00	−8°-59.915	11° 30.619	8				
07.04.	18:00	−9° -7.614	10° 39.039	7				
08.04.	06:00	−8°-35.342	9° 38.083	7	Cucon		Cc	vgv
08.04.	12:00	−8°-47.511	8° 49.869	5	Cucon	Actra	Cc	vgv
09.04.	06:30	−9°-34.932	9° 24.689	7	Cucon	AC		gv
09.04.	13:45	−9°-56.221	8° 24.947	7	Cucon	Actra	Cc	gv
10.04.	06:00	−10°-17.273	7° 9.881	7	Cufra		CI,Cs	gv
10.04.	18:00	−11°-19.481	7° 26.346	7	Cucon	AC	Cs	gv
11.04.	06:00	−10°-51.424	8° 48.647	3	Cufra		CI,Cs	gv

Table 9.1: Cloud observation (continued)

date	time	latitude	longitude	ci	low_cl	mid_c	high_cl	comments
11.04.	09:30	−10°-42.033	9°19.794	1				gv, N0159
11.04.	12:00	−10°-36.810	9°36.544	1	Cufra			
12.04.	06:00	−10°-30.166	11°52.186	5	Cucon		Cf	gv
12.04.	08:45	−10°-29.844	12°19.988	4	Cucon		Cf	gv
12.04.	12:00	−10°-29.985	12°44.330	0				
12.04.	13:15	−10°-29.988	12°48.098	1	Cbcap		Cf	
12.04.	16:00	−10°-29.882	13°11.054	6	Cbcap		CI,Cs	
12.04.	16:45	−10°-30.035	13°15.229	7	Cbcap		CI,Cs	
13.04.	06:00	−12° -0.029	13°19.922	5	Cufra	Actra		gv
13.04.	08:45	−12° -0.525	13° 3.401	1	Cucon		Cc	gv
13.04.	12:43	−12° -0.005	12°33.638	1			Cc	gv
13.04.	17:00	−11°-59.950	11°58.494	2	Cbcap	AS	Cs	vgv
14.04.	06:00	−12° -0.377	10°10.063	5		NS		gv
14.04.	10:00	−11°-59.750	9°29.478	7		NS	Cc	gv
14.04.	16:20	−12° -0.276	8°44.251	5		Actra	Cc,Cf	vgv
15.04.	06:30	−12°-59.971	7°59.724	7	Cufra	Actra		gv
15.04.	13:00	−13°-50.450	8° 0.057	4	Cucon	Actra		gv
15.04.	15:00	−14° -0.078	7°59.563	5	Cucon			gv
16.04.	06:00	−15°-38.164	8° 0.127	4		Actra	Cc	gv
16.04.	10:30	−16° -0.959	7°59.686	1	Cucon			vgv
16.04.	17:00	−15°-46.626	8°48.974	7	Cufra		Cc	gv
17.04.	06:00	−15°-16.416	10°12.106	6		Actra		gv
17.04.	07:30	−15°-12.003	10°24.710	4		Actra	Cc	vgv
17.04.	17:00	−14°-59.995	11°30.801	1			Cf	gv
18.04.	06:00	−14°-59.927	11°58.565	1			Cc	gv
18.04.	08:00	−15° -0.006	11°48.543	2			Cispi	gv
18.04.	09:30	−14°-59.935	11°39.792	0				gv
18.04.	17:00	−15°-17.728	10°59.817	0				ms,gw, seaspray
19.04.	06:00	−16°-19.574	11° 1.252	1	Cufra			gv,gw
19.04.	12:00	−16°-47.925	11°25.287	0				gv,gw
19.04.	15:00	−17° -0.121	11°34.694	0				gv
20.04.	06:00	−17° -0.617	10°11.868	5	Cufra		Cf	gv
20.04.	10:15	−16°-59.972	9°41.626	4	Cucon			gv
20.04.	16:00	−17° -0.101	9°10.415	6	Cufra			vgv
21.04.	06:00	−17°-17.100	7°59.881	7	Sc			gv
21.04.	14:00	−18°-11.313	8° 0.028	1	Sc			gv
21.04.	17:30	−18°-40.765	8° 0.005	4	Cucon		Cf	gv

Table 9.1: Cloud observation (continued)

date	time	latitude	longitude	ci	low_cl	mid_c	high_cl	comments
22.04.	06:00	−19°-46.562	8° 0.739	4	Cuhum			gv
22.04.	17:00	−20°-17.709	8°10.554	1	Sccu			gv
23.04.	06:00	−19°-55.914	9°17.953	5	Sc			gv
23.04.	13:30	−19°-45.337	9°49.518	0				vgv
23.04.	17:00	−19°-38.230	10°10.222	0				gs,gw
24.04.	06:00	−19°-16.545	11°20.365	3	Cufra	Acflo		
24.04.	09:20	−19°-11.223	11°34.488	6	Cuhum			gv
24.04.	11:10	−19°-13.431	11°36.288	3	Cuhum			gv
24.04.	14:00	−19° -8.184	11°47.310	5	Cufra			gv
24.04.	17:00	−19° -5.615	11°58.623	5	Cufra			gv
25.04.	06:00	−20° -0.084	12°46.336	7	Sc			gv
25.04.	12:00	−20° -0.881	12° 8.827	8	Sc			gv
25.04.	17:00	−20° -2.815	11°47.367	8	Sc			gv
26.04.	06:00	−21°-21.894	11°37.093	1	Cufra	AC		gv
26.04.	07:30	−21°-30.085	11°37.710	6	Cufra			gv
26.04.	10:13	−21°-25.165	11°59.024	2	Cufra			gv
26.04.	13:00	−21°-17.874	12°16.103	0				gv
26.04.	16:00	−21°-11.913	12°35.923	0				gv

List of abbreviations

Cu	Cumulus	CI	Cirrus
Cucon	Cumulus congestus	Cf	Cirrus fibratus
Cuhum	Cumulus humilis	Cc	Cirrocumulus
Cucap	Cumulus capillatus	Cs	Cirrostratus
Cufra	Cumulus fractus	Cispi	Cirrus Spissatus
Cb	Cumulonimbus	Ciunc	Cirrus unicus
Cbcap	Cumulonimbus capillatus		
Sc	Stratocumulus		
Sccu	Stratocumulus cumulogenitis		
AC	Altocumulus	vgv	very good visibility
Actra	Altocumulus translucidus	gv	good visibility
Acflo	Altocumulus floccus	mv	medium visibility
AS	Altostratus		
NS	Nimbostratus	gw	gale force wind

9.4 Ichthyoplankton diversity, abundance and vertical distribution in the South East Atlantic Equatorial Current Region

9.4.1 Introduction

The general background of the biological survey

Besides taxonomy and systematics, marine biogeography is the main task of the Taxonomische Arbeitsgruppe (TAG). TAG runs a long-term project to describe the species composition of fish larvae in the Atlantic Ocean, and their specific abundances and vertical distributions. The horizontal and vertical patterns found are explained in a multidisciplinary context, using in-situ as well as literature data. The survey described below covers an area so far mainly investigated by non-quantitative methods, contrary to the NW African area. For reviews see HEMPEL (1982), JOHN and ZELCK (1997), or for Namibian waters OLIVAR and SHELTON (1993).

The actual contexts of the biological surveys

1. Zonal equatorial currents

The biological literature is highly contradictory in respect to the colonization of the equatorial islands in the Atlantic Ocean, whether their fauna is replenished from the American or African continents, respectively, see e.g. BRIGGS (1974), SCHELTEMA (1986) and literature therein. Historical conclusions were generally based on only surface current systems, plus the occurrence of amphiatlantic species, and often (although not exclusively) suggest gene flow westwards. More quantitative faunistic comparisons, however, suggest an eastward dispersal from Brazil, EDWARDS and LUBBOCK (1983). So far, no studies are known to have traced the occurrence, depth distribution, or abundance gradients of planktonic organisms in respect to individual components of the equatorial current system, which show a high complexity of opposite current directions both horizontally (within scales as narrow as two degrees of latitude) and vertically (within some tens of meters near the surface, or some hundred meters down to at least 1200 m depth). For details see e.g. STRAMMA and SCHOTT (1996), and literature therein.

2. Eastern boundary currents, undercurrents and biogeography

VOITURIEZ and HERBLAND (1982) suggested that eastward equatorial currents and, particularly, undercurrents are retroflected polewards at the African continental slope, feeding poleward slope undercurrents formerly believed to be individual parts of upwelling ecosystems. MITTELSTAEDT (1989) suggested that these slope undercurrents are in fact one spatially consistent and permanent current (although superimposed by seasonal and shorter signals), which reaches temperate latitudes at least off NW Africa and Europe. For this hypothesis multidisciplinary surveys including plankton investigations yielded evidence (Stöhr et al. 1997, JOHN and ZELCK 1997, JOHN et al. 1998). Consequently, distribution patterns of slope-dwelling ("pseudoceanic") meso- and benthopelagic species contrast widely from those controlled by the surface flow or temperature field.

3. The role of subthermoclinal domes and frontal zones

VOITURIEZ & HERBLAND (1982) also suggested that further retroflections of the poleward undercurrents occur at the subthermoclinal domes in the eastern Atlantic, see e.g. SIEDLER et al. (1992), and literature therein. Polewards of these domes (Guinea Dome in the north, Angola Dome in the south) frontal zones separate tropical from subtropical-temperate water masses (e.g. KLEIN (1992) for the Cape-Verde-Frontal-Zone "CVFZ" and MEEUWIS and LUTJEHARMS (1990) for the Angola-Benguela-Front "ABF"). These fronts coincide with a change from tropical to subtropical shore fish species, or even cold-water forms in upwelling areas (MAURIN (1968), PENRITH 1978). For NW Africa it has been proven that the CVFZ is tresspassed by the descending slope undercurrent, South Atlantic Central Water filaments offshore, and current branches recirculating around the Guinea Dome into the North Equatorial Current (HAGEN and SCHEMAINDA (1984) and (1987), FIEKAS et al. (1992), MITTELSTAEDT (1991). JOHN and ZELCK (1997) showed that all these branches entrain fish larvae. The quantitative ichthyoplankton data south of the Angola Dome (JOHN and ZELCK, 1998) yielded most of the biological tracers used off NW Africa. Some of the very same tracers were also found south of the ABF off northern Namibia, OLIVAR and FORTUÕ (1991). On basis of a hypothesis of symmetrical systems on both hemispheres it is herewith postulated, that tresspassing by a slope undercurrent, filaments, and recirculation into the South Equatorial Current occurs at the ABF, too.

4. The training component

Scientists from the adjacent countries Angola and Namibia used the biological survey to learn how to handle modern plankton samplers, from preparing and shooting the net, data recording, saving the catch, to microscopical analysis of the zooplankton composition. They learned the ecological significance of the major zooplankton orders, methods of ichthyoplankton identification, and to distinguish those fish larvae which may serve as tracers for advective processes into (or out of) their home areas.

9.4.2 Methods

Equipment

1. The biological sampling was done by an obliquely-towed Hydro-Bios multiple-opening-closing-net (MCN) and a neuston net (NEU) after DAVID. Sampling depths of the neuston nets were the microlayers 0 to 8 cm (upper net) and 10 to 25 cm (lower net). The MCN sampled the depth layers 200 to 150 m, 150 to 100 m, 100 to 50 m, 50 to 25 m and 25 to 0 m, unless bottom depths shallower than 200 m interfered.

The survey strategy

Using a ship of opportunity meant to compromise in the overall cruise track, staff, station location and -time, and lab space (not to mention bad weather...). Furthermore, quantitative plankton analysis is too time consuming to sample a station grid such as that covered by the physical oceanographers. Consequently, a "meridional" transect across the Equatorial Current system from the southern limit of the EEZ off Ivory Coast towards Luanda actually slanted east-southeast (Figure 2.1). Its projected meridional spacing of approximately 32 nautical miles (n.m.) gave a representative coverage of the zonal current system. This transect will below be referred to as the Equatorial transect.

The biological tracers found useful by JOHN and ZELCK (1997) are a mixture of larvae of open-ocean mesopelagic species, teleplanktonic neritic larvae of widely differing depth ranges, and neritic larvae of short planktonic phase. Therefore, a truly meridional transect along 8°E was run from 6.5°S to 20°S, to obtain the "normal" open ocean species composition, vertical distribution and the respective faunistic boundaries, previously unknown for the eastern Atlantic. Cross-slope profiles were (besides the data from "Meteor" cruise 28 along 11.5°S) one transect along 17°S, and a second transect slanting east-northeast and crossing 20°S offshore at 9°E. This transect named here the NE-transect (abf_700 in Figure 2.2) was expected to be long enough to cover the postulated filaments in the open ocean. Furthermore a shorter line at 20°S, coinciding with the Namibian Sea Fisheries Institute's time series line, was repeated to elucidate any slope-undercurrent transport. These four more zonal transects were expected to show the ichthyoplankton structures north of the ABF, in the frontal zone itself, and (if it would have been a climatologically normal year) about 100 n.m. south of the ABF. The comparison of the meridional and zonal diversity structures should allow to elucidate interactions between the open ocean and the coastal zone.

9.4.3 Results

Samples taken

Along the equatorial transect 20 plankton stations (140 - 162) ran without any problems, except that due to a handling error MCN-station 162 yielded an integrated tow 0 - 200 - 0 m only, instead of vertically stratified sampling. The towing conditions for both types of samplers were good. However, with the neuston samples some problems preserving the catch occurred during the first 20 hauls due to lack of staff. These problems did not occur subsequently.

The meridional transect was somewhat out of sequence, including plankton stations 173 - 206, 225 - 229, and making additionally use of station 152 (Table B.5). At station 225 the catch of the lower NEU stratum was lost due to an excessive amount of gelatinuous zooplankton.

The transect along 17°S consisted of 9 stations (207 - 225, see Table B.5). At stations

206 - 224 the NEU could not be used due to gale-force winds. From station 227 onwards NEU-tows were shortened due to high amounts of salps and, later, phytoplankton.

The NE-transect comprised the ships stations 229 - 241, but at station 234 only the NEU could be shot due to bad weather, and no plankton sampling was possible along the slope stations 235 and 236. At station 239 the upper NEU-bucket and its catch was lost, from the same station onwards the MCN-tows were shortened slightly due to excessive amounts of phytoplankton.

The 20°S-transect covered the Namibian shelf and upper slope waters by stas. 242 - 249. Station 245 did not yield any MCN-catches due to a CTD break-down in the sampler. At station 249 again the MCN yielded an integrated double-oblique tow due to a handling error.

For all plankton tows the filtered areas were calculated already on board, and individually for any sampling horizon. On an average, the MCN filtered 4.06 m^2 ($\pm 1.43\,m^2$, n = 226), and the NEU 1434.6 m^2 ($\pm 322.7\,m^2$, n = 34) over most of the survey. The reduced towing times yielded average catches as follows: MCN = 3.13 m^2 ($\pm 0.97\,m^2$, n = 45); NEU = 394.3 m^2 ($\pm 91.2\,m^2$, n = 16).

The weather took its toll, by, as mentioned, losing one NEU bucket including its catch, and by wearing out and tearing two NEU and 3 MCN net bags, respectively, the latter luckily without affecting the catch.

Analysis on board

Only NEU-uppernet-samples 140 to 160 plus MCN haul 173 (see Fig. 9.47 for the latter) could be microscopically analysed for gross zooplankton composition, and fish and oceanic insect Halobates micans were extracted quantitatively. Preserving the catch, a coarse macroscopical check was done for most samples, with occasional microscopic identification of individual fishes of relevance for the project. Adult myctophids, abundant in nighttime catches, underwent a quick-look identification to sort out and deep-freeze reference specimens for a world-wide genetic and enzymatic study of this family. The cruise yielded 137 specimens of at least 16 taxa, sent to South African Museum, Cape Town.

Taxonomy

MCN-station 173 yielded a hitherto undescribed larval specimen of family Bathylagidae, filling a developmental gap in material already available for descriptive work in progress. NEU 153 yielded 5 transforming larvae of genus Coryphaena, similar in pigmentation to C. hippurus, but differing from larvae of both nominal species in having a deeply forked caudal fin and deviating dorsal and anal fin meristics. Larval Sardinops ocellata, Diaphus hudsoni and Acanthurus monroviae were not previously available to Zoologisches Museum Hamburg. The same is true for a developmental series of an (still unidentified for lack of literature) Angolan Carangidae species.

Biogeography

Figure 9.48 presents the gross abundance and number of fish species caught in the first 18 NEU-tows along the equatorial transect. As well described for tropical latitudes, daytime abundances exceeded nightime values by far, whilst during night the number of species increased. Also conform with previous knowledge was that during daytime ichthyoneuston is almost exclusively composed by beloniform fishes (shortwing flying fish being the most abundant), whilst at night myctophid fishes dominate (Fig. 9.49). This is caused by lack of orientation and vertical dispersal in positive phototactic Beloniformes, whilst daytime-mesopelagic Myctophidae (and, less abundant, Photichthyidae and Gonostomatidae) ascend to the surface at night to feed. Among Myctophidae, Myctophum affine and M. nitidulum prevailed, with only few individuals of few other species present. Myctophidae along this transect were almost exclusively of small size. At 6 stations larvae of shallow-water trigger-fish Canthidermis maculatus were caught. Neritic invertebrate taxa (Sergestidae, Phyllosoma, Branchiostoma) were observed at the same stations, but frequently also in adjacent ones.

Noteworthy in Fig.9.48 is the increase in abundance towards Angolan waters. Although not visible in gross diversity, this coincided with a change in composition of Beloniformes. Genus Exocoetus occurred at the northernmost stations of the equatorial transect, but was not found further southwards, including most of the meridional transect. Exocoetidae off Angola were dominated by genera Prognichthys and Cypselurus, which is unusual for oceanic waters. Along the 17°S -transect (i.e. in the ABF), and also southwards of the ABF Myctophidae attained normal sizes. At plankton station 219 the first specimen of genus Symbolophorus appeared, with many more to follow farther southwards. Exocoetus reappeared from station 225 onwards for few stations, where also O. micropterus was replaced by dwarf saury, Nanichthys simulans. Stations 225 - 229 thus showed a fauna characteristic for the South Atlantic Central Gyre. However, at station 228 also a syngnathid specimen was caught at a surprising distance away from its coastal habitat. The NE-transect gradually acquired a prevailing neritic characteristic towards the coast from statio 233 onwards, with postflexion (i.e. elder) larvae of blennies and horse mackerel becoming abundant. The 20°S -transect had a prevailing neritic characteristic, except at its station farthest offshore. It is noteworthy, that besides N. simulans the temperate saury Scomberesox saurus was found here.

9.4.4 Conclusions

The equatorial currents of the eastern Gulf of Guinea had a somewhat impoverished fauna, although they entrained planktonic organisms originating from distant coastal areas. Off Angola, ichthyoplankton abundance (but not its diversity), increased noticeably when the transect reached the northern periphery of the Angola Dome, as depicted by a shallowing of the pycnocline and oxycline (compare the Figures in Chapter 9). In contrast, the relative NEU diversity maximum coincided with a frontal structure of salinity and oxygen plus a core of westward flow (Figures 9.1 and 9.39) in the mesopelagic realm. MCN-station 173 was located within the Angola Dome itself, causing extremely shallow vertical distributions of normally deep living larvae and shallow diversity gradients, but normal patterns in and above the thermocline. The meridional transect south of the Angola Dome seemed to have normal abundances. However, an increase in diversity and, apparently, size particularly of mesopelagic fish species, was noticed towards the south. At the Angola-Benguela-Front (Figure 9.9) coastal fishes appeared in the samples of the meridional transect, suggesting westward flow along the front. South of the front the offshore fauna revealed characteristics of the South Atlantic Central Gyre. Along the zonal transect the faunal character became prevailing neritic, with temperate (i.e. Benguela-ecosystem) species prevailing nearshore in upwelled waters.

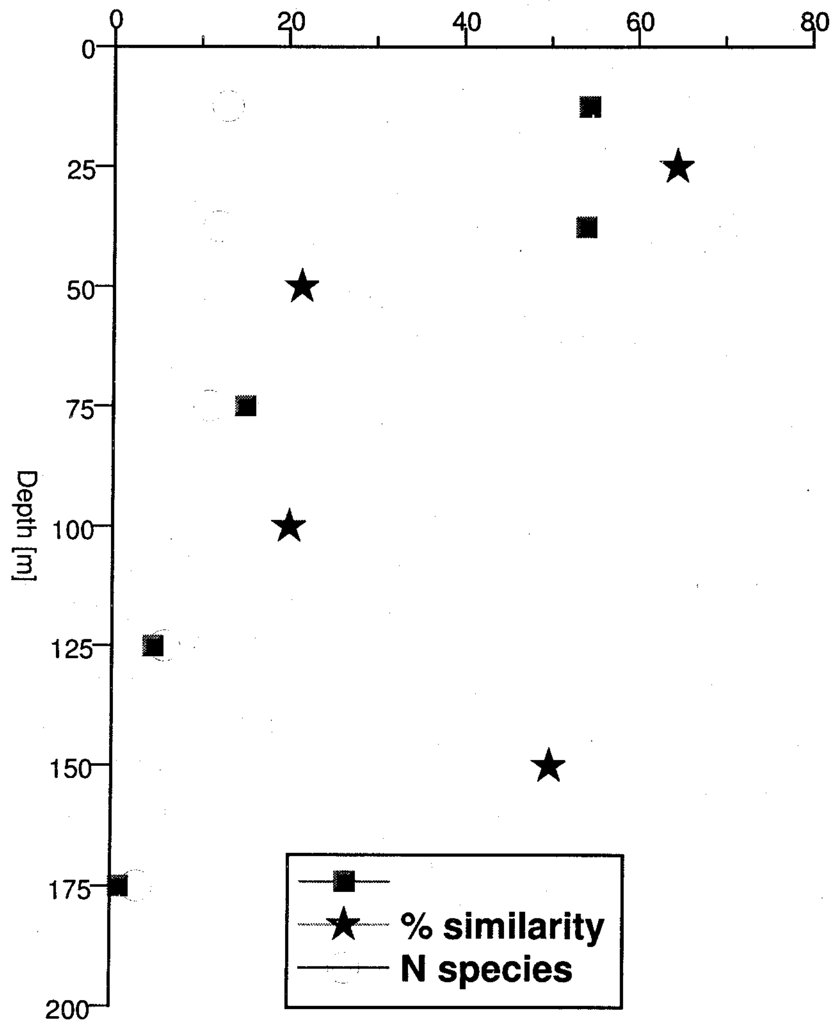

Figure 9.47: The abundance of fish larvae per step, their number of species, and the percentage similarity between steps in the multinet haul within the Angola Dome (ship station 173).

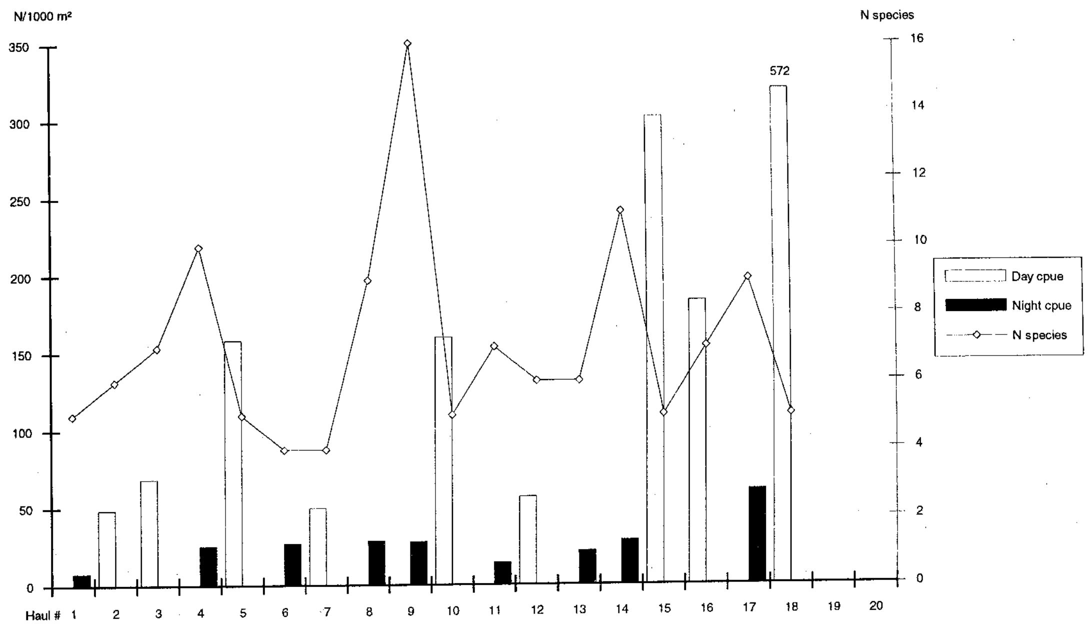

Figure 9.48: The catch per unit of effort (cpue, columns) and number of species (diamonds) caught by the upper neuston net along the equatorial transect. Plankton tows 19 and 20 have not yet been analysed.

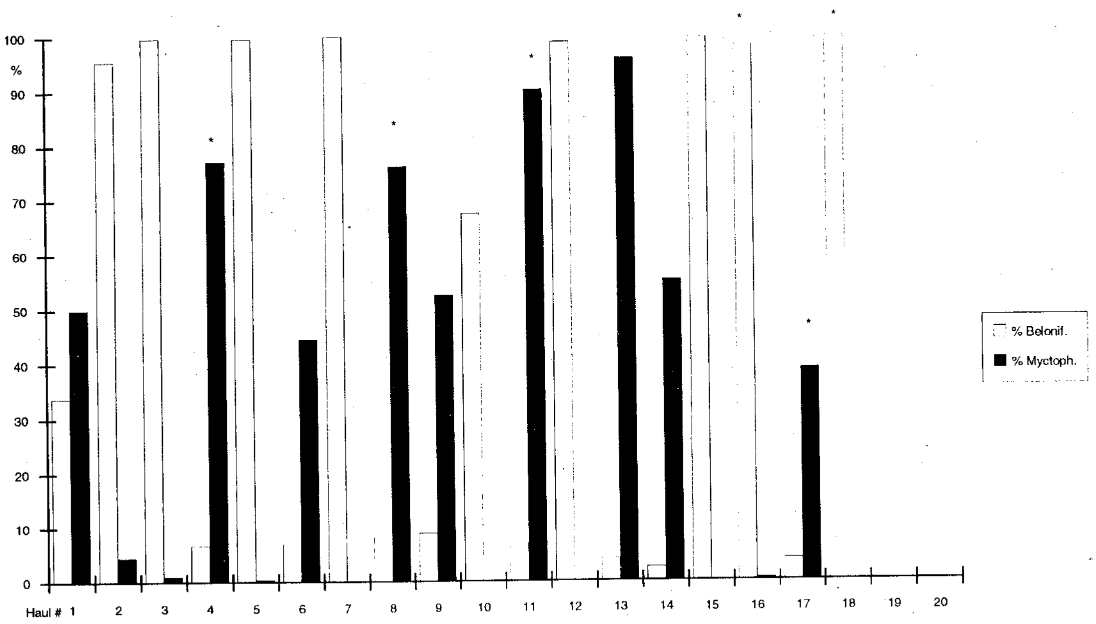

Figure 9.49: The percentages of order Beloniformes, respectively family Myctophidae, among the total number of fish along the equatorial transect. Asterisks above the columns indicate the presence of neritic fish species.

Acknowledgement

This cruise with R/V "Poseidon" was made possible by the cooperation of many people whose help and support should be appreciated here.

The idea for a joint scientific cruise of Angolan, German and Namibian students and scientists was suggested by Prof. Gotthilf Hempel during the International BENEFIT Symposion "On the variability of the marine ecosystems off the southern Africa" in Swakopmund, 1998. As the result of strong efforts of several organisations, institutions and outstandig persons this cruise could be realized with R/V "Poseidon". The support by the "Bundesminister für Bildung Forschung", (BMBF 03F154A) and the "Gesellschaft für Technische Zusammenarbeit", (GTZ, 81024061) is greatly acknowledged.

The cruise participants also wish to thank Prof. v. Bodungen (IOW), Prof. Kortum (IfM Kiel), Prof. Charles Hocutt, Dr. H.-U. Lass, the German Embassies in Luanda and Windhoek and the authorities of the National Marine Information and Research Center in Swakopmund and of the Fisheries Institute in Luanda as well.

Technical support of Siegfried Krüger and his team (IOW), and of the "Poseidon" crew is greatly acknowledged here.

Bibliography

BRIGGS, J. C., 1974: Mar. Zoogeogr. McGraw-Hill, New York.

EDWARDS, A. and R. LUBBOCK, 1983: Marine Zoogeography of St. Pauls's Rocks. J. Biogeogr., 10(1-2), 65-72.

FIEKAS, V., ELKEN, J., MÜELLER, J., AITSAM, A. and W. ZENK, 1992: A View of the Canary Basin Thermocline Circulation in Winter. J. Geophys. Res., 97(C8), 12.495-12.510.

FILIPE, V. L.L. The Angola Dome observed in April 1997, 1998: Proceedings of international symposion and "On the variability of the marine ecosystems off the southern Africa", Swakopmund.

FIRING, E., RANADA, J. and P. CALDWELL, 1995: Processing ADCP data with CODAS Software, Version 3.1. Technical Report, Joint Institute for Marine and Atmospheric Reserch, University of Hawai, USA, 218 S.

GORDON, A. L. and K. L. BOSLEY, 1991: Cyclonic gyre in the tropical South Atlantic. Deep-Sea Res., 38(suppl. 1A), 323-343.

GRASSHOFF, K., EHRHARDT, M. and K. KREMLING, 1983: Methods of Seawater Analysis. Chapter 4: Determination of nutrients. Verlag Chemie, Weinheim.

GRASSHOFF, K., EHRHARDT, M. and K. KREMLING, 1983: Methods of Seawater Analysis. Chapter 4: Determination of nutrients. Verlag Chemie, Weinheim.

HAGEN, E. and R. SCHEMAINDA, 1984: Der Guineadom im ostatlantischen Stromsystem. Beitr. Meereskd., 51, 5-27.

HAGEN, E. and R. SCHEMAINDA, 1987: On the zonal distribution of South Atlantic Central Water (SACW) along a section off Cape Blanc, Northwest Africa. Oceanolog. Acta, SP, 61-70.

HEMPEL, G., editor, 1982: The Canary Current: Studies of an upwelling system., volume 180. Rapp. Proc.-Verb. Réun. Cons. Int. Explor. Mer.

JOHN, H.-CH. and C. ZELCK, 1997: Features, boundaries and connecting mechanisms of the Mauretanian Province exemplified by oceanic fish larvae. Helgoländer Meeresunters., 51(2), 213-240.

JOHN, H.-CH. and C. ZELCK, 1998: Fish Larval Abundance, Diversity, and Zonation across the Tropical South Atlantic at 11°S. J. Ichthyol., 38(2), 190-198.

JOHN, H.-CH., MITTELSTAEDT, E. and K. SCHULZ, 1998: The boundary circulation along the western European continental slope as transport vehicle for two calanid copepods in the Bay of Biscay. Oceanolog. Acta, 21(2), 307-318.

KLEIN, B., 1991: Die Kapverden - Frontalzone. Ber. Inst. Meeresk. Kiel, 227, 191S.

LASS, H. U., SCHMIDT, M., MOHRHOLZ, V. and G. NAUSCH, 2000: Hydrographic and current measurements in the Angola-Benguela front area. J. Phys. Oceanogr. (accepted).

MAURIN, C., 1968: Écologie ichthyologique des fonds chalculatables atalntiques (de la baie Ibéro - Marocaine a la Maurenanie) et de la Méditerranée occidentale. Rev. Trav. Inst. Pêch. marit., 32, 1-147.

MAZEIKA, P. A., 1967: Thermal domes in the Eastern Atlantic Ocean. Limnol. Oceanogr., 12, 537-539.

MEEUWIS, J. M. and J. R. E. LUTJEHARMS, 1990: Surface Thermal Characteristics of the Angola - Benguela Front. S. Afr. J. mar. Sci., 9, 261-279.

MITTELSTAEDT, E., 1989: The subsurface circulation along the Maroccan slope. In Neshyba, S.J., Mooers, C.N.K., Smith, R.L. and Barber, R.T., editor, Coast. Estuar. Stud., 34. Springer-Verlag.

MITTELSTAEDT, E., 1991: The ocean boundary along the northwest African coast. Progr. Oceanogr., 26, 307-355.

MOLINARI, R. L., 1982: Observations of eastward currents in the tropical South Atlantic Ocean: 1978-1980. J. Geophys. Res., 87, 9707-9714.

MOLINARI, R. L., VOITUREZ, B. and P. DUNCAN, 1981: Observations in the subthermocline undercurrent of the South Atlantic Ocean: 1978 - 1980. Oceanolog. Acta, 4, 451-456.

MOROSHKIN, K. V., BUBNOV, V. A. and R. P. BULATOV, 1970: Water circulation in the eastern South Atlantic Ocean. Oceanology, 10(1), 27-34.

OLIVAR, M.-P. and J.-M. FORTUÑO, 1991: Guide to ichthyoplankton of the Southeast Atlantic. (Benguela Current Region). Sci. Mar., 55(1), 1-383.

OLIVAR, M.-P. and P. A. SHELTON, 1993: Larval fish assembalge of the Benguela Current. Bull. Mar. Sci., 53(2), 450-474.

PENRITH, M. J., 1978: An annotated check-list of the inshore fishes of southern Angola. Cimbebasia, A 4(11), 179-190.

REID, J. L., JR., 1964: Evidence of a South Equatorial Counter Current in the Atlantic Ocean in July 1963. Nature London, 203, 182S.

ROHDE, K. H. and D. NEHRING, 1979: Die Bestimmung von Nährstoffen und Schadstoffen im Meer- und Brackwasser..

SCHELTEMA, R., 1986: Epipelagic meroplancton of tropical seas: Its role for biogeography of sublittoral invertebrate species. UNESCO tech. Pap. mar. sci., 49, 242-249.

SIEDLER, G., ZANGENBERG, N., ONKEN, R. and A. MORLIERE, 1992: Seasonal changes in the tropical Atlantic circulation: Observation and simulation of the Guinea Dome. J. Geophys. Res., 97(C1), 703-715.

STÖHR, S., HAGEN, E., JOHN, H.-CH. MITTELSTAEDT, E., SCHULZ, K., VANICEK, M. and H. WEIKERT, 1997: Poleward plankton transport along the Maroccan and Iberian continental slope. Ber. Biol. Anst. Helogoland, 12, 1-53.

STRAMMA, L. and F. SCHOTT, 1996: Western equatorial circulation and interhemisperal exchange. In W. Krauss, editor, The warmwatersphere of the North Atlantic Ocean, pages 195-222. Borntraeger, Berlin.

TOMCZAK, M., 1998: Water mass analysis as a Tool for Climate Research, a workshop held in IAMAS/IAPSO General Assambly in Melbourne, 1997. International WOCE Newsletter, 30, 43S.

VOITURIEZ, B., 1981: Les sous-courants équatoriaux nord et sud et la formation des dômes thermiques tropicaux. Oceanologica Acta, 4, 497-506.

VOITURIEZ, B. and A. HERBLAND, 1982: Comparaison des systèmes productifs de l'Atlantique Tropical Est: dômes thermiques, upwellings côtiers et upwelling équatorial. Rapp. Proc.-Verb. Réun. Cons. Int. Explor. Mer, 180, 114-130.

WACONGNE, S. and B. PITON, 1992: The near-surface circulation in the northeastern corner of the South Atlantic ocean. Deep Sea Res., 39(7/8), 1273-1298.

WLOST, K. P., 1999: IOW-ReiseAssistent-Softwarepaket..

WOCE, 1990: WOCE Hydrographic Operations and Methods. Dissolved Oxygen., unpublished.

YAMAGATA, I. and S. IIZUKA, 1995: Simulation of the Subtropical Domes in the Atlantic: A Seasonal Cycle. J. Phys. Oceanogr., 25(9), 2129-2124.

List of Figures

List of Tables

Appendix A Device configuration

Table A.1: SeaBird SBE 911+ (hardware)

Hardware	
SBE-911plus Underwater Unit	SN 09P7807-0306
Depth capability (CTD and sensor housings)	6 800 m
Pressure sensor range	0 - 10.000 psia (0 - 6.885 dbar)
Digiquartz pressure sensor (with temperature comp.)	SN 51392
Modulo 12P	SN MOD12P-0448
Temperature sensor (SBE 3-02/F)	SN 1592
Conductivity sensor (SBE 4-02/0)	SN 1150
Oxygen sensor (IOW)	SN O023
Oxygen sensor (IOW) Type B	SN 0001
Dr. Haardt BackScat II-Fluorometer (model 1101.1)	SN 2070
Pump (SBE 5T)	SN 51991
HYDRO-BIOS / IOW Rosette water sampler	
Altimeter (Datasonics PSA-900D)	SN A17
Logic Board EPROM Version 1.0	
Modem Interface Installed	
Modem Board Microcontroller Vers. 2.0 IOW	
HYDRO-BIOS Rosette Interface Installed	

Table A.2: SeaBird SBE 911+ (software)

Software	
Seasoft (SBE)	version 4.233 (1999)
presscor, do_om, depth (IOW)	version 3.5 (11.05.1997)
Reise für WINDOWS (IOW)	version 5.77 (1998)

For each station a configuration file *stationname.cnf* is written which contains the complete parameter set, especially sensor coefficients used for the conversion of raw data (frequencies) to standard output format.

Table A.3: Configuration of the VMADCP

Command	Parameter	Value
menu options	average interval	300 s
of software	bin number	60
ue4	transducer depth	4 m
	bin length	8 m
	pulse length	16 m
	blank after transmit	4 m
	ping interval	as soon as possible
	ping per ensemble	1
	ens treshold	25
	en treshold	32676 $\frac{mm}{s}$
	heading offset	0 deg
	pitch offset	0 deg
	roll offset	0 deg
	frequence transmit	65535 Hz
	band width	narrow band
	bottom tracking	none
	top reference bin	4
	bottom reference bin	20
	heading bias	173.3 deg

The configuration of each particulary profile was saved into the CODAS database during the data postprocessing.

Table A.4: Configuration of the LADCP

Command	Parameter	Value
ES35	salinity	35
EX11111	co-ordinates	use earth co-ordinates
TE00:00:01.00	time per ensemble	1 s
TP00:00.00	time between pings	as soon as possible
LD111000000	data output	vel, corr, intensity, percent good
LF0400	blank after transmit	4 m
LP00003	ping per ensemble	3
LJ1	receiver gain	1
LN020	number of depth cells	20
LS0800	bin length	8 m
LV250	correlation velocity	2.5 $\frac{m}{s}$
LW1	band width	narrow band
LZ30,220	Amplitude, Correlation Thresholds	
EZ1111111	sensor source	use all
EA00000	heading alingment	0 deg
EB-XXX	heading bias	XXX deg local magnetic deviation

At the equatorial transect for stations 140 to 148 the following parameters differ from the configuration given above.

Command	Parameter	Value
TP00:01.00	time between pings	1 s
LF0200	blank after transmit	2 m
LP00001	ping per ensemble	1
LN032	number of depth cells	32
LS0400	bin length	4 m

Appendix B Station lists

The CTD-casts can be identified from a consecutive station number from 140 to 256 (shown in figure 2.1) and a station label. Additionally the station list shows station date, time and position as well as the bottom depth and the number of water samples (bt).

LADCP-casts are termed by a consecutive deployment number from 1 to 107 and a deployment name, according to the CTD station number.

Table B.1: List of CTD stations

File	St. nr.	St. label	time and date [UTC]	position	depth [m]	bt
0140F01	140	A0000	21:07:15 28-03	01 27.60 N 05 45.17 W	5133.0	11
0141F01	141	A0001	04:42:15 29-03	00 59.99 N 05 00.14 W	5095.0	11
0142F01	142	A0002	14:37:00 29-03	00 21.39 N 03 57.08 W	5105.5	11
0143F04	143	A0003	01:44:00 30-03	00 16.49 S 02 55.72 W	5088.5	11
0144F01	144	A0004	12:24:45 30-03	00 56.32 S 01 50.02 W	4600.0	11
0145F01	145	A0005	22:34:45 30-03	01 35.34 S 00 46.12 W	4900.0	11
0146F01	146	A0006	08:38:55 31-03	02 13.34 S 00 15.95 E	4600.0	11
0147F01	147	A0007	00:05:10 31-03	02 51.80 S 01 19.03 E	4400.0	10
0148F01	148	A0008	02:50:20 01-04	03 30.81 S 02 23.06 E	4458.5	11
0149F01	149	A0009	12:01:55 01-04	04 07.44 S 03 23.34 E	5100.0	10
0150F01	150	A0010	22:50:30 01-04	04 43.09 S 04 26.90 E	5032.0	11
0151F01	151	A0011	07:51:35 02-04	05 15.52 S 05 35.02 E	4796.5	11
0152F01	152	A0012	17:53:50 02-04	05 47.95 S 06 43.07 E	4526.5	11
0153F01	153	A0013	02:59:10 03-04	06 19.00 S 07 48.00 E	4214.5	10
0154F01	154	A0016	09:17:00 03-04	06 59.91 S 08 00.02 E	4239.5	10
0155F01	155	A0017	16:36:50 03-04	07 59.88 S 08 00.01 E	4450.5	11
0156F01	156	A0019	23:12:10 03-04	08 00.10 S 09 00.02 E	4270.5	11
0157F01	157	A0014	06:55:40 04-04	06 54.19 S 09 00.05 E	3966.5	11
0158F01	158	A0015	14:58:25 04-04	07 22.06 S 10 00.16 E	3906.5	11
0159F01	159	A0020	23:11:55 04-04	08 00.06 S 11 00.03 E	2689.5	11
0160F01	160	A0021	07:18:20 05-04	08 30.08 S 11 59.63 E	1857.5	11
0161F01	161	A0022	13:17:20 05-04	08 35.56 S 12 30.04 E	1347.5	11
0162F01	162	A0023	17:15:15 05-04	08 39.01 S 12 48.89 E	775.5	10
0163F01	163	N0101	23:05:55 06-04	09 00.32 S 12 55.23 E	223.5	11
0164F01	164	N0102	00:26:35 07-04	09 00.12 S 12 45.03 E	467.5	9
0165F01	165	N0103	01:59:55 07-04	09 00.15 S 12 34.88 E	943.5	11
0166F01	166	N0104	03:49:55 07-04	09 00.05 S 12 24.86 E	1285.5	11
0167F01	167	N0105	06:45:30 07-04	09 00.04 S 12 05.16 E	2103.5	11
0168F01	168	N0106	10:11:15 07-04	08 60.00 S 11 40.21 E	2150	11
0169F01	169	N0107	15:04:20 07-04	08 59.99 S 11 00.41 E	2975	11
0170F01	170	N0108	20:42:15 07-04	09 17.37 S 10 12.17 E	4306.5	11
0171F01	171	A0024	02:51:20 08-04	08 30.07 S 09 59.95 E	4095.5	11
0172F01	172	A0025	10:05:50 08-04	08 45.06 S 09 00.07 E	4478.5	11
0173F02	173	A0018	17:53:10 08-04	09 00.01 S 08 00.25 E	4690.5	11
0174F01	174	N0109	05:04:35 09-04	09 32.95 S 09 29.25 E	4405	11
0175F01	175	N0110	10:53:50 09-04	09 49.89 S 08 44.99 E	4600.5	11
0176F01	176	N0111	16:26:40 09-04	10 04.96 S 07 59.80 E	4832.5	11

Table B.1: List of CTD stations (continued)

File	St. nr.	St. label	time and date [UTC]	position	depth [m]	bt
0177F01	177	A0026	00:11:40 10-04	09 29.94 S 07 09.89 E	4957.5	11
0178F01	178	N0112	06:53:00 10-04	10 24.45 S 07 09.75 E	5026.5	11
0179F01	179	N0162	14:47:55 10-04	11 24.75 S 07 11.03 E	5089.5	11
0180F01	180	N0161	21:43:30 10-04	11 07.01 S 07 59.90 E	4856.5	11
0181F01	181	N0160	04:13:15 11-04	10 53.99 S 08 40.03 E	4813.5	11
0182F01	182	N0159	09:23:30 11-04	10 42.03 S 09 19.85 E	4603.5	11
0183F01	183	N0158	14:39:30 11-04	10 30.15 S 09 59.88 E	4355	11
0184F01	184	N0157	19:13:55 11-04	10 30.10 S 10 33.91 E	2899.5	11
0185F01	185	N0156	23:38:35 11-04	10 29.99 S 11 06.98 E	3764.5	11
0186F01	186	N0155	04:12:00 12-04	10 30.19 S 11 42.08 E	1871.5	11
0187F01	187	N0154	08:52:55 12-04	10 29.85 S 12 20.14 E	1605.5	11
0188F01	188	N0153	12:30:45 12-04	10 29.93 S 12 48.05 E	1128.5	11
0189F01	189	N0152	15:04:45 12-04	10 30.02 S 13 04.87 E	351.5	9
0190F01	190	N0151	16:33:05 12-04	10 30.04 S 13 14.96 E	106	7
0191F01	191	N0150	17:53:05 12-04	10 29.78 S 13 24.93 E	128	7
0192F01	192	N0251	03:33:20 13-04	12 00.03 S 13 30.03 E	168.5	8
0193F01	193	N0252	05:47:00 13-04	11 60.00 S 13 20.00 E	708.5	10
0194F01	194	N0253	07:50:10 13-04	12 00.16 S 13 04.95 E	1227.5	11
0195F01	195	N0254	11:14:30 13-04	11 59.94 S 12 39.98 E	1826.5	11
0196F01	196	N0255	15:05:10 13-04	11 59.86 S 12 10.07 E	2145.5	11
0197F01	197	N0256	19:52:55 13-04	11 59.88 S 11 29.99 E	3383.5	11
0198F01	198	N0257	00:34:25 14-04	12 00.04 S 10 49.85 E	3646.5	11
0199F01	199	N0258	05:16:10 14-04	12 00.08 S 10 09.89 E	4051.5	11
0200F01	200	N0259	10:16:45 14-04	12 00.20 S 09 27.92 E	4301	11
0201F01	201	N0260	15:34:10 14-04	12 00.07 S 08 44.10 E	4511.5	11
0202F01	202	N0261	20:47:25 14-04	11 59.90 S 07 60.00 E	4813.5	11
0203F01	203	N0270	05:41:30 15-04	12 59.96 S 07 59.88 E	4799.5	11
0204F01	204	N0271	14:13:20 15-04	14 00.01 S 07 59.98 E	4743.5	11
0205F01	205	N0272	23:04:20 15-04	14 59.98 S 07 59.94 E	4853	11
0206F01	206	N0410	09:23:35 16-04	15 59.94 S 07 59.95 E	4960	11
0207F01	207	N0409	17:14:55 16-04	15 46.37 S 08 50.06 E	4591	11
0208F01	208	N0408	22:09:25 16-04	15 34.55 S 09 22.94 E	4215	11
0209F01	209	N0407	03:00:55 17-04	15 22.78 S 09 55.64 E	3844	11
0210F01	210	N0406	07:33:30 17-04	15 11.98 S 10 24.71 E	3580	11
0211F01	211	N0405	12:33:15 17-04	15 00.01 S 11 00.13 E	3073	11
0212F01	212	N0401	05:01:30 18-04	14 59.92 S 12 05.34 E	290.5	9
0213F01	213	N0402	06:28:30 18-04	14 59.89 S 11 55.11 E	1270.5	11
0214F01	214	N0403	09:00:15 18-04	15 00.04 S 11 40.05 E	1990	11
0215F01	215	N0404	11:47:30 18-04	15 00.00 S 11 25.02 E	2620	11
0216F01	216	N0601	14:25:40 19-04	16 59.82 S 11 35.30 E	85	7
0217F01	217	N0602	15:48:25 19-04	16 59.87 S 11 27.87 E	114.5	7
0218F01	218	N0603	17:24:25 19-04	16 59.76 S 11 20.27 E	155.5	7
0219F01	219	N0604	20:39:35 19-04	16 59.95 S 10 59.76 E	2137	11
0220F01	220	N0605	01:02:15 20-04	17 00.08 S 10 35.02 E	3010	11
0221F01	221	N0606	04:18:25 20-04	17 00.06 S 10 12.75 E	3614	11
0222F01	222	N0607	10:27:40 20-04	17 00.07 S 09 40.40 E	4021	11
0223F01	223	N0608	15:27:25 20-04	17 00.12 S 09 10.52 E	4443	11

Table B.1: List of CTD stations (continued)

File	St. nr.	St. label	time and date [UTC]	position	depth [m]	bt
0224F01	224	N0609	20:22:15 20-04	17 00.05 S 08 39.72 E	4698	11
0225F01	225	N0610	02:22:40 21-04	17 00.06 S 08 00.04 E	4916.5	11
0226F01	226	N0611	11:13:20 21-04	18 00.08 S 07 59.92 E	5004.5	11
0227F01	227	N0612	20:01:15 21-04	18 59.96 S 07 59.97 E	5081	11
0228F01	228	N0613	03:37:10 22-04	19 42.08 S 07 59.94 E	4902	11
0229F01	229	N0712	14:18:00 22-04	20 22.82 S 07 58.87 E	3122.5	11
0230F01	230	N0711	18:55:00 22-04	20 14.04 S 08 27.04 E	2047.5	11
0231F01	231	N0710	00:24:45 23-04	20 06.01 S 08 51.93 E	2282	11
0232F01	232	N0709	06:00:55 23-04	19 55.92 S 09 17.95 E	2385	11
0233F01	233	N0708	12:28:25 23-04	19 44.50 S 09 49.93 E	2044	11
0234F01	234	N0707	18:12:50 23-04	19 35.37 S 10 19.48 E	1398	11
0235F01	235	N0706	22:54:15 23-04	19 27.42 S 10 44.77 E	1189	11
0236F01	236	N0705	02:47:00 24-04	19 21.51 S 11 05.27 E	1061	11
0237F01	237	N0704	05:54:40 24-04	19 16.61 S 11 20.37 E	652.5	10
0238F01	238	N0703	09:46:30 24-04	19 09.96 S 11 36.92 E	314	10
0239F01	239	N0702	12:47:45 24-04	19 06.01 S 11 46.96 E	309.5	10
0240F01	240	N0701	15:54:35 24-04	19 02.94 S 11 58.98 E	226	10
0241F01	241	N0700	19:01:55 24-04	18 59.98 S 12 10.97 E	121.5	7
0250F01	250	N0907	07:13:00 26-04	21 30.08 S 11 37.85 E	2032.5	11
0251F01	251	N0906	10:26:20 26-04	21 25.08 S 11 59.99 E	1426.5	11
0252F01	252	N0905	13:19:05 26-04	21 18.04 S 12 18.08 E	849	11
0253F01	253	N0904	16:51:30 26-04	21 11.87 S 12 35.53 E	402.5	9
0254F01	254	N0903	19:16:15 26-04	21 06.93 S 12 54.43 E	280.5	8
0255F01	255	N0902	20:44:20 26-04	21 02.55 S 13 04.98 E	131.5	6
0256F01	256	N0901	21:57:30 26-04	21 00.08 S 13 15.06 E	119.5	6

Table B.2: List of LADCP casts

Station number	Station label	LADCP cast	LADCP deploy name	max depth of cast (m)	yeared change of misalign (deg E)	magnetic deviation result (deg W)	heading bias para-meter
140	A0000	1	aq140	1200	1.0640	9.08	-908
141	A0001	2	aq141	1249	1.0731	8.97	-897
142	A0002	3	aq142	1301	1.0822	8.80	-880
143	A0003	4	aq143	1301	1.0913	8.67	-867
144	A0004	5	aq144	1311	1.1004	8.54	-854
145	A0005	6	aq145	1307	1.1095	8.43	-843
146	A0006	7	aq146	1308	1.1186	8.32	-832
147	A0007	8	aq147	1305	1.1277	8.22	-822
148	A0008	9	aq148	1304	1.1368	8.14	-814
149	A0009	10	aq149	1310	1.1459	8.06	-806
150	A0010	11	aq150	1309	1.1550	7.96	-796
151	A0011	12	aq151	1400	1.1641	7.79	-779
152	A0012	13	aq152	1313	1.1732	7.64	-764
153	A0013	14	aq153	1307	1.1823	7.49	-749
154	A0016	15	aq154	1305	1.1823	7.78	-778
155	A0017	16	aq155	1307	1.1823	8.27	-827
156	A0019	17	aq156	1304	1.1823	7.88	-788
157	A0014	18	aq157	1304	1.1914	7.34	-734
158	A0015	19	aq158	1305	1.2005	7.16	-716
159	A0020	20	aq159	1302	1.2096	7.06	-706
160	A0021	21	aq160	1316	1.2187	6.89	-689
161	A0022	22	aq161	1311	1.2278	6.66	-666
162	A0023	23	aq162	775	1.2369	6.56	-656
163	N0101	24	aq163	220	1.3500	6.67	-667
164	N0102	25	aq164	480	1.3500	6.74	-674
165	N0103	26	af165	940	1.3500	6.81	-681
166	N0104	27	af166	1275	1.3500	6.90	-690
167	N0105	28	af167	1309	1.3500	7.03	-703
168	N0106	29	af168	1310	1.3500	7.21	-721
169	N0107	30	af169	1304	1.3500	7.46	-746
170	N0108	31	af170	1309	1.3500	7.93	-793
171	A0024	32	af171	1301	1.3500	7.63	-763
172	A0025	33	af172	1313	1.3500	8.14	-814
173	A0018	34	af173	1307	1.3500	8.63	-863
174	N0109	35	af174	1305	1.3500	8.34	-834
175	N0110	36	af175	1306	1.3500	8.75	-875
176	N0111	37	af176	1308	1.3500	9.24	-924
177	A0026	38	af177	1303	1.3500	9.31	-931
178	N0112	39	af178	1329	1.3500	9.85	-985
179	N0162	40	af179	1308	1.3500	10.40	-1040
180	N0161	41	af180	1310	1.3500	9.88	-988
181	N0160	42	af181	1305	1.3500	9.48	-948
182	N0159	43	af182	1312	1.3500	9.11	-911
183	N0158	44	af183	1304	1.3500	8.68	-868

Table B.2: List of LADCP casts (continued)

Station number	Station label	LADCP cast	LADCP deploy name	max depth of cast (m)	yeared change of misalign (deg E)	magnetic deviation result (deg W)	heading bias para-meter
184	N0157	45	af184	1309	1.3500	8.45	-845
185	N0156	46	af185	1303	1.3500	8.25	-825
186	N0155	47	af186	1306	1.3500	8.02	-802
187	N0154	48	af187	1319	1.3500	7.75	-775
188	N0153	49	af188	1105	1.3500	7.54	-754
189	N0152	50	af189		1.3500	7.44	-744
190	N0151	51	af190	104	1.3500	7.37	-737
191	N0150	52	af191	60	1.3500	7.27	-727
192	N0251	53	af192	161	1.3500	8.05	-805
193	N0252	54	af193	678	1.3500	8.12	-812
194	N0253	55	af194	1203	1.3500	8.21	-821
195	N0254	56	af195	1302	1.3500	8.40	-840
196	N0255	57	af196	1307	1.3500	8.58	-858
197	N0256	58	af197	1309	1.3500	8.90	-890
198	N0257	59	af198	1303	1.3500	9.19	-919
199	N0258	60	af199	1310	1.3500	9.50	-950
200	N0259	61	af200	1316	1.3500	9.81	-981
201	N0260	62	af201	1305	1.3500	10.13	-1013
202	N0261	63	af202	1310	1.3500	10.45	-1045
203	N0270	64	af203	1308	1.3500	11.07	-1107
204	N0271	65	af204	1303	1.3500	11.73	-1173
205	N0272	66	af205	1308	1.3500	12.36	-1236
206	N0410	67	af206	1306	1.3500	13.01	-1301
207	N0409	68	af207	1306	1.3500	12.49	-1249
208	N0408	69	af208	1309	1.3500	12.08	-1208
209	N0407	70	af209	1320	1.3500	11.70	-1170
210	N0406	71	af210	1313	1.3500	11.38	-1138
211	N0405	72	af211	1305	1.3500	10.95	-1095
212	N0401	73	af212	277	1.3500	10.47	-1047
213	N0402	74	af213	1264	1.3500	10.55	-1055
214	N0403	75	af214	1317	1.3500	10.65	-1065
215	N0404	76	af215	1304	1.3500	10.76	-1076
216	N0601	77	af216	85	1.3500	12.00	-1200
218	N0603	78	af218	145	1.3500	12.11	-1211
219	N0604	79	af219	1308	1.3500	12.30	-1230
220	N0605	80	af220	1301	1.3500	12.49	-1249
221	N0606	81	af221	1305	1.3500	12.65	-1265
222	N0607	82	af222	1309	1.3500	12.92	-1292
223	N0608	83	af223	1310	1.3500	13.17	-1317
224	N0609	84	af224	1306	1.3500	13.39	-1339
225	N0610	85	af225	1304	1.3500	13.72	-1372
226	N0611	86	af226	1304	1.3500	14.38	-1438
227	N0612	87	af227	1308	1.3500	15.08	-1508
228	N0613	88	af228	1310	1.3500	15.51	-1551

Table B.2: List of LADCP casts (continued)

Station number	Station label	LADCP cast	LADCP deploy name	max depth of cast (m)	yeared change of misalign (deg E)	magnetic deviation result (deg W)	heading bias para-meter
229	N0712	89	af229a	2708	1.3355	15.99	-1599
229	N0712	90	af229	1303	1.3355	15.99	-1599
230	N0711	91	af230	1306	1.3300	15.70	-1570
231	N0710	92	af231	1302	1.3245	15.41	-1541
232	N0709	93	af232	1308	1.3190	15.14	-1514
233	N0708	94	af233	1303	1.3135	14.77	-1477
234	N0707	95	af234	1309	1.3080	14.41	-1441
235	N0706	96	af235	1169	1.3025	14.14	-1414
236	N0705	97	af236	1033	1.2970	13.93	-1393
237	N0704	98	af237	627	1.2915	13.71	-1371
238	N0703	99	af238	306	1.2860	13.58	-1358
239	N0702	100	af239	293	1.2805	13.44	-1344
240	N0701	101	af240	209	1.2750	13.28	-1328
241	N0700	102	af241	130	1.2750	13.14	-1314
250	N0907	103	af250	1311	1.0500	15.38	-1538
251	N0906	104	af251	1310	1.0800	15.14	-1514
252	N0905	105	af252	844	1.1100	14.89	-1489
253	N0904	106	af253	280	1.1400	14.67	-1467
253	N0904	107	af253	381	1.1400	14.67	-1467

Table B.3: Mapa de realização e localizaçã das estações oceanográfcas (Phytoplankton stations)

Data Hora (1999)(utc)	No est.	Latitude Longitude	Profundidade 5-20 m	20-50 m	50-90 m	Termo-clina [m]	Halo-clina [m]
07-04 15:04	169	8 59.99 S 11 00.41 E	5.4	27.5	70.5	25	25
08-04 10:05	172	8 45.06 S 9 00.07 E	5.4	36.5	55.5	20	20
09-04 05:04	174	9 32.95 S 9 29.25 E	5.4	30.5	70.6	25	12
09-04 16:26	176	10 04.96 S 7 59.80 E	5.6	40.5	70.5	30	20
10-04 06:53	178	10 24.45 S 7 09.75 E	5.5	40.5	70.5	25	18
10-04 21:43	180	11 07.01 S 7 59.90 E	5.5	45.5	60.5	25	22
11-04 09:23	182	10 42.03 S 9 19.85 E	5.3	45.5	60.5	25	25
11-04 19:13	184	10 30.10 S 10 33.91 E	5.4	43.5	60.5	25	25
12-04 04:11	186	10 30.19 S 11 42.08 E	5:3	43.5	80.6	37	18
12-04 12:30	188	10 29.93 S 12 48.05 E	5.4	30.5	45.5	30	27
12-04 16:33	190	10 30.04 S 13 14.96 E	5.5	24.5	60.5	33	20
12-04 17:53	191	10 29.78 S 13 24.98 E	5.4	24.5	60.5	12	8
13-04 04:26	192	11 59.92 S 13 30.34 E	20.5	32.5	40.5	25	25
13-04 05:47	193	11 60.00 S 13 20.00 E	5.3	24.5	60.5	50	25
13-04 15:05	196	11 59.86 S 12 10.07 E	5.4	45.5	65.5	30	20
14-04 00:34	198	12 00.04 S 10 49.85 E	5.3	47.6	80.5	30	20
14-04 10:16	200	12 00.20 S 9 27.92 E	5.6	45.5	80.5	33	33
15-04 05:41	203	12 59.96 S 7 59.88 E	5.5	50.5	80.4	30	30
15-04 23:04	205	14 59.98 S 7 59.94 E	5.4	50.5	80.4	30	30
16-04 17:14	207	15 46.37 S 8 50.06 E	5.5	45.5	80.5	36	40
17-04 03:00	209	15 22.78 S 9 55.64 E	15.5	45.5	80.5	20	27
17-04 12:33	211	15 00.O1 S 11 00.13 E	5.4	30.5	65.5	30	40
18-04 05:01	212	14 59.92 S 12 05.34 E	5.5	30.5	80.5	20	20
18-04 09:00	214	15 00.04 S 11 40.05 E	5.5	45.5	80.4	35	35
19-04 14:25	216	16 59.82 S 11 35.30 E	5.4	45.5	80.5	55	50
20-04 06:02	221	17 00.20 S 10 12.27 E	5.5	45.4	80.5	40	40
21-04 02:22	225	17 00.06 S 8 00.04 E	5.5	65.5	80.5	42	42
22-04 14:18	229	20 22.82 S 7 58.87 E	5.5	45.4	80.4	42	42
23-04 22:54	235	19 27.42 S 10 44.77 E	10.5	30.5	65.5	38	37
24-04 05:54	237	19 16.61 S 11 20.37 E	10.4	30.5	65.6	63	63
24-04 15:54	240	19 02.94 S 11 58.98 E	10.5	45.5	80.5	40	40
26/04 20:44	255	21 02.55 S 13 04.98 E	10.5	30.5	70.5	20	15

Table B.4: Distribuição dos principais grupos de fitoplâncton nas diferentes estações de amostragem (Abundance of phytoplankton groups)

Data Hora (1999)(utc)	No est.	Latitude Longitude	Profundidade 20-50m	Grupos fitoplanctónicos
07-04 15:04	169	8 59.99 S 11 00.41 E	27.5	dinoflagelados (+) peq. algas flageladas (+)
08-04 10:05	172	8 45.06 S 9 00.07 E	36.5	dinoflagelados (+)
09-04 05:04	174	9 32.95 S 9 29.25 E	30.5	diatomáceas (*,++) peq. algas flageladas (++)
09-04 16:26	176	10 04.96 S 7 59.80 E	40.5	dinoflagelados (+) peq. algas flageladas ++
10-04 06:53	178	10 24.45 S 7 09.75 E	40.5	dinoflagelados(+) peq. algas flageladas (++), diatomáceas (*,++)
10-04 21:43	180	11 07.01 S 7 59.90 E	45.5	diatomáceas (*,+) peq. algas flageladas (++)
11-04 09:23	182	10 42.03 S 9 19.85 E	45.5	dinoflagelados (+) diatomáacias (**,+)
11-04 19:13	184	10 30.10 S 10 33.91 E	43.5	dinoflagelados(+) diatomáceas (* *,+)
12-04 04:11	186	10 30.19 S 11 42.08 E	43.5	peq. algas flageladas (+)
12-04 12:30	188	10 29.93 S 12 48.05 E	30.5	peq. algas flageladas (+)
12-04 16:33	190	10 30.04 S 13 14.96 E	24.5	peq. algas flageladas (+)
12-04 17:53	191	10 29.78 S 13 24.98 E	24.5	dinoflagelados (+) diatomáceas (**,+)
13-04 04:26	192	11 59.92 S 13 30.34 E	32.5	−−
13-04 05:47	193	11 60.00 S 13 20.00 E	24.5	peq. algas flageladas (++) dinoflagelados (+)
13-04 15:05	196	11 59.86 S 12 10.07 E	45.5	peq. algas flageladas (+) dinoflagelados (+)
14-04 00:34	198	12 00.04 S 10 49.85 E	47.6	peq. algas flageladas (+)
14-04 10:16	200	12 00.20 S 9 27.92 E	45.5	peq. algas flageladas (+)
15-04 05:41	203	12 59.96 S 7 59.88 E	50.5	peq. algas flageladas (+)
15-04 23:04	205	14 59.98 S 7 59.94 E	50.5	dinoflagelados (+) peq. algas flageladas (++)
16-04 17:14	207	15 46.37 S 8 50.06 E	45.5	dinoflagelados(+) peq. algas flageladas (++)
17-04 03:00	209	15 22.78 S 9 55.64 E	45.5	diatomáceas (**,+) peq. algas flageladas (++)
17-04 12:33	211	15 00.O1 S 11 00.13 E	30.5	dinoflagelados (+) peq. algas flageladas (++)
18-04 05:01	212	14 59.92 S 12 05.34 E	30.5	(−−)
18-04 09:00	214	15 00.04 S 11 40.05 E	45.5	dinoflagelados (+) peq. algas flageladas (++)
19-04 14:25	216	16 59.82 S 11 35.30 E	45.5	diatomáceas peq. algas flageladas (++)
20-04 06:02	221	17 00.20 S 10 12.27 E	45.4	peq. algas flageladas (++)
21-04 02:22	225	17 00.06 S 8 00.04 E	65.5	peq. algas flageladas (++)
22-04 14:18	229	20 22.82 S 7 58.87 E	45.4	(−−)

+ *pouco abundantes,* ++ *abundantes* +++ *muito abundantes,*
* *células pequenas,* ** *células grandes,* (−−) *estações ou amostras não observadas*

Table B.4: Distribuição dos principais grupos de fitoplâncton nas diferentes estações de amostragem (Abundance of phytoplankton groups (continued))

Data Hora (1999)(utc)	No est.	Latitude Longitude	Profundidade 20-50m	Grupos fitoplanctónicos
23-04 22:54	235	19 27.42 S 10 44.77 E	30.5	diatomáceas (*,+++)
24-04 05:54	237	19 16.61 S 11 20.37 E	30.5	diatomáceas (*,+++)
24-04 15:54	240	19 02.94 S 11 58.98 E	45.5	diatomáceas (*,+++)
26/04 20:44	255	21 02.55 S 13 04.98 E	30.5	diatomáceas (*,+++)
				peq. algas flageladas (++)

+ pouco abundantes, ++ abundantes +++ muito abundantes,

** células pequenas, ** células grandes, (−−) estaçõões ou amostras não observadas*

Table B.5: List of Multi net hauls

Station nb.	CTD-File name	haul nb.	Date dd.mm	Start UTC	Latitude	Longitude	Bottom depth
0140	A0000	1	28.03	20:22	01 27.65 N	005 45.12 W	5133
0141	A0001	2	29.03	05:40	00 59.99 N	005 00.14 W	5095
0142	A0002	3	29.03	16:10	00 21.41 N	003 57.00 W	5108
0143	A0003	4	30.03	02:05	00 16.46 S	002 55.03 W	5088
0144	A0004	5	30.03	13:20	00 56.31 S	001 50.01 W	4600
0145	A0005	6	31.03	00:15	01 35.27 S	000 46.11 W	4900
0146	A0006	7	31.03	09:35	02 13.25 S	000 15.94 E	4600
0147	A0007	8	31.03	18:45	02 51.80 S	001 19.03 E	4400
0148	A0008	9	1.04	04:20	03 30.80 S	002 23.04 E	4458
0149	A0009	10	1.04	12:50	04 07.41 S	003 23.27 E	5100
0150	A0010	11	1.04	23:45	04 43.09 S	004 26.90 E	5032
0151	A0011	12	2.04	09:30	05 15.51 S	005 35.01 E	4798
0152	A0012	13	2.04	18:40	05 47.95 S	006 43.07 E	4526
0153	A0013	14	3.04	04:50	06 19.00 S	007 48.00 E	4214
0157	A0014	15	4.04	08:10	06 54.16 S	009 00.01 E	3960
0158	A0015	16	4.04	16:10	07 22.05 S	010 00.08 E	3884
0159	A0020	17	5.04	00:05	08 00.08 S	011 00.00 E	2698
0160	A0021	18	5.04	08:00	08 30.05 S	011 59.69 E	1872
0161	A0022	19	5.04	14:10	08 35.54 S	012 30.07 E	1341
0162	A0023	20	5.04	17:45	08 38.99 S	012 48.94 E	772
0173	A0018	21	8.04	17:15	08 59.60 S	008 01.40 E	4682
0176	A0111	22	9.04	17:20	10 05.00 S	007 59.20 E	4829
0180	A0161	23	10.04	22:30	11 07.40 S	007 59.50 E	4841

Table B.5: List of Multi net hauls (continued)

Station nb.	CTD-File name	haul nb.	Date dd.mm	Start UTC	Latitude	Longitude	Bottom depth
0202	A0261	24	14.04	22:11	12 00.10 S	007 59.50 E	4813
0203	A0270	25	15.04	06:34	13 00.00 S	007 59.70 E	4794
0204	A0271	26	15.04	15:03	14 00.10 S	007 59.50 E	4755
0205	A0272	27	15.04	23:53	15 00.40 S	007 59.60 E	4850
0206	A0410	28	16.04	10:13	16 00.20 S	007 59.57 E	4973
0216	A0601	29	19.04	14:37	17 03.70 S	011 31.30 E	92
0217	A0602	30	19.04	15:59	16 59.80 S	011 27.70 E	112
0218	A0603	31	19.04	17:36	16 59.70 S	011 20.10 E	158
0219	A0604	32	19.04	21:32	16 59.90 S	010 59.30 E	2161
0221	A0607	33	20.04	06:12	17 00.70 S	010 11.70 E	3630
0222	A0608	34	20.04	11:16	17 00.10 S	009 40.10 E	4051
0223	A0605	35	20.04	16:17	17 00.10 S	009 10.30 E	4439
0224	A0609	36	20.04	21:12	17 00.10 S	008 39.50 E	4698
0225	A0610	37	21.04	03:20	17 00.50 S	007 59.70 E	4912
0226	A0611	38	21.04	03:12	18 00.80 S	007 59.50 E	5002
0227	A0612	39	21.04	20:51	19 00.00 S	007 59.70 E	5081
0228	A0613	40	22.04	04:31	19 42.40 S	007 59.60 E	4906
0229	A0712	41	22.04	13:14	20 20.40 S	007 58.60 E	3097
0230	A0711	42	23.04	19:49	20 14.30 S	008 26.50 E	2044
0231	A0710	43	23.04	10:21	20 06.40 S	008 51.50 E	2274
0232	A0709	44	23.04	06:53	19 56.29 S	009 17.30 E	2343
0233	A0708	45	23.04	13:21	19 44.70 S	009 49.40 E	2044
0234	A0707	46	23.04	19:03	19 35.50 S	010 19.20 E	1380
0237	A0704	47	24.04	06:24	19 16.40 S	011 20.30 E	651
0238	A0703	48	24.04	10:05	19 09.90 S	011 36.90 E	314
0239	A0702	49	24.04	13:10	19 05.90 S	011 46.90 E	310
0240	A0701	50	24.04	16:13	19 02.90 S	011 58.90 E	225
0241	A0700	51	24.04	19:16	18 59.90 S	012 10.90 E	117
0242	A0751	52	25.04	04:56	19 58.90 S	012 50.60 E	103
0243	A0752	53	25.04	07:31	20 00.00 S	012 41.00 E	125
0244	A0753	54	25.04	08:16	20 00.00 S	012 29.90 E	153
0245	A0754	55	25.04	10:08	19 59.80 S	012 20.00 E	200
0246	A0755	56	25.04	11:44	19 59.90 S	012 09.00 E	278
0247	A0756	57	25.04	13:53	19 59.90 S	011 57.80 E	347
0248	A0757	58	25.04	16:10	20 00.00 S	011 49.00 E	446
0249	A0758	59	25.04	19:21	19 59.90 S	011 25.90 E	844

Meereswissenschaftliche Berichte

MARINE SCIENCE REPORTS

---

29 (1998) Matthäus, Wolfgang; Nausch, Günther; Lass, Hans Ulrich; Nagel, Klaus; Siegel, Herbert:
Hydrographisch-chemische Zustandseinschätzung der Ostsee 1997

30 (1998) Fennel, Katja:
Ein gekoppeltes, dreidimensionales Modell der Nährstoff- und Planktondynamik für die westliche Ostsee

31 (1998) Lemke, Wolfram:
Sedimentation und paläogeographische Entwicklung im westlichen Ostseeraum (Mecklenburger Bucht bis Arkonabecken) vom Ende der Weichselvereisung bis zur Litorinatransgression

32 (1998) Wasmund, Norbert; Alheit, Jürgen; Pollehne, Falk; Siegel, Herbert; Zettler, Michael L.:
Ergebnisse des Biologischen Monitorings der Ostsee im Jahre 1997 im Vergleich mit bisherigen Untersuchungen

33 (1998) Mohrholz, Volker:
Transport- und Vermischungsprozesse in der Pommerschen Bucht

34 (1998) Emeis, Kay-Christian; Struck, Ulrich (Editors):
Gotland Basin Experiment (GOBEX) - Status Report on Investigations concerning Benthic Processes, Sediment Formation and Accumulation

35 (1999) Matthäus, Wolfgang; Nausch, Günther; Lass, Hans Ulrich; Nagel, Klaus; Siegel, Herbert:
Hydrographisch-chemische Zustandseinschätzung der Ostsee 1998

36 (1999) Schernewski, Gerald:
Der Stoffhaushalt von Seen: Bedeutung zeitlicher Variabilität und räumlicher Heterogenität von Prozessen sowie des Betrachtungsmaßstabs - eine Analyse am Beispiel eines eutrophen, geschichteten Sees im Einzugsgebiet der Ostsee (Belauer See, Schleswig-Holstein)

37 (1999) Wasmund, Norbert; Alheit, Jürgen; Pollehne, Falk; Siegel, Herbert, Zettler, Michael L.:
Der biologische Zustand der Ostsee im Jahre 1998 auf der Basis von Phytoplankton-, Zooplankton- und Zoobenthosuntersuchungen

38 (2000) Wasmund, Norbert; Nausch, Günther; Postel, Lutz; Witek, Zbigniew; Zalewski, Mariusz; Gromisz, Sławomira; Łysiak-Pastuszak, Elżbieta; Olenina, Irina; Kavolyte, Rima; Jasinskaite, Aldona; Müller-Karulis, Bärbel; Ikauniece, Anda; Andrushaitis, Andris; Ojaveer, Henn; Kallaste, Kalle; Jaanus, Andres:
Trophic status of coastal and open areas of the south-eastern Baltic Sea based on nutrient and phytoplankton data from 1993 - 1997

39 (2000) Matthäus, Wolfgang; Nausch, Günther; Lass, Hans Ulrich; Nagel, Klaus; Siegel, Herbert:
Hydrographisch-chemische Zustandseinschätzung der Ostsee 1999

40 (2000) Schmidt, Martin; Mohrholz, Volker; Schmidt, Thomas; John, H.-Christian; Weinreben, Stefan; Diesterheft, Henry; Iita, Aina; Filipe, Vianda; Sangolay, Bomba-Bazik; Kreiner, Anja; Hashoongo, Victor; da Silva Neto, Domingos:
Data report of R/V "Poseidon" cruise 250 ANDEX'1999